

**ELUCIDATING BACTERIAL-FUNGAL CROSSTALK THROUGH
BACTERIAL PEPTIDOGLYCAN SENSING AND DETECTION IN THE
HUMAN COMMENSAL CANDIDA ALBICANS**

by

Geneva Maddison Crump

A dissertation submitted to the Faculty of the University of Delaware in partial fulfillment of the requirements for the degree of Doctor of Philosophy in Chemistry and Biochemistry

Fall 2022

© 2022 Geneva Maddison Crump
All Rights Reserved

**ELUCIDATING BACTERIAL-FUNGAL CROSSTALK THROUGH
BACTERIAL PEPTIDOGLYCAN SENSING AND DETECTION IN THE
HUMAN COMMENSAL CANDIDA ALBICANS**

by

Geneva Maddison Crump

Approved: _____

Joel Rosenthal, Ph.D.
Chair of the Department of Chemistry and Biochemistry

Approved: _____

John A. Pelesko, Ph.D.
Dean of the College of Arts and Sciences

Approved: _____

Louis F. Rossi, Ph.D.
Vice Provost for Graduate and Professional Education and
Dean of the Graduate College

I certify that I have read this dissertation and that in my opinion it meets the academic and professional standard required by the University as a dissertation for the degree of Doctor of Philosophy.

Signed:

Catherine L. Grimes, Ph.D.
Professor in charge of dissertation

I certify that I have read this dissertation and that in my opinion it meets the academic and professional standard required by the University as a dissertation for the degree of Doctor of Philosophy.

Signed:

Brian J. Bahnson, Ph.D.
Member of dissertation committee

I certify that I have read this dissertation and that in my opinion it meets the academic and professional standard required by the University as a dissertation for the degree of Doctor of Philosophy.

Signed:

Dennis D. Wykoff, Ph.D.
Member of dissertation committee

I certify that I have read this dissertation and that in my opinion it meets the academic and professional standard required by the University as a dissertation for the degree of Doctor of Philosophy.

Signed:

Karl R. Schmitz, Ph.D.
Member of dissertation committee

ACKNOWLEDGMENTS

The work presented here would not be possible without the generous support of my multiple mentors. First and foremost, I would like to express my deepest gratitude for my advisor Dr. Catherine Leimkuhler Grimes. You have not only provided me with the necessities to conduct research in your lab, but you have provided me with a nurturing environment and a strong depiction of a successful female scientist. Thank you for being the trailblazer that you are and for leading by example. I would next like to thank my committee members Dr. Brian Bahnson, Dr. Dennis Wykoff, and Dr. Karl Schmitz. Thank you for your guidance and support throughout my time as a graduate student.

My time as a graduate student was also enhanced severely by the members of the Grimes Laboratory. Over the course of my time here, we have laughed, learned, and even cried together on occasion. I am especially grateful for Ashley Brown and Ophelia Ukaegbu. They were my biggest supports both behind and in front rows. I would also like to thank other lab members Stephen Hyland and Thi Thu Ha Le. While Stephen and I had a rocky relationship early on, he has quickly become the little brother I love but never wanted. Thi Thu Ha Le has been my late night and early morning commiseration buddy and she has been instrumental in keeping me going when I was at wits end. My last year here at the University of Delaware was enhanced by one of the labs newest members, Caroline Williams. Her passion and enthusiasm for this project gave me a renewed sense of drive for this project. It was a pleasure to

mentor her and I am excited to see the new directions that she will drive this project into going forward.

Last but never least, I would like to thank my family and friends who have support me wholeheartedly. My husband Scott Crump Jr. has been my biggest supporter and comforter through this process. Thank you for leaving your warm home state of Georgia to not only marry me, but to follow me from Connecticut to Delaware and now to Massachusetts. You are an awesome teammate and I'm grateful for the life we share. I'm also grateful for my lovely miracles from above, Maddison and Connor Crump. You two have given me so much purpose and you truly are the reason that I am the woman I am today. After a long day of failed experiments and bad data, I was always reassured that your beautiful, full of life, smiling faces would renew me for the next day. My little "bubba" Connor will always be one of the best parts of my graduate school journey, as he was born during my third year. To my dad Glen Barratt, I thank you for choosing me. Not only did you choose me, but you have supported me every step of the way. From bringing me to America, to helping me through college, to walking me down the aisle, and now graduate school. In every literal sense, I would not be where I am today without you. Thank you, thank you, thank you. I love you beyond measure!

DEDICATION

I dedicate this dissertation to my dad Edgar Barratt; your hard work and continuous support has paved the way for this degree to possible.

TABLE OF CONTENTS

LIST OF TABLES	xi
LIST OF FIGURES.....	xii
ABSTRACT.....	xxi
Chapter	
1 INTRODUCTION.....	1
1.1 The Innate Immune System	1
1.2 The Human Microbiota	2
1.2.1 The Human Mycobiome	3
1.3 Bacterial Peptidoglycan	5
1.3.1 Peptidoglycan Sensing and Recognition.....	8
1.4 Leucine Rich Repeat Proteins	12
1.4.1 Leucine Rich Repeat Protein Families.....	16
1.5 Candida albicans	18
1.5.1 Candida albicans Hyphae and Psuedohyphae	21
1.6 Adenylate Cyclases	23
1.7 Candida. albicans Cyr1p	25
1.8 Dissertation Overview.....	27
REFERENCES.....	29
2 PURIFICATION AND CHARACTERIZATION OF A STABLE, MEMBRANE- ASSOCIATED PEPTIDOGLYCAN RESPONSIVE ADENYLATE CYCLASE LRR DOMAIN FROM HUMAN COMMENSAL CANDIDA ALBICANS.....	37
2.1 Introduction.....	37

2.2	Materials and Methods	42
2.2.1	Molecular cloning in <i>S. cerevisiae</i> expression host	42
2.2.2	Kyte-Doolittle Hydrophathy Plots	43
2.2.3	Expression of Cyr1-LRR domain in <i>S. cerevisiae</i>	43
2.2.4	Purification of Cyr1-LRR domain from <i>S. cerevisiae</i>	44
2.2.4.1	Cellular Lysis	44
2.2.4.2	Membrane Isolation and Solubilization	44
2.2.4.3	Purification of Cyr1p-LRR from Membranes.....	45
2.2.4.4	Circular Dichroism Spectroscopy	45
2.2.4.5	CD Thermal Denaturation Analysis.....	46
2.2.4.6	Peptidoglycan Fragment Immobilization to Magnetic Beads	46
2.2.4.7	Protein Enrichment Assay Using Peptidoglycan Immobilized Beads: Cellular Lysate2	47
2.2.4.8	Protein Enrichment Assay Using Peptidoglycan Immobilized Beads: Purified Protein	47
2.3	Results and Discussions	48
2.3.1	Growth of Yeast for Protein Expression	48
2.3.2	Homology of adenylate cyclases from <i>Candida</i> Species	50
2.3.3	Characterization of Cyr1-LRR.....	50
2.3.4	Cyr1-LRR Domain Predicted Biophysical Parameters.....	52
2.3.5	Cyr1-LRR Purification from <i>S. cerevisiae</i> Membranes.....	53
2.3.6	Cyr1-LRR Characterization	60
2.3.6.1	CD Spectroscopy of Purified Protein.....	60
2.3.6.2	Cyr1p-LRR Binds Bacterial Peptidoglycan Fragments.....	63
	REFERENCES.....	69
3	PEPTIDOGLYCAN FRAGMENTS DIFFERENTIALLY REGULATE HYPHAL GROWTH IN WILDTYPE <i>CANDIDA ALBICANS</i>	72
3.1	Introduction.....	72
3.2	Materials and Methods.....	77
3.2.1	Materials.....	77
3.2.2	Budding <i>C. albicans</i> Peptidoglycan Sensitivity.....	78
3.2.3	Filamentous <i>C. albicans</i> Peptidoglycan Sensitivity.....	78

3.2.4	<i>C. albicans</i> Wildtype Phenotypic Characterization in the Presence of Bacterial Peptidoglycan Fragments	78
3.3	Results and Discussions	79
3.3.1	Budding <i>C. albicans</i> Peptidoglycan Sensitivity	79
3.3.2	Filamentous <i>C. albicans</i> Peptidoglycan Sensitivity	81
3.3.3	<i>C. albicans</i> WT Phenotypic Characterization in the Presence of Bacterial Peptidoglycan Fragments.....	84
REFERENCES.....		94
4	ANOMALOUS HYPHAE SPECIFIC GENE EXPRESSION PROFILES IN <i>C. ALBICANS</i> CELLS TREATED WITH BACTERIAL PEPTIDOGLYCAN FRAGMENTS	98
4.1	Introduction	98
4.2	Materials and Methods.....	103
4.2.1	Materials.....	103
4.2.2	Growth of cells for RNA Isolation.....	103
4.2.3	RNA Isolation	104
4.2.4	cDNA Synthesis	104
4.2.5	RT-qPCR of mRNA levels.....	105
4.3	Results and Discussions	106
REFERENCES.....		111
5	FUTURE DIRECTIONS	116
5.1	Characterization of Cyr1p.....	116
5.1.1	Cyr1p-LRR binding pocket elucidation	116
5.2	Peptidoglycan stimulated hyphal growth.....	117
5.3	Hyphae transcriptional regulation.....	118
5.4	RNA sequence analysis.....	119
Appendix		
A	MOLECULAR CLONING IN <i>E. COLI</i>	121
A.1	Molecular cloning of constructs in <i>E. coli</i>	121

A.1.1	Molecular cloning in <i>E. coli</i>	121
A.2	Expression of Cyr1-LRR domain constructs in <i>E. coli</i>	123
B	MOLECULAR CLONING OF GFP TAGGED LRR IN SACCHAROMYCES CEREVISIAE.....	124
B.1	Molecular Cloning of GFP tagged Cyr1-LRR in <i>S. cerevisiae</i>	124
B.2	Molecular cloning of Full-length Cyr1 in <i>S. cerevisiae</i>	124
C	PHOTOAFFINITY LABELING ANALYSIS OF CYR1-LRR.....	125
C.1	Introduction.....	125
C.2	Results and Discussions.....	127
C.3	REFERENCES.....	128
D	PUBLICATION PERMISSIONS.....	129

LIST OF TABLES

Table 1.1: Subfamilies of LRR proteins.....	16
Table 2.1: Detergents used in this study. * CMC values obtained from anatrace.com.	57
Table 4.1: cDNA Synthesis protocol.....	105
Table 4.2: Primers used in this study for RT-qPCR analysis	105
Table A.1: Cyr1p-LRR Expression Constructs.....	121
Table C.1: Components of the PAL experiment.	127

LIST OF FIGURES

- Figure 1.1: The human microbiome.** The human microbiome encompasses the collection of microbes that inhabit the human body. These microbes are found primarily in the gut, and offer many advantages to the human host 4
- Figure 1.2: Schematic representation of peptidoglycan and corresponding fragments upon enzymatic digestion.** Left: Cross-linked peptidoglycan. Depicted in green is N-acetyl glucosamine and in blue N-acetyl muramic acid with the corresponding representative peptide linkage. Right: representative set of possible PG fragments upon digestion with enzymes such as Lysozyme and Carboxypeptidases. Note that MDP is a synthetic fragment and has not been shown to be produced in a biological context. 7
- Figure 1.3: Pathogen Recognition Receptor interplay in bacterial cell wall recognition.** Homologous PG receptors exist for mammals, plants, and insects. A common domain found in these receptors is the evolutionary and structurally conserved Leucine Rich Repeat protein domain, which is not only responsible for the sensing and detection of PG fragments, but is found across innate immune receptors. 10
- Figure 1.4: Evolutionarily Conserved Leucine Rich Repeat.** Crystal structure depicts the secondary structure of porcine ribonuclease inhibitor, the first LRR to be structurally characterized. Crystal structure demonstrates the conserved structure of the LRR, featuring a horseshoe shaped tertiary structure with β -strands lining the concave surface and α -helices on the convex face. 13
- Figure 1.5: The juxtaposition of leucine rich repeat domains across Kingdoms.** The leucine rich repeat (LRR) domain is found in pattern recognition receptors in plants, bacteria, fungi, humans, and viruses. 15

- Figure 1.6: The interaction between bacterial cell wall fragments and the human immune system.** PG turnover and subsequent fragment release to the environment; non-septic PG fragments appear to enter the bloodstream. The innate immune system response to potential PG antigen is the first line of defense against infection. Many of the cells in the innate immune system (such as dendritic cells, macrophages, mast cells) produce cytokines or interact with other cells directly to activate the adaptive immune system. $\gamma\delta$ T cells and Nature Killer cells are lymphocytes without antigen specificity. Therefore, they are considered to be innate cells with some similarities to effector lymphocytes. The adaptive immune system is based on clonal selection of lymphocytes with antigen receptors (B cell receptors and T cell receptors)⁸³ and recent studies suggest that antibodies for specific PG fragment exist. A more detailed understanding of PG related immune response provides new opportunities for improving immunotherapy for autoimmune diseases..... 18
- Figure 1.7: The Morphological growth forms of *Candida albicans*.** *Candida albicans* growth forms are associated with pathogenicity. Under budding growth, cells are typically commensal. The morphological transition to pseudohyphae/ hyphae lends the fungi the ability to penetrate human epithelial cells and cause disseminated infections..... 20
- Figure 1.8: Bacterial peptidoglycan is a potent molecular signal for the yeast to hyphae morphological transition.** In the presence of some bacterial peptidoglycan fragments budding *C. albicans* cells morphologically transition to hyphal cells..... 22
- Figure 1.9: The adenylate cyclase Cyr1p from the human commensal *Candida albicans*.** From N to C terminus, this receptor consists of a G α domain, a ras associating domain (RA), 14 Leucine Rich Repeats, a proteinphosphatase 2C (PP2C) domain, a catalytic cyclase (CYC) domain, and a C-terminal catalytic binding domain (CBD). 26

- Figure 2.1:** **A:** The adenylate cyclase Cyr1p contains a $G\alpha$ domain, a Ras associating domain, 14 Leucine Rich Repeats (LRR), a Protein Phosphatase 2 domain, a guanylate cyclase domain, and a catalytic binding domain. Our newly designed expression vector for Cyr1p LR LRR domain contains residues from 435 up to the PP2C domain. The construct contains 14 repeats of the LRR domain and is expressed in *S. cerevisiae*. Our previous construct did not include all of the Leucine Rich Repeat. **B:** Tertiary structure prediction of the 1690 amino acid adenylate cyclase by AlphaFold2. Model is depicted with respect to the LRR domain, red= $G\alpha$ domain, Blue= Ras association domain, Teal+ Leucine Rich Repeat domain, Grey= Protein Phosphatase 2C domain, Orange= Adenylyl/ guanylyl cyclase domain. All uncharacterized, or disordered domains are depicted in green. 40
- Figure 2.2: Cyr1p LRR in episomal plasmid pESC-Ura.** **A:** The recombinant construct consists of an N-terminal 6xHis tag, and a C-terminal Spot-Tag. **B:** Western blot analysis of protein expression using an anti-Spot nanobody raised against the Spot-Tag. In the absence of Galactose (-Control) no protein expression is observed. Optimal protein expression is observed in the presence of 2% galactose final concentration. 49
- Figure 2.3: LRR induction analysis.** Optimal induction times are between 9.5 to 11 hours. After 11 hours, protein expression decreases noticeably. Dashed line indicates time points that were removed. 49
- Figure 2.4: Sequence homology of the adenylate cyclase from 5 *Candida*. spp.** Blast analysis of the adenylate cyclase genes from *Candida*. spp *Candida. albicans*, *Candida. glabrata*, *Candida. parapsilosis*, *Candida. auris*, and *Candida. dubliniensis* revealed several highly conserved residues in red and less conserved residue in blue. The LRR domain was cloned from residue 435 at the N-terminus, and residue 1004 at the C-terminus, where sequence conservation decreases significantly as indicated by the gray dashed lines. 50

Figure 2.5: Purification of Protein Detergent Complexes. Protein solubilized from isolated membranes were purified under native conditions. **A:** Western blot analysis against the Spot-Tag shows successful purification of the LRR domain C-terminus. From left to right, MW marker, Flow through, washes 1-6, and elutions 1-3. **B:** Western blot analysis against the His₃ Tag shows successful purification of the LRR domain N-terminus. From left to right, MW marker, Flow through, washes 1-6, and elutions 1-3. **C:** Coomassie staining reveals that the sample in elution is composed primarily of full-length Cyr1-LRR and there are no major impeding impurities. From left to right, Flow Through (FT), Washes 1-6 (W1-W6), followed by elution 1, 2 and 3 (E1, E2, E3 respectively) using Spot Peptide in PBS. Dashed lines indicate truncated gel..... 51

Figure 2.6: Hydropathy Plot of the Cyr1-LRR domain. Possible transmembrane segments were calculated using the linear weight variation model. Y axis represents the hydropathy score, and X axis represents the window number or amino acid position. **A:** Surface regions can be identified by peaks below the midline, and transmembrane proteins can be identified by peaks with scores greater than 1.6. **B:** Potential for a transmembrane domain exists between amino acid residues 500 and 600, at the C-terminus. 52

Figure 2.7: Hydrophobic residues in Cyr1-LRR. Red color signifies negative charge, blue signifies positive, and white denoting neutral. Electrostatic potential maps demonstrate that there are several localized areas of negative charges distributed in the LRR. **A:** Side view of a ribbon diagram depicting hydrophobic amino acids residues in yellow. **B:** Side view of an electrostatic potential map of the LRR domain, where areas of negative charge are observed in red. **C:** Top-down view of the LRR in a ribbon diagram depicting hydrophobic residues in yellow. **D:** Top-down view of the LRR electrostatic potential map depicts localization of negative charges towards the N and C terminus. Figures were generated using PyMol..... 53

Figure 2.8: Membrane solubilization of the Cyr1p-LRR. Expected MW is 68.5 kD. **A:** LRR can be extracted from cellular membranes using high ionic strength alone. Solubilization of the LRR can be achieved with 0.5 M NaCl in the absence of detergent. At 1 M NaCl, decrease in protein solubilization was observed due to salting out. At 100 mM NaCl, protein precipitated was observed from the buffer. **B:** Detergent screens with a salt concentration of 0.5 M demonstrate that the Fos-choline class of detergents is best suited for the solubilization of the LRR from the fractionized cellular membranes. **C:** From the Fos family of detergents, Fos-Choline 16 provided the most solubilized protein from cellular membranes with a salt concentration of 0.5 M. **D** Chemical Structure of the solubilizing detergent Fos-Choline-16..... 55

Figure 2.9: Chemical Structures of detergents used for membrane solubilization. Detergents used in the solubilization trials of the LRR are as follows: n-Dodecyl-B-D-Maltoside (DDM), Octaethylene glycol monododecyl ether (C₁₂E₈), n-Hexadecylphosphocholine (Fos-C16), -n-Dodecylphosphocholine (Fos-C12), n-Octyl-β-D-Glucoside (OG), Dodecylpho-N-Methylethanolamine (FOS-MEA-16) and N-Lauroylsarcosine sodium salt (Sarkosyl). 58

Figure 2.10: Secondary Structure of Cyr1p-LRR. **A:** Circular Dichroism spectroscopy reveals that the LRR domain is well folded and consists of 28.8% alpha helix, and 16.41% β strands. **B:** AlphaFold2 secondary structure prediction agrees with the experimental observations from CD spectroscopy. 61

Figure 2.11: Concentrated purified protein. Purified membrane solubilized protein is prone to oligomerization upon concentration. This high propensity to coexist in multiple oligomerization states is a hindrance to spectroscopic analysis such as Circular Dichroism spectroscopy. 62

Figure 2.12: LRR Secondary Structure Perturbations. Slight perturbations in secondary structure was observed when the LRR was subjected to 95°C temperatures. While the protein remains largely folded, there is some loss of secondary structure observed. Particularly, there is some loss of α- helical and antiparallel β-sheets..... 62

Figure 2.13: Membrane-associated Cyr1p–LRR domain can bind synthetic peptidoglycan fragments. (a) Schematic of magnetic bead functionalization. Terminal carboxylic acids are activated with NHS and subsequently coupled to an amine-functionalized peptidoglycan derivative. (b) Structures of 2-NH ₂ muramyl dipeptide (MDP), muramyl tripeptide (MTP), and 2-NH ₂ muramic acid (MA) coupled to the magnetic beads through an amine functionality. (c) Western blot analysis and quantification of Cyr1p–LRR domain affinity purification relative to the unfunctionalized beads (ethanolamine control). Error bars represent the standard deviation between replicates.	63
Figure 2.14: Cellular Lysate enrichment biological replicate 1. A: Immunoblotting against the C-terminal Spot-Tag. B: Densitometric analysis was used to quantify the binding of Cyr1p-LRR and was normalized to ethanolamine. Relative to Ethanolamine, increased binding is observed for PG fragments, MTP, MDP, and MA. X denotes empty lanes	65
Figure 2.15: Cellular Lysate enrichment biological Replicate 2. A: Immunoblotting against the C-terminal Spot-Tag. B: Densitometric analysis was used to quantify the binding of Cyr1p-LRR and was normalized to ethanolamine. Relative to Ethanolamine, increased binding is observed for PG fragments, MTP, MDP, and MA.	66
Figure 2.16: Purified protein binding to PG functionalized beads. Background binding to the ethanolamine control is undetectable using purified protein. In addition, purified protein binds MTP with higher affinity relative to ethanolamine control.....	67
Figure 3.1: Bacterial Peptidoglycan Fragments Synthesized by former members of the Grimes Laboratory. A suite of in house synthesized bacterial peptidoglycan fragments were analyzed for their ability to induce consistent hyphal morphology in wildtype (WT) yeast <i>C. albicans</i> . The selected bacterial peptidoglycan fragments are at large, MDP, MA, and glucose derivatives.	79
Figure 3.2: Growth of budding yeast characterized in the presence of 6-amino-D - glucose and 2-amino-muramic acid. A slight increase in cellular growth was observed at a concentration of 1mM for both fragments, as evident by a shift in the growth curve to the left.	80

Figure 3.3: Growth of budding yeast in the presence of MDP derivatives. No changes were observed in growth in the presence of these bacterial peptidoglycan fragments at concentrations of 50, 100 and 1000 μ M.	81
Figure 3.4: Filamentous growth assessment in the presence of 1 mM 6-amino-D-glucose and 2-amino-muramic acid. At 1 mM of each peptidoglycan fragment, a slight increase in filamentous growth is observed, similar to growth as budding yeast.	82
Figure 3.5: Filamentous growth of wildtype cells treated with 1 mM 6-amino MDP-(LL)- ester, 6-amino-MMP ester, and 2-amino-γ-amino-butyryl MDP.	83
Figure 3.6: Filamentous growth analysis in presence of a:6-amino MDP ester, b: 6-N-acetyl muramic acid methyl ester, and C: MDP-(LL). Where stereochemistry is not denoted, the biologically active stereoisomer MDP (LL) is implied.	84
Figure 3.7: Hyphal assessment control used to ensure proper cellular responses. FBS and MDP have been documented hyphal inducers of filamentous growth in <i>C. albicans</i> . Where stereochemistry is not denoted, the biologically active stereoisomer MDP-(LD) is implied.	85
Figure 3.8: Filament assessment in the presence of MDP esters. True hyphae were only observed in the presence of 6-amino MDP ester. MDP ester alone and the 6-amino MDP-(LD)- ester failed to form true hyphae. Where stereochemistry is not denoted, the biologically active stereoisomer MDP-(LL) is implied.	86
Figure 3.9: Filamentous assessment in the presence of substituted MDP derivatives 2-amino-β-alanyl MDP, and 2-amino-γ-amino butyryl MDP. At 22 hours post induction, 2-amino- β -alanyl MDP maintained hyphae. Comparitevely, 2-amino- γ -amino butyryl MDP failed to form true hyphae. At 8 hours, pseudo hyphae can be observed, but cells readily reverted to budding at 22 hours post induction. Where stereochemistry is not denoted, the biologically active stereoisomer MDP- (LL) is implied.	87

Figure 3.10: Filamentous assessment in the presence of muramic derivates. 2-amino-muramic acid was the most potent inducer of hyphal morphology comparatively to N-acetyl muramic acid and 6-N-acetylmuramic acid methyl ester. The former produced hyphae at 8 hours, and maintained this morphology throughout 22 hours, while the latter did not produce true hyphae and displayed pseudohyphae.....	89
Figure 3.11: Filament assessment in the presence of 6-amino- d-glucose and 6-amino-MMP ester. 6-amino- d-glucose was able to maintain hyphae at 22 hours, but 6-amino MMP ester only induced pseudohyphae at 8 hours, with complete reversion to budding observed at 22 hours.....	90
Figure 3.12: Heat map representation of the hyphal inducing ability of peptidoglycan fragments assayed. Fragments that induced and maintained hyphal morphology were MDP, 2-amino- β -alanyl MDP, and 2-amino-muramic acid.	91
Figure 4.1: Hyphae specific gene regulatory pathways in <i>C. albicans</i>. Several major pathways are involved in the regulation of the morphological plasticity of <i>C. albicans</i> . Morphological regulation can occur via acidic pH, bacterial peptidoglycan, quorum sensing molecules, etc. ...	100
Figure 4.2: Hyphae Specific Gene expression in cells treated with 10% FBS. The HWP1 transcript was not consistently upregulated during the 22-hour time course treatment. TUP1 was downregulated at 8 hours but appeared upregulated at 22 hours relative to the 8-hour time point. ECE1 was downregulated over the treatment course.....	108
Figure 4.3: Hyphae specific gene expression in cells treated with a) NAM and b) 2-amino muramic acid. NAM treated cells showed a consistent upregulation of HWP1 throughout the 22-hour time course, downregulation of ECE1, and TUP1. MA treated cells displayed no trends in expression patterns of HSGs, as well as HWP1, ECE1, and TUP1 transcripts were neither consistently increased nor decreased throughout the 22-hour analysis window.....	109
Figure 5.1: Photoactivatable crosslinking of Cyr1p-LRR.....	117
Figure 5.2: Synthetic bacterial peptidoglycan fragments. While some of the fragments were tested for their ability to induce hyphal formation, MDP-(LL) remains to be analyzed.....	118

Figure 5.3: Bacterial peptidoglycan fragments. The fragment MTP and its synthetic derivatives remained to be analyzed for their ability to induce hyphae.	118
Figure 5.4: Morphological assay to RNA isolation workflow. The morphological assay samples can be further processed to conduct whole RNA sequencing analysis to capture the full range of RNA transcript upregulation and or downregulation.	120
Figure C.1: MTP photoactivatable probe. MTP was functionalized with a diazirine moiety and a bioorthogonal alkyne handle for use in copper-catalyzed azide-alkyne click chemistry.	126
Figure C.2: Preliminary photoactivatable crosslinking of Cyr1p-LRR. In gel fluorescence demonstrates increased fluorescent intensity in the presence of UV light in Cyr1p-LRR and probe complexes.	128
Figure Appendix D.1: Permission for use of material from the publication: Purification and Characterization of a Stable, Membrane-Associated Peptidoglycan Responsive Adenylate Cyclase LRR Domain from Human Commensal <i>Candida albicans</i>	129
Figure D.2: Permission for use of the following publication: <i>Revisiting peptidoglycans sensing: interactions with host immunity and beyond</i>	130
Figure D.3: Permission for the use of Figure 4.1 from the following publication: Hyphae-Specific Genes HGC1, ALS3, HWP1, and ECE1, and Relevant Signaling Pathways in <i>Candida albicans</i>	131

ABSTRACT

The human innate immune system is composed of functionally distinct modules that has evolved to provide different forms of protection against invading pathogens. The adaptive immune system provides long lasting pathogen specific immune responses. The innate immune system, though less specific to pathogens, serves as the body's first line of defense against invading pathogens. The innate immune system is a conserved host response that entails the sensing of pathogen-associated molecular patterns (PAMPS) through germline-encoded pattern recognition receptors (PRRs), which initiate pathway-specific signaling networks, resulting in rapid responses that serve as the hosts' first line of defense. Such germline encoded PRRs include but are not limited to Toll-like receptors (TLRs), RIG-I-Like (RLRS), NOD-like receptors (NLRs), and DNA receptors. PRRs are an irrefutable asset for the proper maintenance of human health. While they are traditionally known to recognize microbial molecules during infection scenarios, ligands for PRRs are not exclusive to foreign pathogens and are abundantly produced by the resident microbiota during normal colonization.

The human microbiota consists of 10-100 trillion symbiotic microbial cells that reside in the body and vastly outnumber human somatic and germ cells. Microorganisms of the microbiota include bacteria, viruses, fungi, and protozoa. Together, these microbes form ecological communities in many anatomical sites. As such, the microbiota affects many vital functions of the human body. One of the most

common residents of the human microbiota is the polymorphic fungi *Candida albicans* (*C. albicans*).

C. albicans is a commensal member of the human microbiota, typically residing in the gut and other mucosal surfaces of the body. In the human host, *C. albicans* interacts with a plethora of bacterial species and relies on these interactions for homeostasis under normal conditions. In the event of microbiota niche disruption, such as immune incompetence of the host, *C. albicans* transcends from a commensal state to a virulent state. Specifically, owing to the virulence of *C. albicans* is the phenotypic switch from budding yeast (blastospore) to filamentous state (hyphae) followed by transcriptional regulation of hyphae specific genes upon introduction of certain environmental signals. Central to transcriptional regulation for virulence associated genes and subsequent pathogenicity, is a spike in the cAMP-PKA cascade. This signaling pathway is upregulated upon binding of the adenylyl cyclase Cyr1p to bacterial peptidoglycan. Cyr1p behaves much like a PRR, in its ability to bind and sense ligands that are foreign to the fungi. Particularly, this protein contains an evolutionary conserved leucine rich repeat (LRR) protein domain commonly found in human PRRs such as TLRs, and NOD like receptors.

Through its LRR domain, Cyr1p can sense and detect bacterial peptidoglycan (PG). PG, being a major culprit for the transition of *C. albicans* from commensal to pathogenic, is a focal point of the bacterial-fungal relationship and is at the molecular interface facilitating these cross-kingdom interactions. We sought to understand bacterial-fungal crosstalk by characterizing the Cyr1p LRR domain, investigating the Cyr1p-LRR-PG interactions, and probing the phenotypic plasticity of *C. albicans* cells in the presence of synthetic PG fragments.

In our efforts to characterize the Cyr1p-LRR domain, we have biochemically classified this domain as a peripheral membrane protein and have demonstrated that the extended membrane associated LRR construct retained the ability to interact with previously known bacterial PG fragments such as Muramyl tripeptide (MTP). We have also shown the differential morphological regulation of *C. albicans* hyphae by various synthetic PG fragments and have correlated these findings to anomalous transcriptional regulation of Hyphae Specific Genes (HSGs). Though maintenance of HSGs at the transcriptional level ensures hyphal growth and elongation, we reasoned that our observed anomalous HSG transcriptional pattern is due to inadequate knowledge of the entire signaling pathways that govern the morphological transition from budding to hyphae and therefore commensalism to pathogenicity.

In this dissertation, the characterization of the long-standing difficult nature of the Cyr1p-LRR domain has been explained, as this domain has been shown to be membrane associated. This may also foreshadow how *C. albicans* can interact with PG fragments that are small, polar, and not readily membrane permeable ligands. Furthermore, the exploration of *C. albicans* morphological plasticity in the presence of synthetic bacterial PG fragments has indicated that there is specificity in the PG ligands that are able to produce true hyphae in the microbe. These findings, along with anomalous HSG regulation, presage that without proper transcriptional regulation, *C. albicans* can readily convert between yeast and hyphal forms.

Chapter 1

INTRODUCTION

This chapter was adapted from the publications below. Further permissions related to the material excerpted should be directed to the designated journal. Reprint (adapted) with permission from the following publication:

Crump, G. M., et al. (2020). "Revisiting peptidoglycan sensing: interactions with host immunity and beyond." Chemical Communications **56**(87): 13313-13322.

1.1 The Innate Immune System

The mammalian immune system has both innate and adaptive components that cooperate to protect the host from infection. The innate immune system is composed of functionally distinct modules that evolved to provide different forms of protection against pathogens. The adaptive immune system, or the acquired immune system is pathogen specific¹ and provides long term immune protection, via memory responses to previously encountered pathogens². During the first critical hours and days of exposure to a new pathogen, humans rely on their innate immune system to protect them from infection, making it the body's first line of defense. The innate immune system is a conserved host response that entails the sensing of pathogen-associated molecular patterns (PAMPS) through germline-encoded pattern recognition receptors

(PRRs), which initiate pathway-specific signaling networks, resulting in rapid responses that serve as the hosts' first line of defense³.

Such germline encoded PRRs include but are not limited to Toll-like receptors (TLRs), RIG-I-Like (RLRS), NOD-like receptors (NLRs), and DNA receptors³. TLRs are perhaps the most characterized of the PRRs, and are considered to be the primary sensor of pathogens⁴. Humans have at least ten TLRs, of which several have been shown to play important roles in innate immune recognition of PAMPs, immunostimulants that are essential for the life cycle of pathogens such as bacterial peptidoglycan and lipopolysaccharides⁵. In addition, molecules related to TLRs have been found to be involved in innate immunity in all multicellular organisms. For instance, in plants, proteins with leucine rich repeats and with domains homologous to the cytosolic portion of TLRs are required for resistance to fungal, bacterial, and viral pathogens⁶. NLRs are cytosolic PRRs that survey intracellular environments for threats. Threat detection leads to oligomerization into large macromolecular scaffolds and the rapid deployment of effector signaling cascades to restore homeostasis⁷.

PRRs are an irrefutable asset for the proper maintenance of human health. While they are traditionally known to recognize microbial molecules during infections, ligands for PRRs are not exclusive to foreign pathogens and are abundantly produced by the resident microbiota during normal colonization.

1.2 The Human Microbiota

The birth of the human microbiota began in the late 1600's, when 17th century scientist Anthony van Leeuwenhoek discovered and illustrated using a handcrafted microscope, that there were five different kinds of bacteria, or animalcules as he termed them at the time, present in his own mouth and the mouths of others. He then

went on to investigate the fecal microbiota, spurring the start a revolutionary field in science. Centuries later, in 1853 Joseph Leidy published a book entitled *A Flora and fauna within Living Animals*, spurring what was considered to be the start of “microbiots” research⁸. Building off of their predecessors, Pasteur, Metchnikoff, Koch, Escherich, Kendall, and several others began laying the foundation of how scientist understand host-microorganism interactions⁹. Specifically, Pasteur developed the germ theory of disease, Metchnikoff believed that the microbiota composition and its interactions with the host were essential for human health, and Escherich spawned the idea that understanding the endogenous flora was a necessity to understand the physiology of digestion and the pathology and therapy of intestinal diseases¹⁰. Though it was not defined as the microbiota at that time, the aforementioned scientist designed the landscape of what is now termed the human microbiota.

The human microbiota consists of 10-100 trillion symbiotic microbial cells that reside in the body (**Figure 1.1**). The microbes that live in and on us outnumber our somatic and germ cells by an estimated 10-fold¹¹. These microorganisms include a large number of bacteria, viruses, fungi, and protozoa¹², and are an assemblage of microorganisms that form ecological communities in many anatomical sites. As such, the microbiota affects many vital functions on the human body.

1.2.1 The Human Mycobiome

The term microbiome at large refers to the bacterial component of the microbes that resides in and on the body. When the Human Microbiome Project was launched, priority was focused on the normal bacterial microbiome of various anatomical sites such as the oral, skin, gut, and vaginal cavities. With the advent of findings regarding human health and disease, there was a significant lack of

characterization of the fungal diversity within the aforementioned anatomical sites. Interestingly, the term microbiome has implied reference to only commensal and pathogenic bacteria¹³. As more interest emerged in the study of the microbial component of the human body, there was shift in 2010 with the branding of the term ‘mycobiome’¹⁴. Mycobiome is a combination of the word ‘mycology’ and ‘microbiome’ and was first used to refer to the fungal microbiome.



Figure 1.1: The human microbiome. The human microbiome encompasses the collection of microbes that inhabit the human body. These microbes are found primarily in the gut, and offer many advantages to the human host

The lesser characterized mycobiome is no less important or physiologically relevant in the context of human health, pathology, and disease progression. There has been a constant increase in the incidence of fungal infections in the past two decades, primarily in opportunistic infections of immunocompromised populations, such as those living with HIV/AIDS, cancer, and other immune suppressing indications¹⁵. Even more alarming, is that several diseases that were formerly considered to have no association with fungi, such as hepatitis B¹⁶, cystic fibrosis^{17, 18}, and inflammatory bowel disease (IBD)¹⁹, are now found to be associated with particular mycobiomes. With the realization that there is a greater interplay between the fungal component of the microbiome (mycobiome), research has expanded in the field of characterizing fungi and their roles in the body.

Like their bacterial counterparts, fungi can occupy multiple anatomical sites and under normal conditions pose no threat to the human host, but in an instance of dysbiosis, these commensals turn pathogenic and can have lethal implications. A hallmark of fungal pathogenies in the human body is the coincidence of bacterial peptidoglycan. Thus, fungal-bacterial interactions within the context of the human microbiome are important for disease pathology and overall human health.

1.3 Bacterial Peptidoglycan

With regards to the human microbiome, bacterium and their associations are an important facet in the overarching context of human health and disease pathology. Specifically, the bacterial cell wall peptidoglycan (PG) is an extremely immune-stimulat agent in the human host. Peptidoglycan, or murein, is an essential and highly specific component of the bacterial cell wall found on the outside of the cytoplasmic

membrane of almost all bacteria. This dynamic structure functions to preserve the overall bacterial cell integrity by withstanding turgor pressure, maintaining homeostasis within the cell, and provides a scaffold for anchoring other cellular envelope components such as proteins and teichoic acids²⁰.

The hallmark of bacterial peptidoglycan is linear glycan strands cross-linked by short peptides. The glycan backbone consists of alternating N-acetylglucosamine and N-acetylmuramic acid (GlcNAc-MurNAc) residues connected via a β -1-4 linkage and the pentapeptide bridges are attached to the lactyl moiety of MurNAc via an amide linkage²⁰. The typical peptide structures: 1) L-alanine, 2) D-glutamate, 3) an amine functionalized amino acid, 4) D-alanine and 5) D-alanine²¹. Importantly, the second and third amino acid are linked via the carboxylic acid in glutamate's side chain, not the α -carboxylic acid (Figure 1). Two of the most prominent examples are the following: in most Gram (-) bacteria, the peptide moiety at the third position is *m*-DAP (*meso*-diaminopimelic acid), and connects the glycan strands through direct *m*-DAP-D-Ala cross linkage, whereas in Gram (+) bacteria the third amino acid is lysine and is cross-linked to other glycan strands via glycine bridges²².

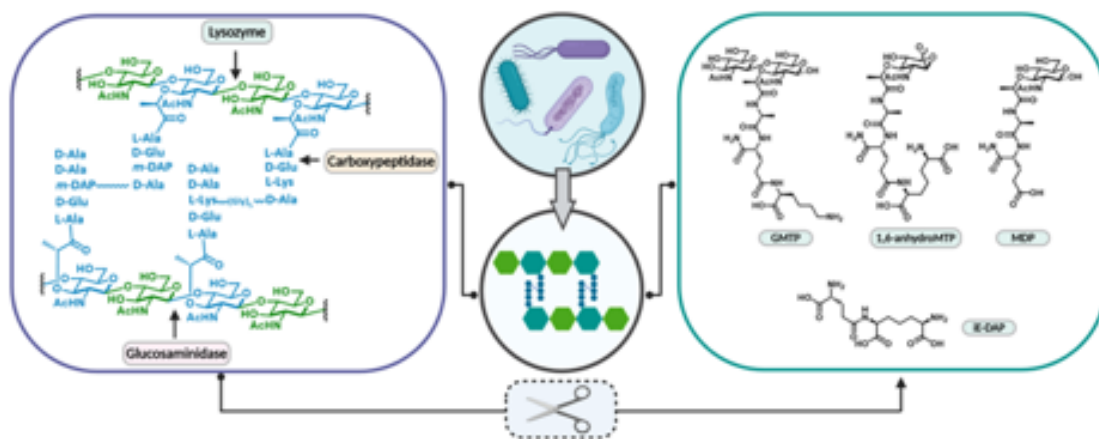


Figure 1.2: Schematic representation of peptidoglycan and corresponding fragments upon enzymatic digestion. Left: Cross-linked peptidoglycan. Depicted in green is N-acetyl glucosamine and in blue N-acetyl muramic acid with the corresponding representative peptide linkage. Right: representative set of possible PG fragments upon digestion with enzymes such as Lysozyme and Carboxypeptidases. Note that MDP is a synthetic fragment and has not been shown to be produced in a biological context.

Though the glycan backbone is generally conserved in bacteria, the peptide moiety exhibits considerable diversity among Gram (-) and Gram (+) bacterium (**Figure 1.2**). Substitution of *m*-DAP by other amino acids such as lanthionine and stereochemical variant LL-DAP has been reported for Gram (-) bacteria *Fusobacterium nucleatum*²³ and *Porphyromonas gingivalis*²⁴ respectively. Similarly, in the Gram (+) bacteria *Herpetosiphon aurantiacus*²⁵ and *Ornithinmicrobium humiphilum*²⁶ *m*-DAP is completely replaced by L-ornithine. Moreover, the peptide stem constitutes the point of covalent anchoring of cell envelope proteins to peptidoglycan. For instance, in *E. coli* and other Gram (-) bacteria, Braun's lipoprotein is the only protein covalently linked to peptidoglycan to date^{27, 28}. Gram (+) bacteria contain many surface proteins

that are anchored to the peptidoglycan and subsequently involved in pathogenic processes. Such proteins include protein A, fibronectin-binding proteins, collagen adhesions, and others²⁹.

The rigid structure of PG lends to its diverse functions that play critical roles for the protection and integrity of the bacterial cell³⁰. Premature or unwanted degradation of PG results in bacterial cell lysis³⁰. The presence of PG is multifaceted, as it serves to preserve and define cellular integrity, as well as scaffold cell components such as lipopolysaccharides³¹. The role of PG is very broad and has scientific relevance from antibacterial development³², to the human microbiome³³, and human innate immune signaling³⁴.

1.3.1 Peptidoglycan Sensing and Recognition

Peptidoglycan is a dynamic structure that continuously undergoes remodeling during bacterial growth and reproduction, which results in the release of fragments from the bacterial cell wall into the localized environment; a process termed peptidoglycan turnover³⁵. Bacteria degrade approximately 40 to 50% of their peptidoglycan per generation as part of their normal peptidoglycan remodeling process required for cell wall expansion³⁶. The heteropolymer must be at least partially degraded to allow for proper cell division before it is reconstructed to yield mature daughter cells³⁷⁻³⁹. During this highly regulated process, small fragments are released into the milieu, and constitute a marker for bacterial presence and activity⁴⁰.

Since peptidoglycan turnover is a highly regulated process, it requires stringent control at the transcriptional level to avoid autolysis and unintentional cell death³⁵. It is therefore controlled by more than one enzyme. Varying enzymatic control equates to multiple fragments that can be placed in the milieu at any given time, thus the

chemical composition of these fragments can vary wildly. For instance, both lysozyme and lytic transglycosylases release disaccharide-peptides but while the hydrolytic reaction of lysozyme generates a terminal reducing MurNAc, the lytic transglycosylase produces anhydromuropeptides which present a 1,6-anhydro ring at the MurNAc thereby producing an anhydroMurNAc moiety⁴¹. PG turnover/recycling is not limited to Gram (-) or Gram (+) but is indeed a facet of both types of bacteria, further increasing the types of fragments produced^{35, 42}.

With the array of fragments that can be encountered by the host, one must imagine that nature has evolved inherent sensing mechanisms to generate the appropriate response. Indeed, this is the case as various hosts have evolved peptidoglycan recognition receptors that aid in its detection and subsequently processing (**Figure 1.3**). The molecular signatures present in bacteria that are absent in host cells (mammals, plants) are defined as microbe-associated molecular patterns (MAMPs)⁴³. The detection of MAMPs is successful through specific receptors termed Pathogen Recognition Receptors (PRRs)⁴⁴. Pathogen Recognition receptors are able to bind peptidoglycan and a plethora of other bacterial derived molecules such as lipopolysaccharides (LPS)⁴⁴. In this dissertation, I elaborate only on PRRs and their activation as it pertains to PG, specifically MurNAc containing fragments, in which many excellent reviews have been written on the innate immune recognition^{21, 34, 40, 45, 46} of.

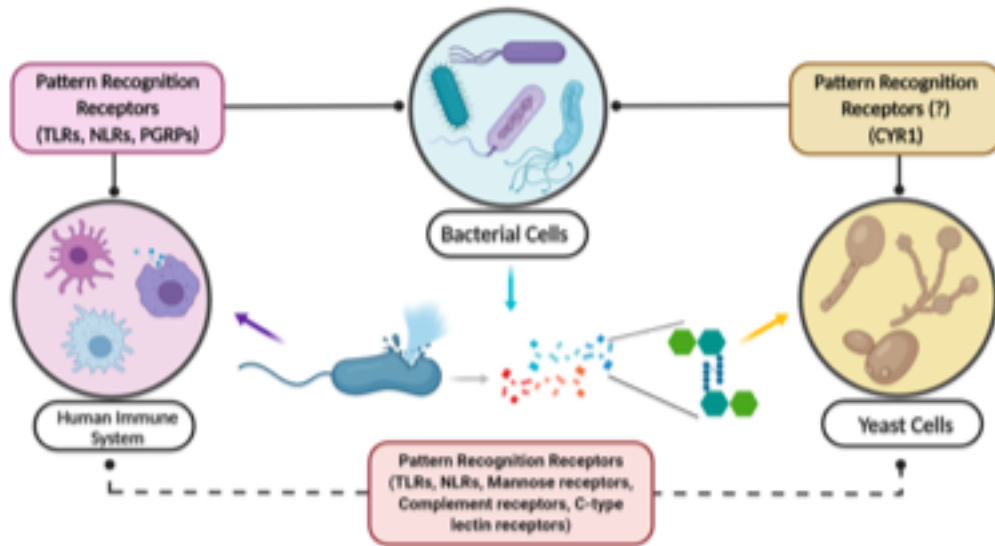


Figure 1.3: Pathogen Recognition Receptor interplay in bacterial cell wall recognition. Homologous PG receptors exist for mammals, plants, and insects. A common domain found in these receptors is the evolutionary and structurally conserved Leucine Rich Repeat protein domain, which is not only responsible for the sensing and detection of PG fragments, but is also found across innate immune receptors.

Plants, insects, and mammals have all evolved a number of germline encoded PRRs and peptidoglycan-recognition receptors⁴⁷. Once these receptors are activated, a host response is elicited for the particular class of invading microbe or bacteria. To date, much research has been conducted on Toll-like receptors (TLRs) and nucleotide oligomerization domain (NOD) like receptors (NLRs)^{4, 48-50}. NOD proteins are intracellular and regulatory proteins that respond to a variety of signaling molecules, including PG fragments^{5, 50} (**Figure 1.6**). NOD1 and NOD2 are multi-domain proteins consisting of one or two CARD domains respectively, and a centrally located NOD domain followed by a number of C-terminal leucine rich repeats (LRRs)⁵⁰.

Our lab and others have demonstrated that the LRR domain of NOD2 binds to the synthetic bacterial PG fragment MDP^{7, 51}. In addition, other labs have focused on NLRP3 and NOD1⁵²⁻⁵⁴, which sense GlcNAc⁵⁵ and *m*-DAP respectively. In contrast to NLRs, TLRs are integral membrane glycoproteins which are localized to the cell surface (TLR1,2,3) or to intracellular compartments (TLR7,9)⁴. Each Toll Like Receptor is composed of an ectodomain with leucine rich repeats that mediate microbe associated molecular patterns recognition, a transmembrane domain, and a cytoplasmic Toll/IL receptor (TOR) domain responsible for downstream signaling⁴⁹. Like Nod Like Receptors, Toll Like Receptors sense pathogens via their LRR domains, with the Pathogen Associated Molecular Patterns binding sites formed by insertions in leucine rich repeat loops. These receptors work in concert to generate the appropriate immune response, with substantial cross-talk between the receptors⁵⁶.

In addition to triggering immunological responses upon activation, NLRs and TLRs, all share a common binding domain. Of particular interest in these PG recognition receptors, is the commonality of the LRR domain. Briefly, leucine rich repeats are generally 20–30 residues long and contain a conserved 11-residue segment with the consensus sequence LxxLxLxxN/CxL, where x can be any amino acid and leucine residues can also be substituted by valine, isoleucine and phenylalanine⁵⁷. Overall, LRRs display a curved shape with parallel β -sheets on the concave side and mostly helical segments on the convex side⁵⁸. A more extensive overview of LRRs can be found in section 1.4.

A less studied LRR that senses bacterial peptidoglycan is the adenylyl cyclase, Cyr1p, from the human commensal *C. albicans*. Although yeasts, being single celled organisms, are not considered to have an immune system, Cyr1p functions very much

like an innate immune receptor by signaling to *C. albicans* that bacterial peptidoglycan fragments are present and ultimately changing the phenotype of the *C. albicans*'s cell. While much literature can be found on NRLs and TLRs, not much has been presented with regards to the sensing and detection of yeast to bacterial peptidoglycan. Nonetheless, it is highly documented in the medical sector that there is a clear association between *C. albicans* pathogenesis and bacterial infections⁵⁹. *C. albicans* infections are often isolated with bacterial infections and in fact worsened in the presence of bacteria^{60, 61}. Shing *et al.* reported that the presence of *C. albicans* can not only promote Group B Streptococcus urinary tract infections, but can also increase bacterial adherence to bladder epithelium thereby promoting bacterial colonization⁶².

1.4 Leucine Rich Repeat Proteins

As previously mentioned, Leucine Rich Repeats (LRRs) are evolutionarily conserved protein domains that are 20-30 amino acid residues in length with sequence motifs ranging from 2-45⁶⁰. Proteins containing LRRs include tyrosine kinase receptors, cell-adhesion molecules, virulence factors, and extracellular matrix-binding glycoproteins^{63, 64}. They are involved in a variety of biological processes, including signal transduction, cell adhesion, DNA repair, recombination, transcription, RNA processing, disease resistance, apoptosis, and the immune responses. This evolutionarily conserved protein domain is a unique structural motif consisting of 2-45 leucine rich repeats that contain the consensus sequence $LxxLxLXX^N/cxL$, where x can be any amino acid and L positions can be occupied by valine, isoleucine, and phenylalanine⁶⁰. Specifically, LRRs are short protein modules characterized by a periodic distribution of hydrophobic amino acids, especially leucine residues, separated by more hydrophilic residues. Early consensus sequences compiled from

LRR containing proteins containing leucine or other aliphatic residues at positions 2,5,7,12,16,21,24, and asparagine, cysteine, or threonine at position 10⁵⁹ demonstrated that most proteins almost exclusively contain asparagine at position 10, but some have exclusively cysteines at this position. Additional conserved amino acid residues are also found in LRR proteins at varying positions. These conserved residues are mostly aliphatic and aromatic amino acids, sometimes glycines and prolines, but seldom other amino acids⁵⁹. In addition, hydrophobic consensus residues in the carboxy-terminal parts of the repeats are commonly spaced by 3, 4, or 7 residues⁵⁹.

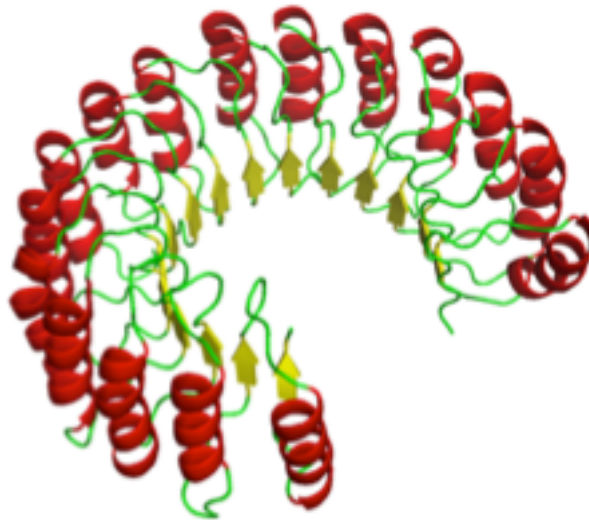


Figure 1.4: Evolutionarily Conserved Leucine Rich Repeat. Crystal structure depicts the secondary structure of porcine ribonuclease inhibitor, the first LRR to be structurally characterized. Crystal structure demonstrates the conserved structure of the LRR, featuring a horseshoe shaped tertiary structure with β -strands lining the concave surface and α -helices on the convex face.

LRRs were first discovered in leucine-rich α 2-glycoprotein, a protein of unknown function from human serum⁶⁵, with the porcine ribonuclease inhibitor (RI) LRR being the first to be sequenced (**Figure 1.4**). In the case of the porcine RI, a cytoplasmic protein that inhibits ribonucleases from the pancreatic superfamily by binding very tightly to an extensive surface area of ribonuclease containing its catalytic site, the LRR domain consists of 15 alternating LRRs that correspond to β - α structural units, consisting of short β -strands and an α -helix approximately parallel to each other⁶⁶.

The structural units are arranged so that all the β -strands and the helices are parallel to a common axis, resulting in a nonglobular horseshoe-shaped, molecule with a curved parallel β -sheet lining the inner circumference of the horseshoe, and helices flanking its outer circumference. Furthermore, regardless of the LRR residue sequence motif length, all LRR domains structurally adopt a horseshoe shape, with the concave face consisting of parallel β -strands and the convex face that is typically occupied by helices⁶⁴. This is readily observed from the very first LRR containing protein to be sequenced, the porcine ribonuclease inhibitor⁶⁷, as well as recent computational algorithms such as LRR predictor that provides insights into the diversification of LRR domains and a robust support for structure informed analysis of LRRs particularly in immune receptors⁶⁸.

LRRs are found in functionally and evolutionarily diverse proteins, from viruses, to bacteria, archaea, and eukaryotes (**Figure 1.5**). All LRR containing proteins appear to be involved in protein-protein interactions, and a vast majority of them partake in signal transduction pathways. Given the nonglobular structure of LRRs, the area available for interaction with smaller globular proteins is significantly increased,

and therefore facilitates more interactions. In addition, the exposed surface of the parallel β -sheets could also aid in protein binding. Though parallel β -sheets occur more frequently in the interior of proteins, where helices or other parallel β -sheets pack against them, in the case of LRR proteins, ligand interactions can substitute for such packing interactions. The specificity of LRR containing proteins with regards to protein-protein interactions and signal transduction can possibly be attributed to the composition of non-consensus residues and may also be influenced the lengths of the repeats and the flanking domains. This owns directly to the evolution of these proteins. The variety of non-consensus residues found in LRR domains lend to the need to characterize LRR proteins into superfamilies.

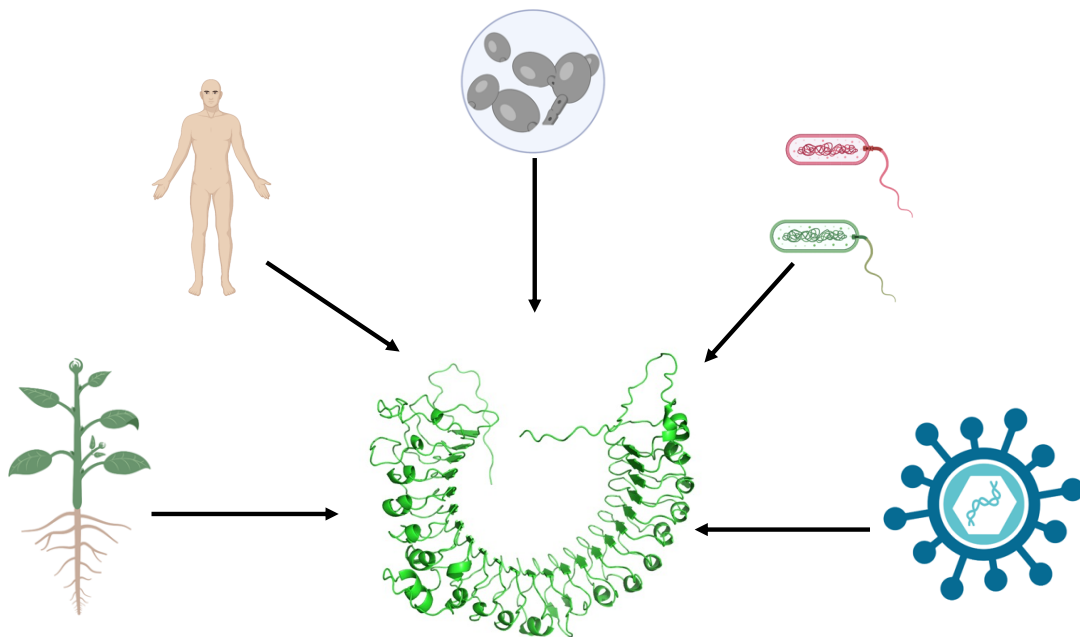


Figure 1.5: The juxtaposition of leucine rich repeat domains across Kingdoms.
The leucine rich repeat (LRR) domain is found in pattern recognition receptors in plants, bacteria, fungi, humans, and viruses.

1.4.1 Leucine Rich Repeat Protein Families

The continuously expanding leucine rich repeat (LRR) superfamily includes intracellular, extracellular and membrane-attached proteins characterized by a common modular architecture especially suited to favor protein-protein interactions. Seven classes of LRR proteins have been identified and are further categorized into subfamilies. Subfamilies are defined as Typical, Ribonuclease inhibitor (RI-like), Cysteine containing (CC), Plant Specific (PS), SD22-like, *Treponema pallidum* and Bacterial⁶⁹. Subfamilies differ in the length of the amino acid residues in the consensus sequence as well as cellular location⁷⁰⁻⁷⁷. A representation of LRR subfamilies and some of their characteristics can be found in Table 1 below.

Table 1.1: Subfamilies of LRR proteins.

LRR Subfamily	Typical LRR Length (range)	Organism of Origin	Cellular Location
RI-like	28-29 (28-29)	Animals	Intracellular
SDS22-like	22 (21-23)	Animals, Fungi	Intracellular
Cysteine Containing	26 (25-27)	Animals, Plants, Fungi	Intracellular
Bacterial	20 (20-22)	Gram-negative bacteria, Animals, Fungi	Extracellular
Typical	24 (20-27)		Extracellular
Plant Specific	24 (23-25)	Plants, primary eukaryotes	Extracellular
TpLRR	23 (23-25)	Bacteria	Extracellular

LRR classification into subfamilies has demonstrated that repeats from different subfamilies never occur simultaneously in the same protein and suggest that they have evolved independently. Subfamily classification along with structural insights have also highlighted important flanking regions of the domain. Particularly, in a typical LRR structure, the hydrophobic core would be exposed to solvent at the

ends, denoting that most LRR proteins contain flanking regions that are an integral part of the domain. C-terminal flanking motifs have been recognized in several LRR proteins and is termed the LRR cap⁷⁸. Hydrophilic N-terminal caps have also been identified in LRRs and have been predicted to function in metal ion binding as well as cellular invasion⁷³.

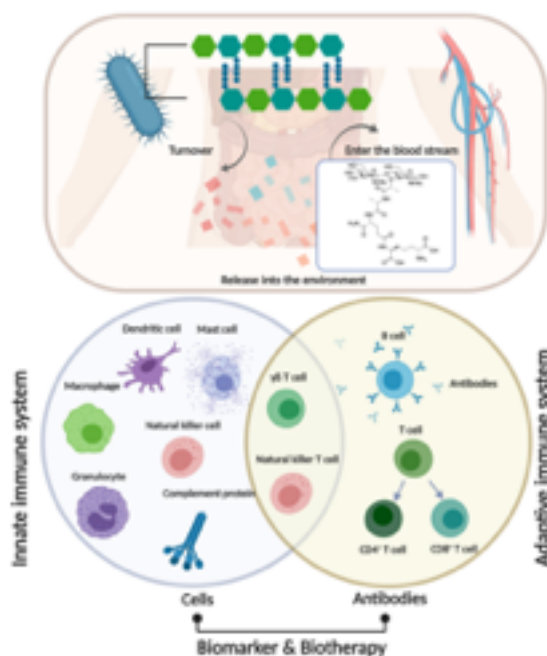


Figure 1.6: The interaction between bacterial cell wall fragments and the human immune system. PG turnover and subsequent fragment release to the environment; non-septic PG fragments appear to enter the bloodstream. The innate immune system response to potential PG antigen is the first line of defense against infection. Many of the cells in the innate immune system (such as dendritic cells, macrophages, mast cells) produce cytokines or interact with other cells directly to activate the adaptive immune system. $\gamma\delta$ T cells and Nature Killer cells are lymphocytes without antigen specificity. Therefore, they are considered to be innate cells with some similarities to effector lymphocytes. The adaptive immune system is based on clonal selection of lymphocytes with antigen receptors (B cell receptors and T cell receptors)⁸³ and recent studies suggest that antibodies for specific PG fragment exist. A more detailed understanding of PG related immune response provides new opportunities for improving immunotherapy for autoimmune diseases.

1.5 *Candida albicans*

C. albicans is a dimorphic fungus that is part of the commensal microbial flora in many healthy individuals⁷⁹⁻⁸¹. As a normal resident of the human body, *C. albicans*

typically coexists with the human host in a symbiotic manner and colonizes several niches in the skin, gastrointestinal and urogenital tracts in almost all healthy individuals⁸². Each site of occupancy delivers a different environment for growth and maintenance of these organisms, yet disruption of such environment leads to similar infectious outputs. The ability of *C. albicans* to occupy multiple anatomical sites both in a commensal and pathogenic state is largely due to multiple distinct regulatory mechanisms upon receiving environmental cues. The ability to thrive in multiple anatomical sites requires a high level of metabolic adaptivity of the species. *C. albicans* must contend with mechanical barriers, biochemical, chemical, and physical antagonist, microbial competition, and the innate and adaptive immune system of the human host⁸³. The most intrusive skill of *C. albicans* is its versatility to strive in host niches that differ dramatically in their environmental conditions, particularly with regards to pH, nutrient availability, O₂ and CO₂ levels, and the presence of immune cells⁸⁴.

Another important adaptability that is now under heavy research is the survivability of *C. albicans* in environments that encompass other microbial species, particularly bacteria. Under most in vivo situations, *C. albicans* will encounter other members of the natural human microbiota and/or coinfecting pathogens. As such, the organism must not only cope with host defense mechanisms, but also compete with other microorganisms for host niches, adhesion sites, nutrients and must deal with toxins and metabolic byproducts of its neighbors to successfully colonize and survive within the human host. As a commensal, *C. albicans* colonizes niches that are co-colonized by a wide range of other microbes forming the natural microbiome of the human host. As such, interactions between *C. albicans* and commensal bacteria have

evolved during the evolution of the human microbiota. Interactions between *C. albicans* and other microbes in the human microbiome are multifaceted and can be mutualistic as well as competitive. These interactions can occur via direct contact of cells, the secretion of signaling molecules or toxins, competition for nutrients/metabolites, or simply via alterations of localized environments in a beneficial or detrimental way for one or all interacting partners^{85, 86, 87}.

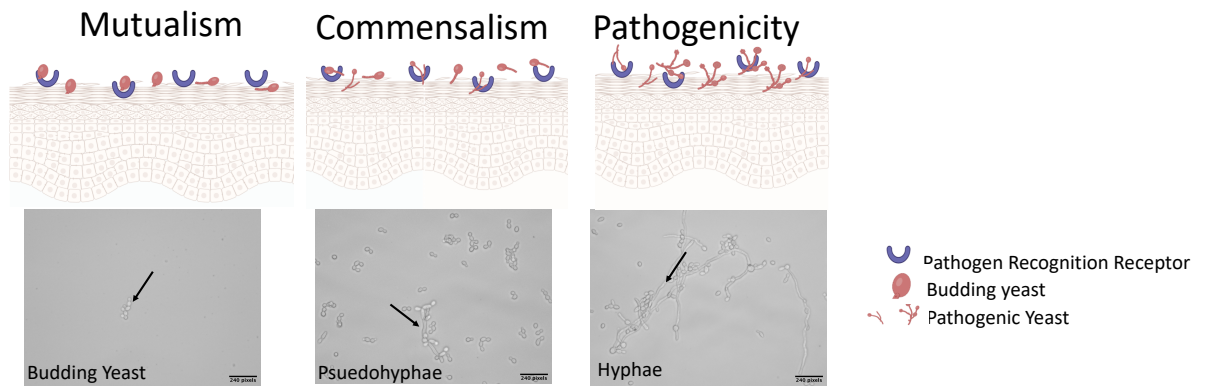


Figure 1.7: The Morphological growth forms of *Candida albicans*. *Candida albicans* growth forms are associated with pathogenicity. Under budding growth, cells are typically commensal. The morphological transition to pseudohyphae/ hyphae lends the fungi the ability to penetrate human epithelial cells and cause disseminated infections.

Rather than planktonic or single-species growth, the most common occurrence of *C. albicans* in nature are in polymicrobial multispecies communities. To that end, 4-8% of all *Candida* associated bloodstream infections involve more than one *Candida spp*^{88, 89}. Furthermore, it was estimated that greater than 20% of *C. albicans* bloodstream infections also have bacteria. For instance, it has been documented that the most common co-isolated species are *Staphylococcus epidermis*, *Enterococcus*

spp., and *Staphylococcus aureus*. Not surprisingly, to survive bacterial attacks or gain beneficial effects from these coinfections, *C. albicans* must sense and communicate with its neighbors. The dynamic between fungal and bacterial interactions is one of necessity to elucidate.

Perhaps one of the most important implications of bacterial-fungal interactions is the pathogenicity that ensues when *C. albicans* senses and detects bacterial peptidoglycan. As previously mentioned, *C. albicans* is capable of altering its morphology from that of a budding yeast to filamentous state (hyphae/pseudohyphae) in response to niche disruption via immune incompetence and/or environmental changes⁹⁰ (**Figure 1.7**). An important and still developing aspect of niche disruption that leads to pathogenicity for this organism, is an encounter with bacterial peptidoglycan in localized environment. *C. albicans* can morph into true hyphae in the presence of certain bacterial peptidoglycan fragments (**Figure 1.8**).

1.5.1 Candida albicans Hyphae and Pseudohyphae

By definition, hyphae or germ tubes are long tube-like filaments with completely parallel sides and the absence of constrictions at the site of separation⁹¹. Contrastingly, pseudohyphae are morphologically distinguishable from hyphae because they have constrictions at the sites of septation and are wider than hyphae. The morphological plasticity of *C. albicans* is a direct virulence determinant, as the hyphal growth form occupies key roles in infection processes. It is hyphal forms that allow *C. albicans* to invade epithelial and endothelial cells during mucosal infections. In addition, access to the bloodstream to establish candidemia requires penetration of mucosal barriers. Several studies have demonstrated that the hyphal form is invasive, as biopsy samples from patients with mucosal infections show that only hyphal forms

1.6 Adenylate Cyclases

Adenylyl Cyclase also termed adenylate cyclase catalyzes the formation of the secondary messenger cyclic adenosine monophosphate (cAMP). cAMP is a universal secondary messenger in signal transduction based on G-protein coupled receptors (GPCR) in eukaryotes⁹⁵. This secondary messenger is responsible for amplifying stimuli received by cells, through the binding and regulation of kinases and ion channels, whose activity subsequently determine cellular responses to stimuli. It is this downstream effect of cellular responses that require the tight regulation of cAMP at the enzymatic level. The adenylyl cyclase framework is seen to function both as a discriminator for environmental signals and as a signal generator.

cAMP was first discovered by Rall et al., and has been a booming field in scientific research to elucidate the mechanisms or regulation of this intracellular concentration of this secondary messenger⁹⁶. A plethora of hormones and neurotransmitters can stimulate and inhibit the rate of cAMP synthesis via pathways that consist of three distinct types of plasma membrane associated proteins: hormone receptors, guanine nucleotide-binding regulatory proteins (G proteins), and adenylyl cyclase's⁹⁷. In its simplest mechanistic manner, binding of a hormone to a stimulatory receptor at the extracellular surface then triggers the activation of the signal transducing G protein, G_s , which then interacts with adenylyl cyclase at the intracellular face of the plasma membrane to stimulate the formation of cAMP⁹⁸. When stimulated, adenylate cyclases produce cAMP, which act through multiple intracellular signals to conduct a plethora of biochemical reactions necessary for the sustenance of life in many organisms. Adenylyl cyclase, being one of the first signal modulators intracellularly for cAMP made the receptor a particularly important enzyme to understand.

The first adenylyl cyclase was cloned from complementary DNA isolated from bovine brain and provided key insights into the structure of and characterization of other enzymes in the family⁹⁸. Data obtained from the first adenylyl cyclase deduced amino acid sequence residues divisible into alternating sets of hydrophobic and hydrophilic domains, with each of the two large hydrophobic domains appearing to contain transmembrane spans⁹⁸. In addition, the two large hydrophilic domains contain sequences that are homologous to single cytoplasmic domains of several guanylyl cyclases. This was the first structural insight into this family of enzymes and has since set the precedence of characterization of this class of enzymes. This information suggested that this enzyme family structure is reminiscent of those that have been proposed for several transporters and channels, due to the common motif of one or more sets of transmembrane spans, large cytoplasmic domains that separate multiple sets of transmembrane spans. Additionally, a striking topographical resemblance was observed between adenylyl cyclase and the P glycoprotein- the product of the multidrug resistance gene⁹⁹.

Since the analysis of the first adenylyl cyclase, there have been several efforts in the field of enzymology to further understand and classify this enzyme with respect to structure function relationships. This has led to the classification of this family of enzyme in various families and subfamilies. The adenylyl cyclase family of enzymes contains 9 enzymes, termed adenylyl cyclase 1-9 (AC1-9), with each member of the family responsible for specific regulatory properties and tissues localization. Thus, Adenylyl cyclases have a structural fingerprint.

1.7 *Candida. albicans* Cyr1p

A key signaling pathway for morphological regulation in *C. albicans* is the cAMP/protein kinase A (PKA) pathway, which is activated by the adenylyl cyclase Cyr1p. Cyr1p is the only adenylyl cyclase present in *C. albicans* and is encoded by the gene caCDC35. The 189.4 kDa protein has a domain structure typical of fungal adenylyl cyclases in addition to mammalian isoforms around the catalytic core. In contrast to mammalian adenylyl cyclases, the fungal isoforms appear to be regulated by Ras through the interaction of a small GTP binding protein with a leucine rich repeat domain in the central region of the adenylyl cyclase.

Previous studies have demonstrated that Cyr1p is indispensable for the pathogenesis of *C. albicans* cells. Furthermore, *C. albicans* cells deleted for both alleles of Cyr1p are viable but grow approximately 2.5-fold slower than wildtype cells¹⁰⁰. Deletion of CaCD35, the gene encoding Cyr1p completely abolishes detectable levels of intracellular cAMP, reverberating that this is the only enzyme capable of producing cAMP in *C. albicans* cells. While Cyr1p mutant cells are viable, meaning that cAMP is not a requirement for vegetative growth, *C. albicans* cells lacking *cyr1p* do not form hyphae, but can be rescued in the presence of endogenous cAMP and subsequently produce hyphae.

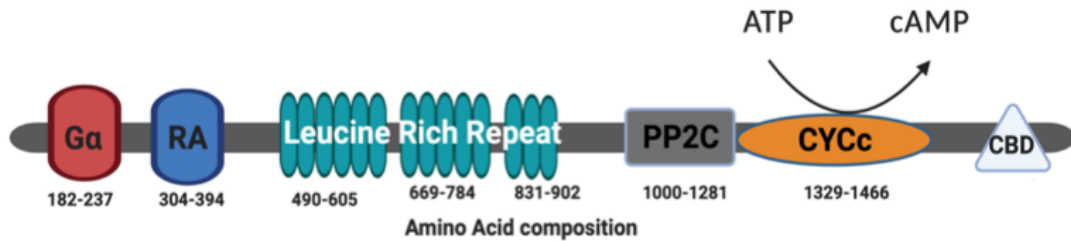


Figure 1.9: The adenylate cyclase Cyr1p from the human commensal *Candida albicans*. From N to C terminus, this receptor consists of a G α domain, a ras associating domain (RA), 14 Leucine Rich Repeats, a proteinphosphatase 2C (PP2C) domain, a catalytic cyclase (CYC) domain, and a C-terminal catalytic binding domain (CBD).

In the early 2000s, it was thought that Cyr1p may be involved directly in signal sensing. Klengel et al. reported that the catalytic domain of Cyr1p behaved as a CO₂ sensor and mediated CO₂ induced filamentous growth, while Hogan et al. reported that a sensory role was suggested for quorum sensing molecules¹⁰⁰. While these findings made major headway in the role of Cyr1p and the morphological regulation of *C. albicans*, the molecular mechanism of signal sensing remained to be elucidated. The ability of Cyr1p to distinguish different stimuli or sense and integrate multiple ones is owed to its several highly conserved domains. One such domain, and pertinent to this dissertation, is the aforementioned LRR domain, common in many innate immune receptors as discussed above.

Several studies have characterized the adenylate cyclase from *S. cerevisiae* to which the *C. albicans* adenylate cyclase shares 42.80% homology^{101, 102}. Data obtained from the *S. cerevisiae* adenylate cyclase has provided much insight into the nature of this protein and have demonstrated the importance of the adenylate cyclase in yeast¹⁰³⁻¹⁰⁶. Elegant work by Wang and coworkers demonstrated that this domain is able to

bind PG fragments¹⁰⁷. Though it was long determined that serum was the most potent activator of the morphological transition from budding yeast to hyphal yeast⁹⁰, the active constituent in serum remained unknown. Wang and co-workers discovered that bacterial peptidoglycan fragments, specifically muramyl-dipeptides (MDPs) in serum (Figure 1), was the causative agent of high-inducing hyphal activity¹⁰⁷. Using biotinylated MDP enrichment assays, data were obtained that demonstrated the association between Cyr1p's LRR and MDP, but direct binding and analytical characterization of this interaction remained unknown. To quantitatively and molecularly characterize this interaction, our lab has successfully expressed and purified an MBP fusion construct of the Cyr1p LRR domain and demonstrated via a sensitive, surface plasmon resonance assay (SPR) that the LRR binds diverse PG fragments with high affinity¹⁰⁵. Briefly, our lab was able to prove that Cyr1p-LRR binds to muramyl tripeptide (MTP) with a K_d of 176 ± 68 nM, and through competition assay demonstrate that binding is strong and specific¹⁰⁵.

1.8 Dissertation Overview

Bacterial-fungal crosstalk in the microbiome are critical interactions for the progression of human health and disease states. Incorrect communication between commensal microbes in the microbiome oftentimes leads to the onset of disease characteristics. Despite the recent outburst of scientific data suggesting this, there is still a lack of basic molecular understanding as to how these microbes sense and detect one another. My dissertation aimed at honing in on the crosstalk between bacterial and fungal components of the microbiome, through elucidating molecular interactions stemming from bacterial peptidoglycan. Particularly, the major goal of my dissertation is to characterize the LRR domain of the adenylate cyclase Cyr1p, as this domain is

the key molecular integrator of bacterial peptidoglycan sensing, and ensuing pathogenicity of the *C. albicans*. By characterizing this receptor, we can begin to gather a comprehensive scope of ligands that make *C. albicans* susceptible to pathogenicity. Once this information is gathered, high throughput inhibitor screens can ensue, that can be used as leads for new antifungals. Chapter 2 details the expression and biochemical classification of the Cyr1p-LRR domain as a peripheral membrane protein. Chapter 3 demonstrates the ability of different bacterial peptidoglycan fragments to elicit hyphal growth at varying timepoints and consistencies. Chapter 4 uncovers transcriptional anomalies in the regulation of hypha specific genes under hyphal induction conditions in response to various bacterial peptidoglycan fragments. Overall, my dissertation has provided new insights into the LRR domain of Cyr1p and demonstrates the differential activation of hyphae growth in wildtype *C. albicans* cells stimulated with various bacterial peptidoglycan fragments. Additionally, I demonstrate that hyphal induction does not correlate with the upregulation of hyphae specific genes when *C. albicans* cells are stimulated with bacterial peptidoglycan fragments. These data are interesting, and mimic observations by Naseem et al¹⁰⁸.

REFERENCES

1. Shaw, A. E.; Hughes, J.; Gu, Q.; Behdenna, A.; Singer, J. B.; Dennis, T.; Orton, R. J.; Varela, M.; Gifford, R. J.; Wilson, S. J.; Palmarini, M., Fundamental properties of the mammalian innate immune system revealed by multispecies comparison of type I interferon responses. *PLOS Biology* **2017**, *15* (12), e2004086.
2. Flajnik, M. F.; Kasahara, M., Origin and evolution of the adaptive immune system: genetic events and selective pressures. *Nat Rev Genet* **2010**, *11* (1), 47-59.
3. Kumar, H.; Kawai, T.; Akira, S., Pathogen recognition by the innate immune system. *Int Rev Immunol* **2011**, *30* (1), 16-34.
4. Lemaitre, B.; Nicolas, E.; Michaut, L.; Reichhart, J.-M.; Hoffmann, J. A., The Dorsoventral Regulatory Gene Cassette *spätzle*/Toll/cactus Controls the Potent Antifungal Response in *Drosophila* Adults. *Cell* **1996**, *86* (6), 973-983.
5. Kawasaki, T.; Kawai, T., Toll-like receptor signaling pathways. *Frontiers in immunology* **2014**, 461.
6. El-Zayat, S. R.; Sibaii, H.; Mannaa, F. A., Toll-like receptors activation, signaling, and targeting: an overview. *Bulletin of the National Research Centre* **2019**, *43* (1), 187.
7. Franchi, L.; Warner, N.; Viani, K.; Nuñez, G., Function of Nod-like receptors in microbial recognition and host defense. *Immunological reviews* **2009**, *227* (1), 106-128.
8. Leidy, J., *A flora and fauna within living animals*. 1853.
9. Farré-Maduell, E.; Casals-Pascual, C., The origins of gut microbiome research in Europe: From Escherich to Nissle. *Human Microbiome Journal* **2019**, *14*, 100065.
10. Escherich, T., *Die Darmbakterien des Säuglings und ihre Beziehungen zur Physiologie der Verdauung*. Enke: Stuttgart, 1886.
11. Turnbaugh, P. J.; Ley, R. E.; Hamady, M.; Fraser-Liggett, C. M.; Knight, R.; Gordon, J. I., The human microbiome project. *Nature* **2007**, *449* (7164), 804-810.
12. Altveş, S.; Yildiz, H. K.; Vural, H. C., Interaction of the microbiota with the human body in health and diseases. *Biosci Microbiota Food Health* **2020**, *39* (2), 23-32.
13. Moyes, D. L.; Naglik, J. R., The mycobiome: influencing IBD severity. *Cell Host Microbe* **2012**, *11* (6), 551-2.
14. Cui, L.; Morris, A.; Ghedin, E., The human mycobiome in health and disease. *Genome Medicine* **2013**, *5* (7), 63.
15. Ghannoum, M. A.; Jurevic, R. J.; Mukherjee, P. K.; Cui, F.; Sikaroodi, M.; Naqvi, A.; Gillevet, P. M., Characterization of the Oral Fungal Microbiome (Mycobiome) in Healthy Individuals. *PLOS Pathogens* **2010**, *6* (1), e1000713.

16. Chen, Y.; Chen, Z.; Guo, R.; Chen, N.; Lu, H.; Huang, S.; Wang, J.; Li, L., Correlation between gastrointestinal fungi and varying degrees of chronic hepatitis B virus infection. *Diagn Microbiol Infect Dis* **2011**, *70* (4), 492-8.
17. Nelson, A.; De Soyza, A.; Bourke, S. J.; Perry, J. D.; Cummings, S. P., Assessment of sample handling practices on microbial activity in sputum samples from patients with cystic fibrosis. *Lett Appl Microbiol* **2010**, *51* (3), 272-7.
18. Willger, S. D.; Grim, S. L.; Dolben, E. L.; Shipunova, A.; Hampton, T. H.; Morrison, H. G.; Filkins, L. M.; O'Toole, G. A.; Moulton, L. A.; Ashare, A.; Sogin, M. L.; Hogan, D. A., Characterization and quantification of the fungal microbiome in serial samples from individuals with cystic fibrosis. *Microbiome* **2014**, *2* (1), 40.
19. Ott, S. J.; Kühbacher, T.; Musfeldt, M.; Rosenstiel, P.; Hellmig, S.; Rehman, A.; Drews, O.; Weichert, W.; Timmis, K. N.; Schreiber, S., Fungi and inflammatory bowel diseases: Alterations of composition and diversity. *Scand J Gastroenterol* **2008**, *43* (7), 831-41.
20. Crump, G. M.; Zhou, J.; Mashayekh, S.; Grimes, C. L., Revisiting peptidoglycan sensing: interactions with host immunity and beyond. *Chemical Communications* **2020**, *56* (87), 13313-13322.
21. Medzhitov, R.; Janeway, C. A., Innate immunity: the virtues of a nonclonal system of recognition. *Cell* **1997**, *91* (3), 295-298.
22. Vollmer, W.; Bertsche, U., Murein (peptidoglycan) structure, architecture and biosynthesis in *Escherichia coli*. *Biochim Biophys Acta* **2008**, *1778* (9), 1714-34.
23. Kato, K.; Umemoto, T.; Sagawa, H.; Kotani, S., Lanthionine as an essential constituent of cell wall peptidoglycan of *Fusobacterium nucleatum*. *Current Microbiology* **1979**, *3* (3), 147-151.
24. Barnard, M. R.; Holt, S. C., Isolation and characterization of the peptidoglycans from selected gram-positive and gram-negative periodontal pathogens. *Can J Microbiol* **1985**, *31* (2), 154-60.
25. Jürgen, U. J.; Meissner, J.; Reichenbach, H.; Weckesser, J., l-ornithine containing peptidoglycan-polysaccharide complex from the cell wall of the gliding bacterium *Herpetosiphon aurantiacus*. *FEMS Microbiology Letters* **1989**, *60* (3), 247-250.
26. Groth, I.; Schumann, P.; Weiss, N.; Schuetze, B.; Augsten, K.; Stackebrandt, E., *Ornithinimicrobium humiphilum* gen. nov., sp. nov., a novel soil actinomycete with L-ornithine in the peptidoglycan. *Int J Syst Evol Microbiol* **2001**, *51* (Pt 1), 81-87.
27. Braun, V.; Rehn, K., Chemical characterization, spatial distribution and function of a lipoprotein (murein-lipoprotein) of the *E. coli* cell wall. The specific effect of trypsin on the membrane structure. *Eur J Biochem* **1969**, *10* (3), 426-38.
28. Braun, V.; Sieglin, U., The covalent murein-lipoprotein structure of the *Escherichia coli* cell wall. The attachment site of the lipoprotein on the murein. *Eur J Biochem* **1970**, *13* (2), 336-46.

29. Marraffini, L. A.; Dedent, A. C.; Schneewind, O., Sortases and the art of anchoring proteins to the envelopes of gram-positive bacteria. *Microbiol Mol Biol Rev* **2006**, *70* (1), 192-221.
30. Girardin, S. E.; Boneca, I. G.; Carneiro, L. A.; Antignac, A.; Jéhanno, M.; Viala, J.; Tedin, K.; Taha, M.-K.; Labigne, A.; Zähringer, U., Nod1 detects a unique muropeptide from gram-negative bacterial peptidoglycan. *Science* **2003**, *300* (5625), 1584-1587.
31. Höltje, J.-V.; Tuomanen, E. I., The murein hydrolases of *Escherichia coli*: properties, functions and impact on the course of infections in vivo. *Microbiology* **1991**, *137* (3), 441-454.
32. Silhavy, T. J.; Kahne, D.; Walker, S., The bacterial cell envelope. *Cold Spring Harbor perspectives in biology* **2010**, *2* (5), a000414.
33. Okuda, S.; Sherman, D. J.; Silhavy, T. J.; Ruiz, N.; Kahne, D., Lipopolysaccharide transport and assembly at the outer membrane: the PEZ model. *Nature Reviews Microbiology* **2016**, *14* (6), 337-345.
34. Janeway Jr, C. A.; Medzhitov, R., Innate immune recognition. *Annual review of immunology* **2002**, *20* (1), 197-216.
35. Arthur, M.; Depardieu, F.; Molinas, C.; Reynolds, P.; Courvalin, P., The vanZ gene of Tn1546 from *enterococcus faecium* BM4147 confers resistance to teicoplanin. *Gene* **1995**, *154* (1), 87-92.
36. Bugg, T. D.; Wright, G. D.; Dutka-Malen, S.; Arthur, M.; Courvalin, P.; Walsh, C. T., Molecular basis for vancomycin resistance in *Enterococcus faecium* BM4147: biosynthesis of a depsipeptide peptidoglycan precursor by vancomycin resistance proteins VanH and VanA. *Biochemistry* **1991**, *30* (43), 10408-10415.
37. Mayer, C.; Kluj, R. M.; Muehleck, M.; Walter, A.; Unsleber, S.; Hottmann, I.; Borisova, M., Bacteria's different ways to recycle their own cell wall. *International Journal of Medical Microbiology* **2019**, *309* (7), 151326.
38. Ursell, L. K.; Metcalf, J. L.; Parfrey, L. W.; Knight, R., Defining the human microbiome. *Nutr Rev* **2012**, *70 Suppl 1* (Suppl 1), S38-S44.
39. Jutras, B. L.; Lochhead, R. B.; Kloos, Z. A.; Biboy, J.; Strle, K.; Booth, C. J.; Govers, S. K.; Gray, J.; Schumann, P.; Vollmer, W., *Borrelia burgdorferi* peptidoglycan is a persistent antigen in patients with Lyme arthritis. *Proceedings of the National Academy of Sciences* **2019**, *116* (27), 13498-13507.
40. Boothby, D.; Daneo-Moore, L.; Higgins, M. L.; Coyette, J.; Shockman, G. D., Turnover of bacterial cell wall peptidoglycans. *Journal of Biological Chemistry* **1973**, *248* (6), 2161-2169.
41. Park, J. T.; Uehara, T., How bacteria consume their own exoskeletons (turnover and recycling of cell wall peptidoglycan). *Microbiology and Molecular Biology Reviews* **2008**, *72* (2), 211-227.
42. McDonald, C.; Inohara, N.; Nuñez, G., Peptidoglycan signaling in innate immunity and inflammatory disease. *Journal of Biological Chemistry* **2005**, *280* (21), 20177-20180.

43. Irazoki, O.; Hernandez, S. B.; Cava, F., Peptidoglycan muropeptides: release, perception, and functions as signaling molecules. *Frontiers in microbiology* **2019**, *10*, 500.
44. Borisova, M.; Gaupp, R.; Duckworth, A.; Schneider, A.; Dalügge, D.; Mühleck, M.; Deubel, D.; Unsleber, S.; Yu, W.; Muth, G., Peptidoglycan recycling in Gram-positive bacteria is crucial for survival in stationary phase. *MBio* **2016**, *7* (5), e00923-16.
45. Mackey, D.; McFall, A. J., MAMPs and MIMPs: proposed classifications for inducers of innate immunity. *Molecular microbiology* **2006**, *61* (6), 1365-1371.
46. Wolf, A. J.; Underhill, D. M., Peptidoglycan recognition by the innate immune system. *Nature Reviews Immunology* **2018**, *18* (4), 243-254.
47. Mogensen, T. H., Pathogen recognition and inflammatory signaling in innate immune defenses. *Clinical microbiology reviews* **2009**, *22* (2), 240-273.
48. Brubaker, S. W.; Bonham, K. S.; Zanoni, I.; Kagan, J. C., Innate immune pattern recognition: a cell biological perspective. *Annual review of immunology* **2015**, *33*, 257.
49. Stokes, B. A.; Yadav, S.; Shokal, U.; Smith, L.; Eleftherianos, I., Bacterial and fungal pattern recognition receptors in homologous innate signaling pathways of insects and mammals. *Frontiers in microbiology* **2015**, *6*, 19.
50. Iwaki, D.; Mitsuzawa, H.; Murakami, S.; Sano, H.; Konishi, M.; Akino, T.; Kuroki, Y., The extracellular toll-like receptor 2 domain directly binds peptidoglycan derived from *Staphylococcus aureus*. *Journal of Biological Chemistry* **2002**, *277* (27), 24315-24320.
51. Boyle, J. P.; Parkhouse, R.; Monie, T. P., Insights into the molecular basis of the NOD2 signalling pathway. *Open biology* **2014**, *4* (12), 140178.
52. Lauro, M. L.; D'Ambrosio, E. A.; Bahnson, B. J.; Grimes, C. L., Molecular recognition of muramyl dipeptide occurs in the leucine-rich repeat domain of Nod2. *ACS infectious diseases* **2017**, *3* (4), 264-270.
53. Grimes, C. L.; Ariyananda Lde, Z.; Melnyk, J. E.; O'Shea, E. K., The innate immune protein Nod2 binds directly to MDP, a bacterial cell wall fragment. *J Am Chem Soc* **2012**, *134* (33), 13535-7.
54. Correa, R. G.; Milutinovic, S.; Reed, J. C., Roles of NOD1 (NLRC1) and NOD2 (NLRC2) in innate immunity and inflammatory diseases. *Bioscience reports* **2012**, *32* (6), 597-608.
55. Conforti-Andreoni, C.; Beretta, O.; Licandro, G.; Qian, H. L.; Urbano, M.; Vitulli, F.; Ricciardi-Castagnoli, P.; Mortellaro, A., Synergism of NOD2 and NLRP3 activators promotes a unique transcriptional profile in murine dendritic cells. *Journal of Leukocyte Biology* **2010**, *88* (6), 1207-1216.
56. Swanson, K. V.; Deng, M.; Ting, J. P. Y., The NLRP3 inflammasome: molecular activation and regulation to therapeutics. *Nature Reviews Immunology* **2019**, *19* (8), 477-489.
57. Wolf, A. J.; Reyes, C. N.; Liang, W.; Becker, C.; Shimada, K.; Wheeler, M. L.; Cho, H. C.; Popescu, N. I.; Coggeshall, K. M.; Arditi, M.; Underhill, D. M.,

- Hexokinase Is an Innate Immune Receptor for the Detection of Bacterial Peptidoglycan. *Cell* **2016**, *166* (3), 624-636.
58. Hajishengallis, G.; Lambris, J. D., Microbial manipulation of receptor crosstalk in innate immunity. *Nature Reviews Immunology* **2011**, *11* (3), 187-200.
59. Kobe, B.; Deisenhofer, J., The leucine-rich repeat: a versatile binding motif. *Trends in Biochemical Sciences* **1994**, *19* (10), 415-421.
60. Kobe, B.; Kajava, A. V., The leucine-rich repeat as a protein recognition motif. *Current Opinion in Structural Biology* **2001**, *11* (6), 725-732.
61. Malic, S.; Hill, K. E.; Ralphs, J. R.; Hayes, A.; Thomas, D. W.; Potts, A.; Williams, D. W., Characterization of *Candida albicans* infection of an in vitro oral epithelial model using confocal laser scanning microscopy. *Oral microbiology and immunology* **2007**, *22* (3), 188-194.
62. Shirtliff, M. E.; Peters, B. M.; Jabra-Rizk, M. A., Cross-kingdom interactions: *Candida albicans* and bacteria. *FEMS microbiology letters* **2009**, *299* (1), 1-8.
63. Rothberg, J. M.; Jacobs, J. R.; Goodman, C. S.; Artavanis-Tsakonas, S., slit: an extracellular protein necessary for development of midline glia and commissural axon pathways contains both EGF and LRR domains. *Genes & development* **1990**, *4* (12a), 2169-2187.
64. Ng, A.; Xavier, R. J., Leucine-rich repeat (LRR) proteins: integrators of pattern recognition and signaling in immunity. *Autophagy* **2011**, *7* (9), 1082-4.
65. Ohkura, H.; Yanagida, M., *S. pombe* gene *sds22+* essential for a midmitotic transition encodes a leucine-rich repeat protein that positively modulates protein phosphatase-1. *Cell* **1991**, *64* (1), 149-157.
66. Lee, F. S.; Vallee, B. L., Structure and Action of Mammalian Ribonuclease (Angiogenin) Inhibitor. In *Progress in Nucleic Acid Research and Molecular Biology*, Cohn, W. E.; Moldave, K., Eds. Academic Press: 1993; Vol. 44, pp 1-30.
67. Kobe, B.; Deisenhofer, J., Crystal structure of porcine ribonuclease inhibitor, a protein with leucine-rich repeats. *Nature* **1993**, *366* (6457), 751-756.
68. Martin, E. C.; Sukarta, O. C. A.; Spiridon, L.; Grigore, L. G.; Constantinescu, V.; Tacutu, R.; Goverse, A.; Petrescu, A. J., LRRpredictor-A New LRR Motif Detection Method for Irregular Motifs of Plant NLR Proteins Using an Ensemble of Classifiers. *Genes (Basel)* **2020**, *11* (3).
69. Kajava, A. V., Structural diversity of leucine-rich repeat proteins | Edited by F. Cohen. *Journal of Molecular Biology* **1998**, *277* (3), 519-527.
70. Price, S. R.; Evans, P. R.; Nagai, K., Crystal structure of the spliceosomal U2B'-U2A' protein complex bound to a fragment of U2 small nuclear RNA. *Nature* **1998**, *394* (6694), 645-650.
71. Hillig, R. C.; Renault, L.; Vetter, I. R.; Drell IV, T.; Wittinghofer, A.; Becker, J., The crystal structure of rnalp: a new fold for a GTPase-activating protein. *Molecular cell* **1999**, *3* (6), 781-791.
72. Zhang, H.; Seabra, M. C.; Deisenhofer, J., Crystal structure of Rab geranylgeranyltransferase at 2.0 Å resolution. *Structure* **2000**, *8* (3), 241-251.

73. Marino, M.; Braun, L.; Cossart, P.; Ghosh, P., Structure of the InlB leucine-rich repeats, a domain that triggers host cell invasion by the bacterial pathogen *L. monocytogenes*. *Molecular cell* **1999**, 4 (6), 1063-1072.
74. Wu, H.; Maciejewski, M. W.; Marintchev, A.; Benashski, S. E.; Mullen, G. P.; King, S. M., Solution structure of a dynein motor domain associated light chain. *Nature structural biology* **2000**, 7 (7), 575-579.
75. Schulman, B. A.; Carrano, A. C.; Jeffrey, P. D.; Bowen, Z.; Kinnucan, E. R.; Finnin, M. S.; Elledge, S. J.; Harper, J. W.; Pagano, M.; Pavletich, N. P., Insights into SCF ubiquitin ligases from the structure of the Skp1-Skp2 complex. *Nature* **2000**, 408 (6810), 381-386.
76. Liker, E.; Fernandez, E.; Izaurralde, E.; Conti, E., The structure of the mRNA export factor TAP reveals a cis arrangement of a non-canonical RNP domain and an LRR domain. *The EMBO journal* **2000**, 19 (21), 5587-5598.
77. Evdokimov, A. G.; Anderson, D. E.; Routzahn, K. M.; Waugh, D. S., Unusual molecular architecture of the *Yersinia pestis* cytotoxin YopM: a leucine-rich repeat protein with the shortest repeating unit. *Journal of molecular biology* **2001**, 312 (4), 807-821.
78. Ceulemans, H.; De Maeyer, M.; Stalmans, W.; Bollen, M., A capping domain for LRR protein interaction modules. *FEBS letters* **1999**, 456 (3), 349-351.
79. Morales, D. K.; Hogan, D. A., *Candida albicans* interactions with bacteria in the context of human health and disease. *PLoS pathogens* **2010**, 6 (4), e1000886.
80. Shing, S. R.; Ramos, A. R.; Patras, K. A.; Riestra, A. M.; McCabe, S.; Nizet, V.; Coady, A., The fungal pathogen *Candida albicans* promotes bladder colonization of group B streptococcus. *Frontiers in cellular and infection microbiology* **2020**, 9, 437.
81. Seed, P. C., The human mycobiome. *Cold Spring Harbor perspectives in medicine* **2015**, 5 (5), a019810.
82. Gilbert, J. A.; Blaser, M. J.; Caporaso, J. G.; Jansson, J. K.; Lynch, S. V.; Knight, R., Current understanding of the human microbiome. *Nature medicine* **2018**, 24 (4), 392-400.
83. Polke, M.; Hube, B.; Jacobsen, I. D., Chapter Three - *Candida* Survival Strategies. In *Advances in Applied Microbiology*, Sariaslani, S.; Gadd, G. M., Eds. Academic Press: 2015; Vol. 91, pp 139-235.
84. Calderone, R. A.; Clancy, C. J., *Candida and candidiasis*. American Society for Microbiology Press: 2011.
85. Lynch, A. S.; Robertson, G. T., Bacterial and fungal biofilm infections. *Annu Rev Med* **2008**, 59, 415-28.
86. Peleg, A. Y.; Hogan, D. A.; Mylonakis, E., Medically important bacterial-fungal interactions. *Nature Reviews Microbiology* **2010**, 8 (5), 340-349.
87. Wargo, M. J.; Hogan, D. A., Fungal-bacterial interactions: a mixed bag of mingling microbes. *Curr Opin Microbiol* **2006**, 9 (4), 359-64.

88. Bouza, E.; Burillo, A.; Muñoz, P.; Guinea, J.; Marín, M.; Rodríguez-Créixems, M., Mixed bloodstream infections involving bacteria and *Candida* spp. *Journal of Antimicrobial Chemotherapy* **2013**, *68* (8), 1881-1888.
89. Nace, H. L.; Horn, D.; Neofytos, D., Epidemiology and outcome of multiple-species candidemia at a tertiary care center between 2004 and 2007. *Diagnostic microbiology and infectious disease* **2009**, *64* (3), 289-294.
90. Limon, J. J.; Skalski, J. H.; Underhill, D. M., Commensal fungi in health and disease. *Cell host & microbe* **2017**, *22* (2), 156-165.
91. Sudbery, P. E., Growth of *Candida albicans* hyphae. *Nature Reviews Microbiology* **2011**, *9* (10), 737-748.
92. Scherwitz, C., Ultrastructure of human cutaneous candidosis. *Journal of Investigative Dermatology* **1982**, *78* (3), 200-205.
93. Lo, H.-J.; Köhler, J. R.; DiDomenico, B.; Loebenberg, D.; Cacciapuoti, A.; Fink, G. R., Nonfilamentous *C. albicans* mutants are avirulent. *Cell* **1997**, *90* (5), 939-949.
94. Hornby, J. M.; Jensen, E. C.; Lisec, A. D.; Tasto, J. J.; Jahnke, B.; Shoemaker, R.; Dussault, P.; Nickerson, K. W., Quorum sensing in the dimorphic fungus *Candida albicans* is mediated by farnesol. *Applied and environmental microbiology* **2001**, *67* (7), 2982-2992.
95. Hanson, M. A.; Stevens, R. C., Discovery of new GPCR biology: one receptor structure at a time. *Structure (London, England : 1993)* **2009**, *17* (1), 8-14.
96. Berthet, J.; Rall, T. W.; Sutherland, E. W., The relationship of epinephrine and glucagon to liver phosphorylase. IV. Effect of epinephrine and glucagon on the reactivation of phosphorylase in liver homogenates. *J Biol Chem* **1957**, *224* (1), 463-75.
97. Robinson, G. A.; Butcher, R. W.; Sutherland, E. W., Cyclic AMP. *Annual Review of Biochemistry* **1968**, *37* (1), 149-174.
98. Krupinski, J.; Coussen, F.; Bakalyar, H. A.; Tang, W.-J.; Feinstein, P. G.; Orth, K.; Slaughter, C.; Reed, R. R.; Gilman, A. G., Adenylyl Cyclase Amino Acid Sequence: Possible Channel- or Transporter-Like Structure. *Science* **1989**, *244* (4912), 1558-1564.
99. Gottesman, M. M.; Pastan, I., The multidrug transporter, a double-edged sword. *J Biol Chem* **1988**, *263* (25), 12163-6.
100. Rocha, C. R.; Schröppel, K.; H Marcus, D.; Marcil, A.; Dignard, D.; Taylor, B. N.; Thomas, D. Y.; Whiteway, M.; Leberer, E., Signaling through adenylyl cyclase is essential for hyphal growth and virulence in the pathogenic fungus *Candida albicans*. *Mol Biol Cell* **2001**, *12* (11), 3631-43.
101. Altschul, S. F.; Madden, T. L.; Schäffer, A. A.; Zhang, J.; Zhang, Z.; Miller, W.; Lipman, D. J., Gapped BLAST and PSI-BLAST: a new generation of protein database search programs. *Nucleic Acids Res* **1997**, *25* (17), 3389-402.
102. Altschul, S. F.; Wootton, J. C.; Gertz, E. M.; Agarwala, R.; Morgulis, A.; Schäffer, A. A.; Yu, Y. K., Protein database searches using compositionally adjusted substitution matrices. *Febs j* **2005**, *272* (20), 5101-9.

103. Zou, H.; Fang, H. M.; Zhu, Y.; Wang, Y., *Candida albicans* Cyr1, Cap1 and G-actin form a sensor/effector apparatus for activating cAMP synthesis in hyphal growth. *Molecular microbiology* **2010**, *75* (3), 579-591.
104. Bai, C.; Xu, X. L.; Wang, H. S.; Wang, Y. M.; Chan, F. Y.; Wang, Y., Characterization of a hyperactive Cyr1 mutant reveals new regulatory mechanisms for cellular cAMP levels in *Candida albicans*. *Molecular microbiology* **2011**, *82* (4), 879-893.
105. Burch, J. M.; Mashayekh, S.; Wykoff, D. D.; Grimes, C. L., Bacterial Derived Carbohydrates Bind Cyr1 and Trigger Hyphal Growth in *Candida albicans*. *ACS Infectious Diseases* **2018**, *4* (1), 53-58.
106. Fang, H. M.; Wang, Y., RA domain-mediated interaction of Cdc35 with Ras1 is essential for increasing cellular cAMP level for *Candida albicans* hyphal development. *Molecular microbiology* **2006**, *61* (2), 484-496.
107. Xu, X. L.; Lee, R. T.; Fang, H. M.; Wang, Y. M.; Li, R.; Zou, H.; Zhu, Y.; Wang, Y., Bacterial peptidoglycan triggers *Candida albicans* hyphal growth by directly activating the adenylyl cyclase Cyr1p. *Cell Host Microbe* **2008**, *4* (1), 28-39.
108. Naseem, S.; Araya, E.; Konopka, J. B., Hyphal growth in *Candida albicans* does not require induction of hyphal-specific gene expression. *Molecular Biology of the Cell* **2015**, *26* (6), 1174-1187.

Chapter 2

PURIFICATION AND CHARACTERIZATION OF A STABLE, MEMBRANE-ASSOCIATED PEPTIDOGLYCAN RESPONSIVE ADENYLATE CYCLASE LRR DOMAIN FROM HUMAN COMMENSAL CANDIDA ALBICANS

This chapter was adapted from the publications below. Further permissions related to the material excerpted should be directed to the designated journal. Reprint (adapted) with permission from the following publication:

Crump, G. M., et al. (2022). "Purification and Characterization of a Stable, Membrane-Associated Peptidoglycan Responsive Adenylate Cyclase LRR Domain from Human Commensal *Candida albicans*." Biochemistry.

2.1 Introduction

Leucine Rich Repeat (LRR) proteins provide an important structural framework for molecular interactions necessary for proper recognition in self vs non-self. They are especially important with regards to the molecular recognition and detection of pathogens and microbes in the human microbiome; a complex multi-kingdom microbial community that lives on and in the human body. This microbial community consists of various bacteria, fungi, and viruses¹. The ability to maintain human health is directly linked to a system of checks and balances that must occur between human and non-human cells in the microbiome². The ability to sense and

detect foreign entities makes the LRR domain a prime candidate to maintain proper symbiosis both in the human host through innate immunity, and through molecular interactions between coexisting species of the microbiome³.

The LRR protein domain is an evolutionarily conserved structural motif of 20-30 amino acids with a characteristic repetitive sequence rich in leucine residues⁴. LRR domains consist of 2-45 leucine rich repeats and structurally adopt a horseshoe shape, with the concave face consisting of parallel β -strands and the convex face that is typically occupied by helices⁵. LRRs contain the consensus sequence $LxxLxLXX^N/cxL$, where 'x' can be any amino acid and 'L' positions can be occupied by valine, isoleucine, and phenylalanine⁶. LRR proteins have been identified in viruses, bacteria, archaea, and eukaryotes. The juxtaposition between the various kingdoms that this domain is present in lies at the interface of innate immunity and protein-protein interactions. LRR containing proteins aid in innate immunity through the sensing of pathogen-associated molecular patterns (PAMPS), protein-protein interactions, and many others⁷.

The importance of the LRR domain and its diversity is readily observed in the polymorphic fungus *Candida albicans* (*C. albicans*), the most common fungal commensal in the human microbiome⁸. It is capable of colonizing multiple anatomical sites such as the mouth, skin, intestine, vagina, etc. The suitability to thrive in multiple anatomical sites with varying microbial niches, and metabolic factors, renders these fungi can produce a range of infections in the human host. *C. albicans* can disseminate from its localized environment and invade almost every internal organ, producing invasive life-threatening infections, particularly if disseminated in the blood stream⁹.

Whereas superficial skin infections pose no severe health complications, disseminated systemic infections known as Candida have a mortality rate exceeding 70%¹⁰.

The margin of commensalism and pathogenicity in *C. albicans* is a morphological transition from that of a budding yeast to an extended hyphal form, with budding being commensal and hyphal denoting pathogenicity and potential virulence. A major signal integrator for this morphological transition is the single adenylyl cyclase, Cyr1p. The fungal adenylyl cyclase Cyr1p, is a Class III adenylyl Cyclase (AC) and catalyzes the formation of the universal secondary messenger cyclic adenosine-3',5'-monophosphate (cAMP) from ATP¹¹ (**Figure 2.1**). Like yeast type ACs, Cyr1p has a multi-domain architecture not found in mammalian ACs. This 1690 amino acid receptor consists of a RAS- associating domain (RasA), Leucine Rich Repeat (LRR), domain, protein phosphatase type 2C catalytic domain (PP2Cc) and a Cyclase homology domain (CHD)¹² (**Figure 2.1**). Though this protein remains unclassified at large, previous studies have proven Cyr1p to be regulated by several strong hyphal inducing signals such as serum, carbon dioxide, and bacterial peptidoglycan^{13, 14}. Interestingly, Xue, et al., were the first to make the connection that Cyr1p contains the evolutionarily conserved LRR domain that is also found in the human innate receptors, NOD1 and NOD2¹⁴. Using biotin-streptavidin pull down assays, they were successful in demonstrating that the LRR domain of Cyr1p does in fact bind the synthetic bacterial peptidoglycan fragment muramyl dipeptide (MDP). In recent work, the team has gone on to characterize this phenotype in the presence of peptidoglycan targeting antibiotics in mouse models¹⁵.

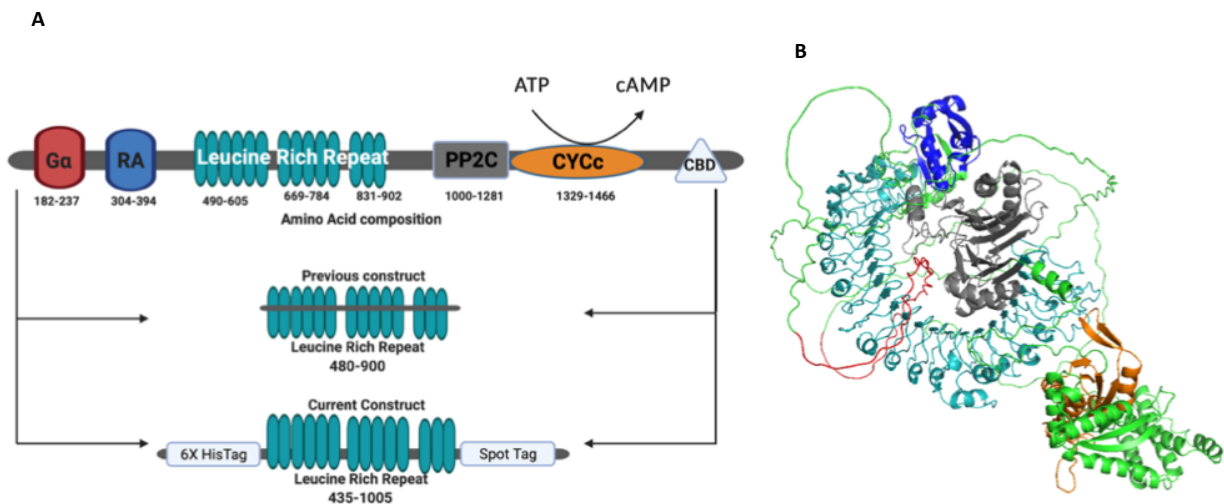


Figure 2.1: **A:** The adenylyl cyclase Cyr1p contains a $G\alpha$ domain, a Ras associating domain, 14 Leucine Rich Repeats (LRR), a Protein Phosphatase 2 domain, a guanylate cyclase domain, and a catalytic binding domain. Our newly designed expression vector for Cyr1p LR LRR domain contains residues from 435 up to the PP2C domain. The construct contains 14 repeats of the LRR domain and is expressed in *S. cerevisiae*. Our previous construct did not include all of the Leucine Rich Repeat. **B:** Tertiary structure prediction of the 1690 amino acid adenylyl cyclase by AlphaFold2. Model is depicted with respect to the LRR domain, red= $G\alpha$ domain, Blue= Ras association domain, Teal+ Leucine Rich Repeat domain, Grey= Protein Phosphatase 2C domain, Orange= Adenylyl/ guanylyl cyclase domain. All uncharacterized, or disordered domains are depicted in green.

Building on this work, we developed interest in quantifying the binding between recombinant Cyr1p and various bacterial derived carbohydrates. Taking inspiration from Xu et al., we recombinantly expressed the LRR domain of Cyr1p using an *E. coli* expression system, and conducted bioanalytical binding assays using a Surface Plasmon Resonance assay (SPR)¹⁶. The binding of recombinantly expressed Cyr1p-Maltose Binding Protein (MBP) to bacterial carbohydrates was successfully quantified as a nM binding event. However, the MBP-fusion proved limited in further characterization experiments due to its expression as aggregates in insoluble inclusion

bodies. This expression profile required a denaturation/renaturation purification scheme that proved inefficient and resulted in a highly unstable construct. Purified protein did not remain soluble in solution once cleaved from the MBP fusion tag, could not undergo freeze thaw cycles, and readily precipitated upon dialysis or buffer exchange. To circumvent these limitations, the recombinant LRR was redesigned here utilizing a biophysical and bioinformatics approach. Biophysical data obtained from a Kyte-Doolittle hydrophathy plots suggested several possible transmembrane helices ¹⁷. In addition, *C. albican*'s adenylate cyclase is 43% homologous to *Saccharomyces cerevisiae*'s (*S. cerevisiae*) adenylate cyclase, which is a peripheral membrane protein ¹⁸⁻²⁰. These parameters led us to hypothesize that Cyr1p may also be a membrane associated protein.

In this chapter we report detailed characterization of a more stable recombinantly expressed LRR domain that spans the entire region of the predicted leucine rich repeat domain using a new expression system with a smaller epitope tag. Inspiration for the amino acid sequences off the LRR was gathered from homology between the adenylate cyclases of four other *Candida* spp. The N terminus contains a His₃ tag, and the C-terminus contains a 1.4 kDa Spot-Tag, The novel Spot-Tag contains an inert 12-amino acid (PDRVRAVSHWSS) peptide-tag and spot-nanobodies that specifically bind to Spot-tagged proteins with high affinity ^{21, 22}. The newly designed recombinant LRR domain was found to be more stable than the previously expressed *E. coli* construct, localized to cellular membranes and retain the ability to bind bacterial peptidoglycan fragments.

2.2 Materials and Methods

Primers were purchased from Eurofins Genomics. Restriction endonucleases were purchased from New England Biolabs. Antibiotics were purchased from Gold Biotechnology. Bacterial expression hosts were purchased from Agilent Technologies, and yeast expression hosts were gifted to us from our collaborator Dr. Dennis Wykoff at Villanova University. Detergents were obtained from Anatrace, DNA molecular weight standards were obtained from New England Biolabs, Protein molecular weight markers were obtained from Bio-Rad, Spot Nanobody was purchased from Chromotek, and anti-llama nanobody from Bethyl Laboratories. All protease inhibitors were purchased from Roche Applied Sciences. All other chemicals were purchased from Sigma- Aldrich, unless otherwise specified. Graphs were generated using GraphPad Prism. All homology models were visualized using the PyMOL software, using a PDB file of the LRR generated for us graciously by Dr. Juan Perilla, utilizing the AlphaFold2 software.

2.2.1 Molecular cloning in *S. cerevisiae* expression host

Codon optimized plasmid containing the Cyr1-LRR domain (amino acid residues 435-1004) with an N-terminal His6 tag and a C-terminal Spot-Tag was synthesized by Genscript. The codon optimized LRR (amino acid residues 435-1004) was synthesized and cloned by Genscript into a pESC-URA expression vector utilizing the restriction sites EcoRI at the N terminus and NotI at the C-terminus, under the control of the GAL10 promoter. The plasmid was transformed into *Saccharomyces. Cerevisiae* cells EY1201 ((*leu2 trp1 ura3 prb1-1122 pep4-1 his3del::pGAL10::GAL4*) that were graciously gifted to us by from Dr. Dennis Wykoff at Villanova University. The Genscript synthesized plasmid encoding the

Cyr1p-LRR domain was transformed into *S. cerevisiae* cells using the lithium acetate (LiOAc) method^{23, 24}. Transformed cells were selected on -uracil synthetic dropout media.

2.2.2 Kyte-Doolittle Hydropathy Plots

Kyte-Doolittle hydropathy plots were generated using ExPASy to indicate potential transmembrane and surface regions of the LRR domain¹⁷. The hydropathy index was analyzed using 2 window positions. First, a window position of 9 amino acids was used to determine the potential for surface regions in the protein. In addition, a window position of 19 was used to determine possible transmembrane segments in the LRR. Hydropathy plots were generated using the linear weight variation model.

2.2.3 Expression of Cyr1-LRR domain in *S. cerevisiae*

A single colony was used to initiate culture by inoculating into 5mL of Synthetic Dropout-Uracil (SD-Ura) medium supplemented with 2% glucose at 30°C. Cells were harvested from the saturated overnight culture and resuspended in Yeast Basic Medium containing (0.67% yeast nitrogen base without amino acids, 0.087% - Uracil amino acid drop out mix, 60% (w/w) sodium lactate, 3% glycerol) and allowed to overcome the diauxic shift from glucose to lactate (approximately 2 days). Protein expression was induced at 30°C with sterile filtered galactose at a final concentration of 2% when cell culture reached an optical density of 0.8 at 600 nm. Cells were harvested at 3500 g for 30 minutes and the supernatant was discarded. Pellets were stored at -80°C until use.

2.2.4 Purification of Cyr1-LRR domain from *S. cerevisiae*

2.2.4.1 Cellular Lysis

A 1 L cell pellet was harvested at 3500 g and resuspended in ice cold lysis buffer (50 mM HEPES pH 7.4, 150 mM NaCl, 0.1 mM MgCl₂, 0.1 mM EGTA, 1 mM PMSF, 10% glycerol, and protease inhibitor cocktail tablet). Resuspended cells were transferred to 7 mL screw cap vials preloaded with 4.5 mL of acid washed glass beads. Cell lysis was performed by disruption with acid washed glass beads using an OMNI Bead Ruptor 12 for 10 cycles of 30 seconds each with intermittent cooling on ice for 1-minute intervals.

2.2.4.2 Membrane Isolation and Solubilization

Total cell lysate was ultracentrifuged at 505,000 g for 2 hours at 4°C to isolate membranes. Membrane pellets were resuspended in membrane solubilization buffer (50mM HEPES pH 7.4, 500mM NaCl, 0.1mM MgCl₂, 0.1mM EGTA, 1mM PMSF, 10% glycerol, and protease inhibitor cocktail tablet). For detergent solubilization, membrane pellets were first homogenized in membrane solubilization buffer, then detergents were added at levels greater than their critical micelle concentration (CMC) (Figure 3). For low CMC detergents DDM, C12E8, the final concentration was 1%. For higher CMC detergents OG, Fos-Choline 12, 16 and Fos-MEA-12, the final concentration was 2% (Figure 2). Membranes were solubilized for 2 hours at 4°C with end-over-end rotation. Insoluble material was removed via centrifugation at 505,000 g for 1 hour at 4 °C to remove unextracted membranes. An equal volume of lysate was used for the membrane isolation to examine the extraction efficiencies for the aforementioned detergents.

2.2.4.3 Purification of Cyr1p-LRR from Membranes

Detergent-solubilized membranes were clarified by ultracentrifugation at 505,000 g for 1 hour at 4 °C. The Spot-Cap affinity matrix was equilibrated in membrane solubilization buffer with 0.5% Fos-choline 16. Solubilized protein was incubated with the resin at 4 °C overnight. Resin was then washed with 4 CVs of membrane solubilization buffer with 0.5% Fos-Choline, followed by washing twice with 5 CVs of wash buffer (50 mM HEPES pH 7.4, 1 M NaCl, 0.1 mM MgCl₂, 0.1 mM EGTA, 1 mM PMSF, 10% glycerol, and protease inhibitor cocktail tablet). Cyr1p-LRR was eluted from the column using spot peptide in PBS to compete for binding to the resin. Elution was carried out in 2 stages, stage 1 utilizing 100 µM spot peptide, and stage 2 utilizing 200 µM spot peptide warmed to 30 °C before elution.

2.2.4.4 Circular Dichroism Spectroscopy

Circular Dichroism (CD) spectra were obtained on a JASCO J1500 spectropolarimeter equipped with a PM-539 detector. All spectra were obtained in a rectangular quartz cell 1mm cuvette at 1nm data pitch, 8 second D.I.T, 1.00nm Bandwidth, and a scanning speed of 50 nm/min over wavelengths 190-260. Spectra were analyzed to the limit of detection per CD buffer. Each spectrum is the average of 5 scans and were obtained with reference to the baseline of the buffer. Mean residue ellipticity ($[\theta]$) was calculated from the following formula: (millidegrees X mean residue weight)/ (pathlength in millimeters X concentration in mg ml⁻¹), where mean residue weight = (molecular weight/ number of backbone amides) = 113.26 and Pathlength= 1mm. The ellipticity of each sample was corrected using buffer containing no protein as the baseline. Purified protein detergent complexes were buffer exchanged using a PD 10 Desalting column into CD compatible buffer (10mM

Potassium phosphate, 50mM (NH₄)₂SO₄, residual detergent) and concentrated down to 0.5 mg/mL. Protein concentration was determined using the Pierce Detergent Compatible Bradford Assay Kit. Spectra was obtained at 20°C.

2.2.4.5 CD Thermal Denaturation Analysis

CD spectroscopy was also used to determine secondary structure alterations with increasing temperature. Purified protein at a concentration of 0.021 mg /mL was subjected to spectral analysis from 0°C to 95°C and 95°C to 0°C in increments of 5 degrees. The Beta Structure Selection (BeStSel) method for the secondary structure determination and fold recognition from protein circular dichroism spectra, was used to predict secondary structure from CD data^{25, 26}. Using this platform, secondary structure was predicted to consist of 16.1% α helix, 10.5% antiparallel β -sheets, 0% parallel β -sheets, 15.4 % turns, 57.9% other structures, 2.7% helix1 (regular), 13.4% helix2 (distorted), 0% Anti1 (left-twisted), 10.5% Anti2 (relaxed) and 16.5% Anti3 (right twisted). A shift in secondary structure was observed at 95°C, where secondary structure composition was predicted to consists of 4.4% α helix, 32.1% antiparallel β -sheets, 0% parallel β -sheets, 21.6 % turns, 41.9% other structures, 1.4% helix1 (regular), 3.0% helix2 (distorted), 0% Anti1(left-twisted), 15.7% Anti2 (relaxed) and 16.5% Anti3 (right twisted) at 95°C.

2.2.4.6 Peptidoglycan Fragment Immobilization to Magnetic Beads

NHS activated beads were equilibrated to room temperature and aliquoted into microcentrifuge tubes (300 μ L). Beads were washed in ice cold 1M hydrochloric acid. Peptidoglycan fragments or ethanolamine were incubated with beads. Peptidoglycan fragments muramyl tripeptide, muramyl dipeptide, and muramic

acid were each dissolved in 50mM borate buffer, pH 8.5 at a concentration of 2.0 mg/mL, ethanolamine was added to the beads at a concentration of 3M, pH 9.0. PG fragments and ethanolamine were incubated with the acid washed beads with end-over-end rotation at 4°C overnight. Beads were washed 3x with 0.1M glycine, pH 2.0, followed by DI water. Immobilized peptidoglycan beads were stored in 300 µL 50mM borate buffer, pH 8.5 + 0.05% sodium azide.

2.2.4.7 Protein Enrichment Assay Using Peptidoglycan Immobilized Beads: Cellular Lysate²

5 µL peptidoglycan immobilized magnetic beads were equilibrated in lysis buffer, or lysis buffer, 5%v bovine serum albumin (BSA). Clarified cellular lysate was incubated with beads overnight at 4°C with end-over-end rotation. Beads were washed 2x with lysis buffer, 1x with lysis buffer + 0.1% Triton-x-100, and 2x with wash buffer (50mM HEPES, 0.5 M NaCl, 0.1 mM EGTA, 0.1 mM MgCl₂, 10% glycerol, pH 7.4). Bound protein was eluted from the beads with 6X Lamelli buffer. To normalize the volumes between supernatant and bead elutions, the bead was resuspended in 10µL 6X Lamelli Buffer, 50µL PBS, supernatant was prepared by 50µL supernatant and 10µL Lamelli Buffer. Samples were analyzed via immunoblotting against the Spot-Tag.

2.2.4.8 Protein Enrichment Assay Using Peptidoglycan Immobilized Beads: Purified Protein

15 µL peptidoglycan immobilized magnetic beads were equilibrated in lysis buffer, 5%v bovine serum albumin (BSA). Purified protein from solubilized cellular membranes was incubated with beads overnight at 4°C with end-over-end rotation.

Beads were washed 2x with lysis buffer, 1x with lysis buffer + 0.1% Triton-x-100, and 2x with wash buffer (50mM HEPES, 0.5 M NaCl, 0.1 mM EGTA, 0.1 mM MgCl₂, 10% glycerol, pH 7.4). Bound protein was eluted from the beads with 6X Lamelli buffer. To normalize the volumes between supernatant and bead elutions, the bead was resuspended in 10μL 6X Lamelli Buffer, 50μL PBS, supernatant was prepared by 50μL supernatant and 10μL Lamelli Buffer. Samples were analyzed via immunoblotting against the Spot-Tag.

2.3 Results and Discussions

2.3.1 Growth of Yeast for Protein Expression

The 68.5 kDa LRR domain (amino acid residues 435-1005), was cloned into a pESC-URA expression vector under the bidirectional GAL:10 promoter in a *S. cerevisiae* expression system, with an N-terminal His₆ tag, and a C-terminal 1.4 kDa Spot-Tag (**Figure 2.2a**). The expression vector was transformed into *S. cerevisiae* cells EY1202 (*leu2 trp1 ura3 prb1-1122 pep4-1 his3del::pGAL10::GAL4*) via the Lithium Acetate method^{23,24}. Optimal Cyr1p-LRR expression was obtained with the addition of 2% galactose final concentration (**Figure 2.2b**) after 10 hours of induction (**Figure 2.3**).

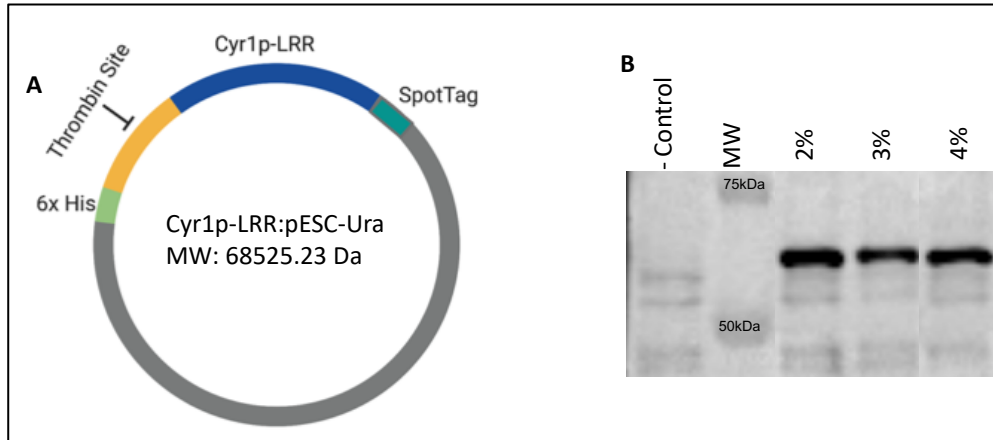


Figure 2.2: Cyr1p LRR in episomal plasmid pESC-Ura. **A:** The recombinant construct consists of an N-terminal 6xHis tag, and a C-terminal Spot-Tag. **B:** Western blot analysis of protein expression using an anti-Spot nanobody raised against the Spot-Tag. In the absence of Galactose (-Control) no protein expression is observed. Optimal protein expression is observed in the presence of 2% galactose final concentration.

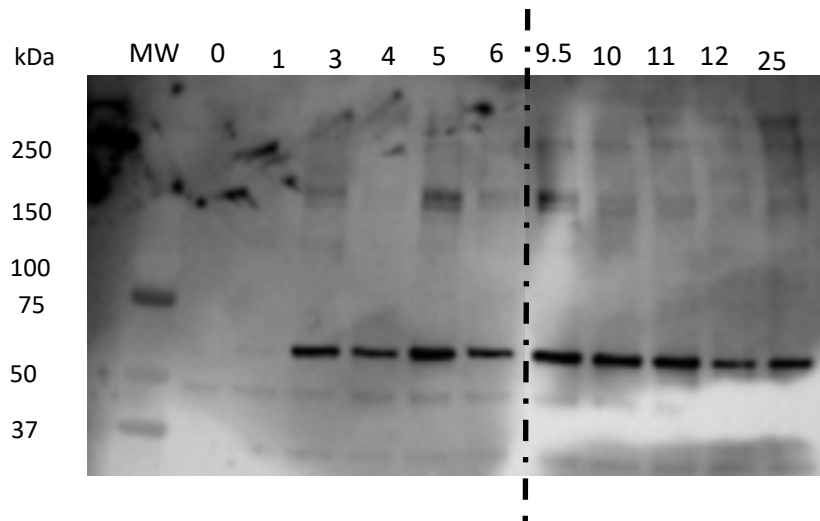


Figure 2.3: LRR induction analysis. Optimal induction times are between 9.5 to 11 hours. After 11 hours, protein expression decreases noticeably. Dashed line indicates time points that were removed.

2.3.2 Homology of adenylate cyclases from Candida Species

Inspiration for the amino acid composition of the newly expressed LRR was gathered from sequence homology data from the adenylate cyclase of *Candida* spp. *Candida. glabrata*, *Candida. parapsilosis*, *Candida. auris*, and *Candida. dubliniensis* (Figure 2.4). At the N-terminus of the aligned adenylate sequences, a high degree of amino acid residue conservation can be observed at proline residue 453 in the *C. albicans* receptor. At the C-terminus, sequence conservation severely subsides after amino acid residue 1004 in the *C. albicans* receptor. As such, the newly designed LRR was cloned from amino acid residues 435-1005.

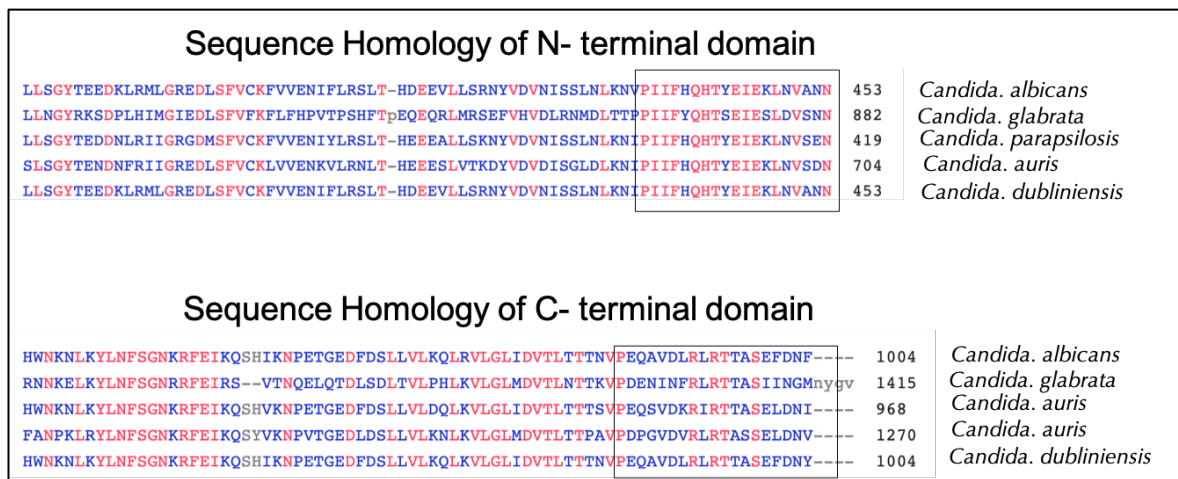


Figure 2.4: Sequence homology of the adenylate cyclase from 5 *Candida* spp. Blast analysis of the adenylate cyclase genes from *Candida* spp. *Candida. albicans*, *Candida. glabrata*, *Candida. parapsilosis*, *Candida. auris*, and *Candida. dubliniensis* revealed several highly conserved residues in red and less conserved residue in blue. The LRR domain was cloned from residue 435 at the N-terminus, and residue 1004 at the C-terminus, where sequence conservation decreases significantly as indicated by the gray dashed lines.

2.3.3 Characterization of Cyr1-LRR

Protein purification was confirmed via immunoblotting using both anti-Spot nanobody raised against the Spot-Tag (Figure 2.5a) and anti-his antibody raised

against the His6 tag (**Figure 2.5b**). Low protein expression levels, determined by overexpressed protein detection via Coomassie staining led to the need to investigate protein enrichment strategies. Interestingly, previous attempts to express this protein in an *E. coli* expression system with various epitope tags also resulted in undetectable expression levels (refer to appendix 1). These observations propelled the investigation into biophysical parameters to better predict protein behavior.

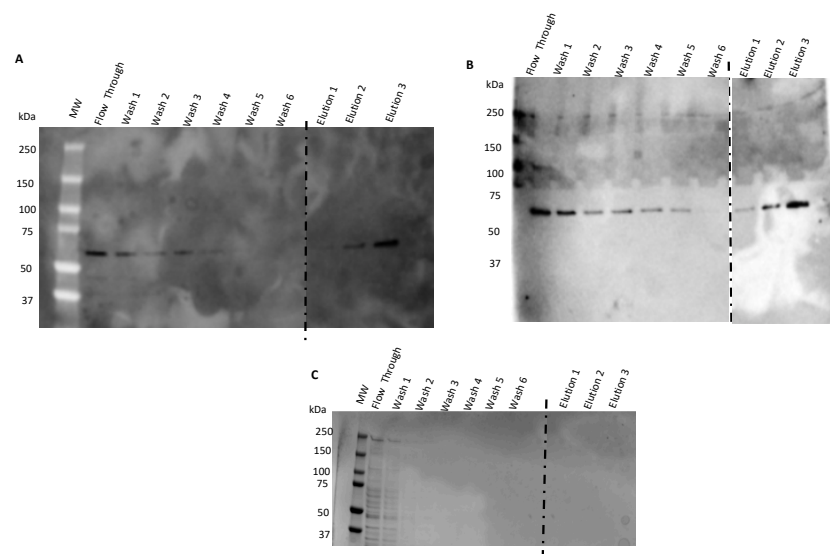


Figure 2.5: Purification of Protein Detergent Complexes. Protein solubilized from isolated membranes were purified under native conditions. **A:** Western blot analysis against the Spot-Tag shows successful purification of the LRR domain C-terminus. From left to right, MW marker, Flow through, washes 1-6, and elutions 1-3. **B:** Western blot analysis against the His₃ Tag shows successful purification of the LRR domain N-terminus. From left to right, MW marker, Flow through, washes 1-6, and elutions 1-3. **C:** Coomassie staining reveals that the sample in elution is composed primarily of full-length Cyr1-LRR and there are no major impeding impurities. From left to right, Flow Through (FT), Washes 1-6 (W1-W6), followed by elution 1, 2 and 3 (E1, E2, E3 respectively) using Spot Peptide in PBS. Dashed lines indicate truncated gel.

2.3.4 Cyr1-LRR Domain Predicted Biophysical Parameters

Results from the Kyte-Doolittle hydrophathy plot of the LRR domain suggests several possible transmembrane associated helices in the LRR domain. Specifically, the plot calculated with a window position of 9 indicate that there are several potential surface regions of the LRR, particularly towards the C-terminus (Figure 2.6a). Results from the plot calculated using a window position of 19 indicate that there is the potential for one transmembrane segment in the LRR (Figure 2.6b). Secondary structure determination by the AlphaFold2 algorithm depicts localized hydrophobic segments on the surface of the LRR domain (Figure 2.7)^{27, 28}. Taken together, these data suggested the possibility that the LRR domain may localize to the cellular membrane.

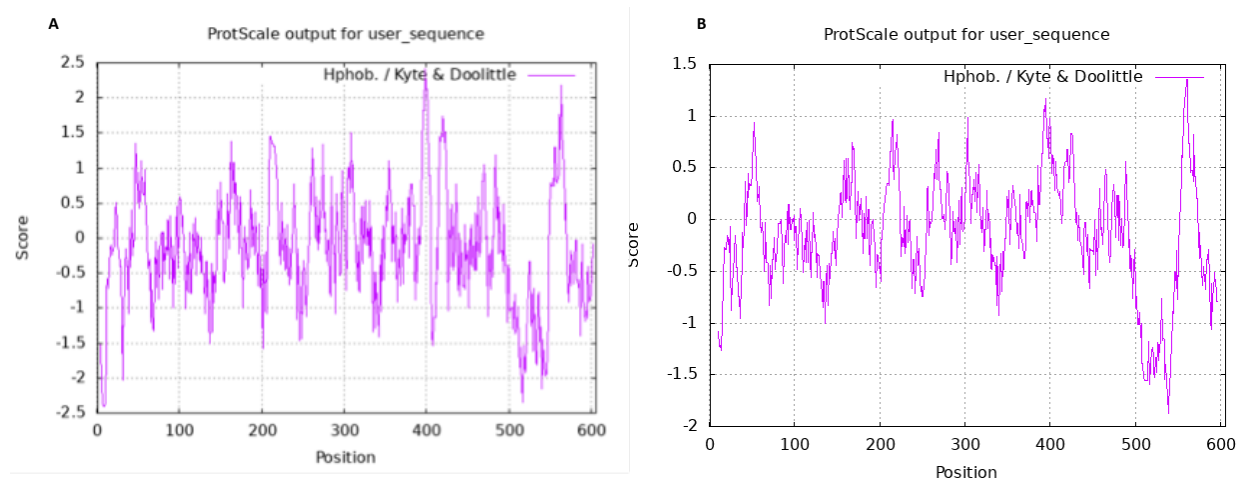


Figure 2.6: Hydrophathy Plot of the Cyr1-LRR domain. Possible transmembrane segments were calculated using the linear weight variation model. Y axis represents the hydrophathy score, and X axis represents the window number or amino acid position. A: Surface regions can be identified by peaks below the midline, and transmembrane proteins can be identified by peaks with scores greater than 1.6. B: Potential for a transmembrane domain exists between amino acid residues 500 and 600, at the C-terminus.

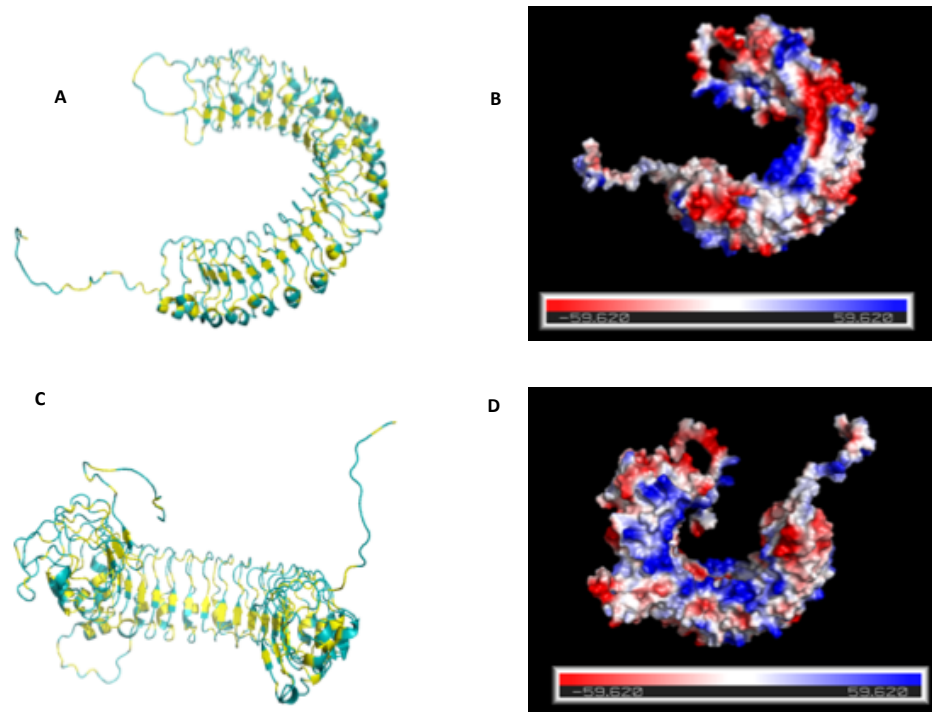


Figure 2.7: Hydrophobic residues in Cyr1-LRR. Red color signifies negative charge, blue signifies positive, and white denoting neutral. Electrostatic potential maps demonstrate that there are several localized areas of negative charges distributed in the LRR. **A:** Side view of a ribbon diagram depicting hydrophobic amino acids residues in yellow. **B:** Side view of an electrostatic potential map of the LRR domain, where areas of negative charge are observed in red. **C:** Top-down view of the LRR in a ribbon diagram depicting hydrophobic residues in yellow. **D:** Top-down view of the LRR electrostatic potential map depicts localization of negative charges towards the N and C terminus. Figures were generated using PyMol.

2.3.5 Cyr1-LRR Purification from *S. cerevisiae* Membranes

To assess the cellular membrane as a possible site of protein localization, clarified total lysate, insoluble cellular debris, and fractionized cellular membranes were analyzed for Cyr1p-LRR levels via SDS and immunoblotting with a Spot nanobody (Methods). Following cellular lysis and membrane fractionization, the majority of Cyr1p-LRR was detected in the total lysate, and significantly decreased when membranes were fractionized from the total lysate by ultracentrifugation. No

Cyr1p-LRR was detected in the insoluble cellular debris following solubilization in 8 M urea and heating to 95 °C (data not shown). Immunoblotting confirmed that Cyr1p-LRR abundance significantly decreased in the cytosolic fraction after ultracentrifugation, indicating that the majority of the protein was localized to the cellular membranes (**Figure 2.8**).

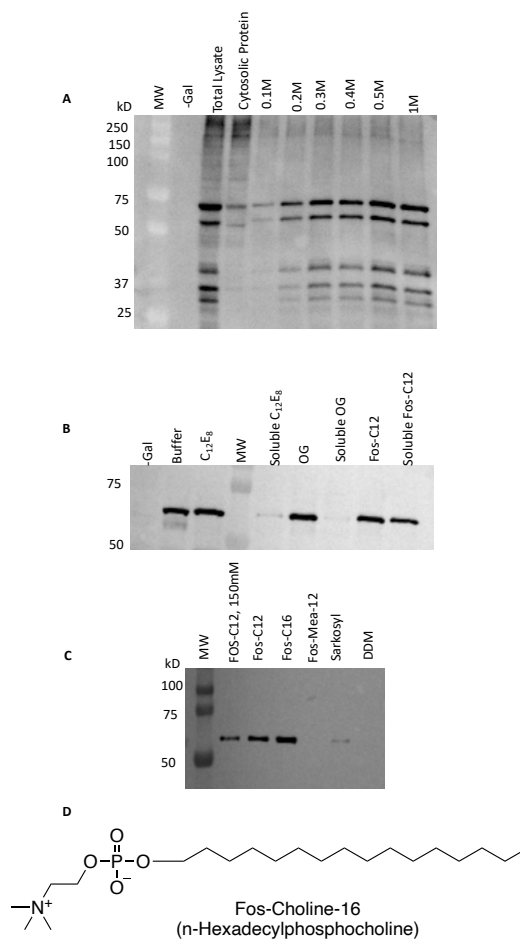


Figure 2.8: Membrane solubilization of the Cyr1p-LRR. Expected MW is 68.5 kD. **A:** LRR can be extracted from cellular membranes using high ionic strength alone. Solubilization of the LRR can be achieved with 0.5 M NaCl in the absence of detergent. At 1 M NaCl, decrease in protein solubilization was observed due to salting out. At 100 mM NaCl, protein precipitated was observed from the buffer. **B:** Detergent screens with a salt concentration of 0.5 M demonstrate that the Fos-choline class of detergents is best suited for the solubilization of the LRR from the fractionated cellular membranes. **C:** From the Fos family of detergents, Fos-Choline 16 provided the most solubilized protein from cellular membranes with a salt concentration of 0.5 M. **D** Chemical Structure of the solubilizing detergent Fos-Choline-16.

Confirmation that the LRR domain was preferentially distributed in the cellular membrane warranted characterization of the protein as either a transmembrane or a peripheral membrane protein. Protein solubilization was conducted from fractionated membranes in the presence of increasing salt concentrations. Solubilized samples were analyzed via immunoblotting against the spot-tag. Immunoblotting confirmed that the Cyr1p-LRR can be solubilized from the membrane effectively at 0.5 M NaCl. Densiometric analysis of immunoblots displayed that at a concentration of 1 M NaCl, Cyr1p-LRR solubility slightly decreased (**Figure 2.8a**). This decrease in solubilized protein at 1 M NaCl concentration was attributed to the salting out effect²⁹. The solubilization of the protein in high salt concentrations without the presence of detergent is indicative of a peripheral membrane protein, as extraction of transmembrane proteins require complete disruption of the lipid bilayer through the use of organic solvents, or detergents³⁰.

Though high ionic conditions are often sufficient to solubilize peripheral membrane proteins, once solubilized in high ionic conditions it is often necessary to remove high salts for further downstream biochemical assays, such as binding assays. Removal of proteins from high ionic environments can confer structural instability and lead to protein aggregation, particularly in the case of hydrophobic proteins. Thus, enhanced stabilizing elements were sought for the solubilization of the LRR in the form of detergents as a means to mitigate possible aggregation once removed from a high ionic buffer. As such, detergent screens were conducted with the aim of obtaining purified protein in its native functional form (**Figure 2.8b-c**). To that end, protein solubilization from the membranes was primarily carried out in mild, non-denaturing detergents that would not disrupt the secondary structure of the LRR (**Figure 2.9**),

such as Octaethylene glycol monododecyl ether (C₁₂E₈), n-Octyl-β-D-Glucoside (OG), n-Dodecylphosphocholine (Fos-C12), n-hexadecylphosphocholine (Fos-C16), Dodecylpho-n-Methylethanolamine (Fos-MEA-12), sodium lauroyl sarcosine (Sarkosyl), and n-Dodecyl-B-D-Maltoside (DDM). Furthermore, selected detergents were sought out based on accessibility, ease of detergent removal, protein functionality, and compatibility with downstream biochemical characterization such as binding assays.

Following isolation, membranes were resuspended in lysis buffer. The protein fraction was analyzed via immunoblotting against the Spot-Tag to ensure that protein loss did not occur due to precipitation upon introduction of detergent. Detergents were added to resuspended membranes at varying percentages (w/v) to ensure that the amount of detergent was orders of magnitude higher than critical micelle concentration (CMC) values **Table 1**. In lysis buffer, the best solubilizing detergent for the LRR domain was found to be from the choline family of detergents (**Figure 2.8b**). Specifically, Fos-C12 was the most efficient detergent for solubilizing the LRR in detergent screens.

Table 2.1: Detergents used in this study. * CMC values obtained from anatrace.com.

Detergent	Abbreviation	MW	*CMC mM
Octaethylene glycol monododecyl ether	C ₁₂ E ₈	538.75	0.09
n-Octyl-β-D-Glucoside	OG	292.40	19
n-Dodecylphosphocholine	Fos-C12	351.50	1.5
n-Hexadecylphosphocholine	Fos-C16	407.50	0.013
Dodecylpho-n-	Fos-MEA-12	323.00	0.43

Methylethanolamine			
n-Lauroylsarcosine sodium salt	Sarkosyl	293.40	14.4
n-Dodecyl-B-D-Maltoside	DDM	510.60	0.17
Triton-x-100	NA	647.00	0.016

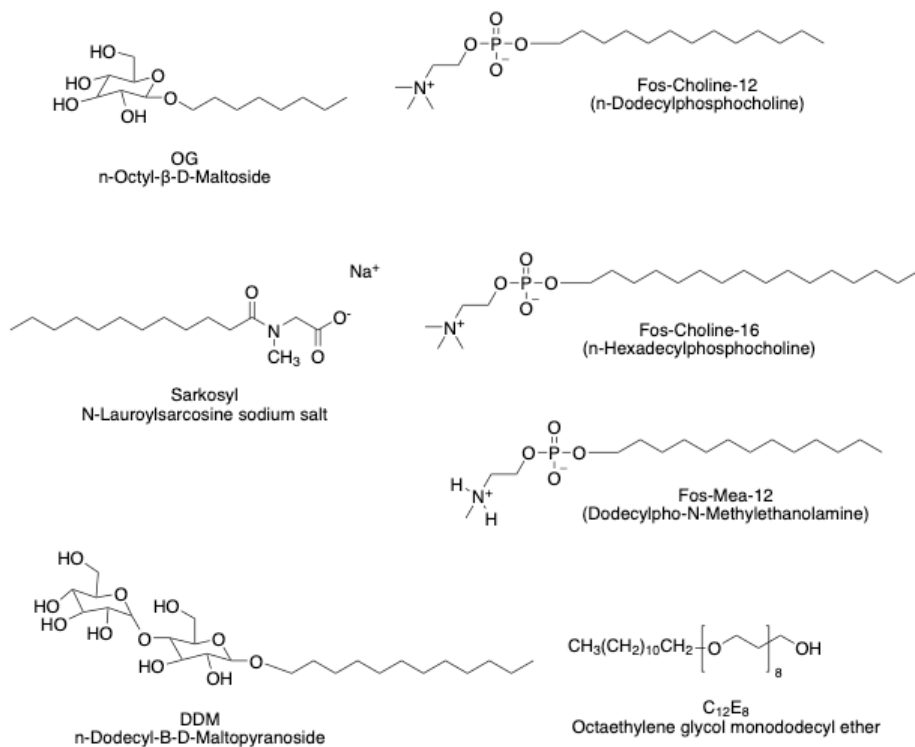


Figure 2.9: Chemical Structures of detergents used for membrane solubilization. Detergents used in the solubilization trials of the LRR are as follows: n-Dodecyl-B-D-Maltoside (DDM), Octaethylene glycol monododecyl ether (C₁₂E₈), n-Hexadecylphosphocholine (Fos-C16), n-Dodecylphosphocholine (Fos-C12), n-Octyl-β-D-Glucoside (OG), Dodecylpho-N-Methylethanolamine (FOS-MEA-16) and N-Lauroylsarcosine sodium salt (Sarkosyl).

Preliminary detergent screens were conducted in lysis buffer utilizing mild conditions, i.e., low salt concentration (150 mM NaCl), however, in the absence of a specific requirement for low ionic strength, a higher ionic strength workflow was explored. Higher salt concentrations can be helpful in the solubilization of membrane proteins as the conditions decrease electrostatic interactions between proteins and charged lipids³¹. With this in mind, solubilization using Fos-Choline detergents were conducted again, with an increased salt concentration of 0.5 M NaCl. In addition to increasing salt concentration, other closely related Fos-choline detergents, Fos-choline 16, and Fos- MEA 12 (**Table 1**), were also analyzed for effective solubilization.

In the presence of 0.5 M NaCl, an increase in the solubilization of Cyr1p was observed from the detergent Fos-C12 and Fos-C16, which has a slightly longer lipid chain (**Figure 2.5d**). Protein solubilization failed in the presence of Fos-MEA 12, and other common detergents such as DDM and Sarkosyl. The longer lipid chain of Fos-C16 may aid in the additional solubilization of some membrane interacting lipids necessary for the stability and subsequent solubility of the LRR, as detergents with longer lipid chains tend to be more solubilizing than detergents with shorter chains³². Interestingly, the methyl group in Fos-MEA-12 inhibited the solubilization of the LRR and promoted protein precipitation, indicating some specificity for the charge of the amine head group.

With enhanced LRR solubilization and enrichment from fractionized membranes, purification was conducted in the optimized conditions (1% Fos-C16, and 0.5 M NaCl). Purified Cyr1p-LRR was used to characterize the functionality of the LRR domain as it pertains to the binding of bacterial peptidoglycan fragments. The decision to undergo purification in the presence of detergent though not necessary was

driven by the added stability the detergent conferred to the LRR when dialyzed from a high ionic buffer. Solubilization in 0.5 M NaCl alone was not deemed an efficient purification scheme as the LRR did not bind resin adequately under such conditions, and readily precipitated upon dialysis into lower ionic strength buffers. In addition, 0.5 M NaCl was not conducive to further downstream biochemical assays, particularly bacterial cell wall binding assays. Upon dialysis to a lower ionic strength buffer, the persistent presence of detergent in the buffer conferred an added advantage of stability and therefore protection from precipitation. Purification was successful in the presence of Fos-C16, as immunoblots were positive against both the N-terminal His₆ Tag, and the C-terminal Spot-Tag, demonstrating that the entire LRR domain was successfully purified in detergent complexes (**Figure 2.5**).

2.3.6 Cyr1-LRR Characterization

2.3.6.1 CD Spectroscopy of Purified Protein

Upon purification, Cyr1p-LRR was dialyzed into buffer containing 0.01% Fos-C16, with no precipitation observed. Circular Dichroism (CD) spectroscopy of purified detergent solubilized protein determined that the LRR domain was properly folded, and agreed with our previous observations¹⁶ (**Figure 2.10a**). Using the K₂D₂ program for estimation of protein secondary structure from CD spectra, the membrane purified construct was predicted to contain 28.8% alpha helix and 16.41% β strand³³, which is in agreement with the predicted secondary structure from AlphaFold2 (**Figure 2.10b**). CD spectroscopy was also used to analyze LRR secondary structure variation under increasing temperatures. Though limited in the ability to produce high concentrations of purified protein in a monomeric state (**Figure 2.11**), data suggest

that there is a change in secondary structure in the presence of high temperatures (**Figure 2.12**). These data suggest that predicted structure from AlphaFold2 is an accurate model of how the construct is folded.

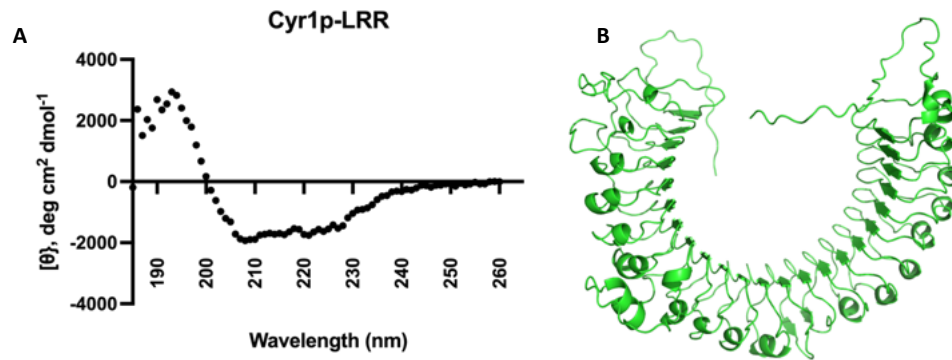


Figure 2.10: Secondary Structure of Cyr1p-LRR. **A:** Circular Dichroism spectroscopy reveals that the LRR domain is well folded and consists of 28.8% alpha helix, and 16.41% β strands. **B:** AlphaFold2 secondary structure prediction agrees with the experimental observations from CD spectroscopy.

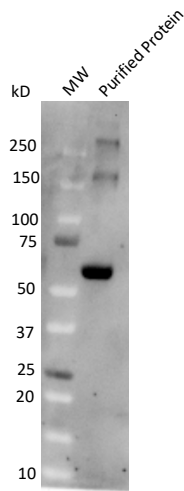


Figure 2.11: Concentrated purified protein. Purified membrane solubilized protein is prone to oligomerization upon concentration. This high propensity to coexist in multiple oligomerization states is a hindrance to spectroscopic analysis such as Circular Dichroism spectroscopy.

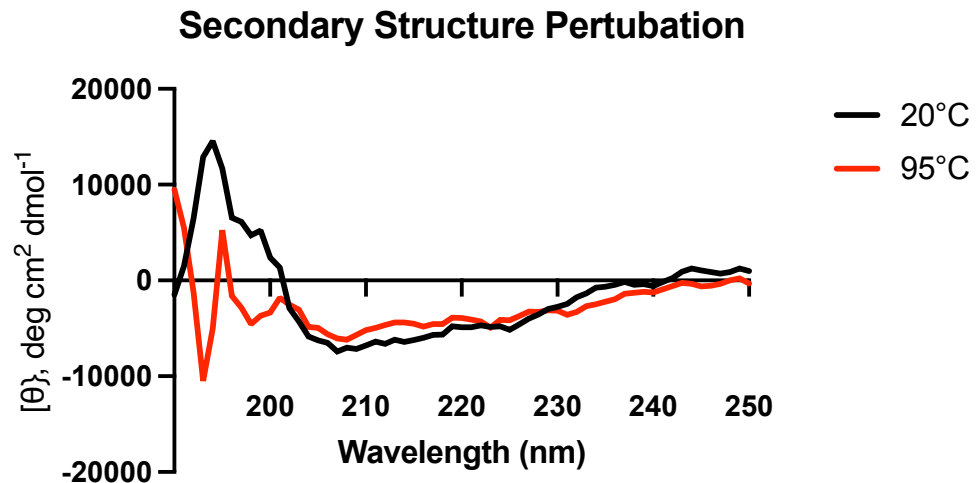


Figure 2.12: LRR Secondary Structure Perturbations. Slight perturbations in secondary structure was observed when the LRR was subjected to 95°C temperatures. While the protein remains largely folded, there is some loss of secondary structure observed. Particularly, there is some loss of α -helical and antiparallel β -sheets.

2.3.6.2 Cyr1p-LRR Binds Bacterial Peptidoglycan Fragments

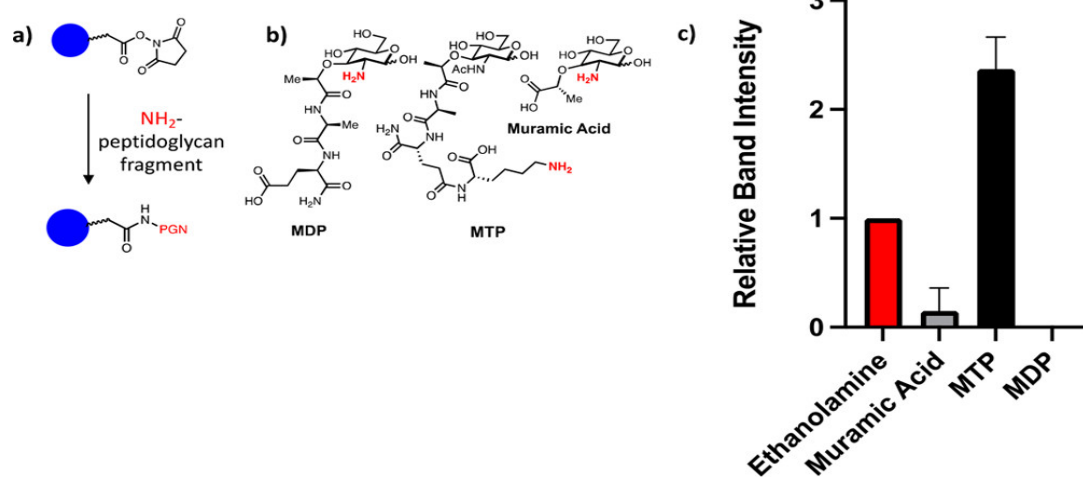


Figure 2.13: Membrane-associated Cyr1p-LRR domain can bind synthetic peptidoglycan fragments. (a) Schematic of magnetic bead functionalization. Terminal carboxylic acids are activated with NHS and subsequently coupled to an amine-functionalized peptidoglycan derivative. (b) Structures of 2-NH₂muramyl dipeptide (MDP), muramyl tripeptide (MTP), and 2-NH₂ muramic acid (MA) coupled to the magnetic beads through an amine functionality. (c) Western blot analysis and quantification of Cyr1p-LRR domain affinity purification relative to the unfunctionalized beads (ethanolamine control). Error bars represent the standard deviation between replicates.

It has previously been reported that the LRR binds to bacterial peptidoglycan fragments¹⁶. The newly expressed Cyr1p-LRR's functionality was assessed for the ability to bind bacterial peptidoglycan (PG) fragments: Muramyl Tripeptide (MTP), Muramyl Dipeptide (MDP), and Muramic Acid (MA) (Figure 2.13). Briefly, PG fragments were coupled to NHS activated magnetic beads using an amine handle contained within each fragment: MTP on the peptide, MDP and MA on the 2-position of the sugar. To assess non-specific binding, ethanolamine coated beads were used as a control. Functionalized, precoated bovine serum albumin (BSA) beads were incubated with clarified cellular lysates with end-over-end rotation at 4 °C overnight.

Beads were washed and bound constituents were eluted off the bead using 6x Lamelli buffer (without heating). Samples were analyzed using immunoblotting against the Spot-Tag. Relative to the ethanolamine functionalized beads, increased binding was observed for the peptidoglycan fragments muramyl tripeptide, muramyl dipeptide and muramic acid. We note that background binding was not decreased upon the addition of BSA (**Figure 2.14, 2.15**). However, when purified Cyr1p-LRR from solubilized membranes was used, limited background binding to ethanolamine was observed (**Figure 2.13**) and substrate preferences changed. Purified Cyr1p-LRR bound to MTP when it was linked through the peptide chain (**Figure 2.13**); these data are in accordance with the previously published SPR assay using *E. coli* LRR. Interestingly, for the human LRRs binding preferences shifted depending on the spatial orientation of the PG ligand³⁴. These data suggest that purified Cyr1p's LRR may behave in a similar manner; as binding is observed when a PG fragment is linked through the peptide but not the carbohydrate (**Figure 2.13c**). These binding preferences could shift depending on the presence of accessory proteins, as it was observed that Cyr1p-LRR in total lysate did not display the same binding preferences as purified protein (**Figure 2.14-15, 2.16**). This is supported by recent work by Hang et al., that show the binding of NOD2 for its peptidoglycan ligand can be enhanced in the presence of the accessory protein Arf6³⁵.

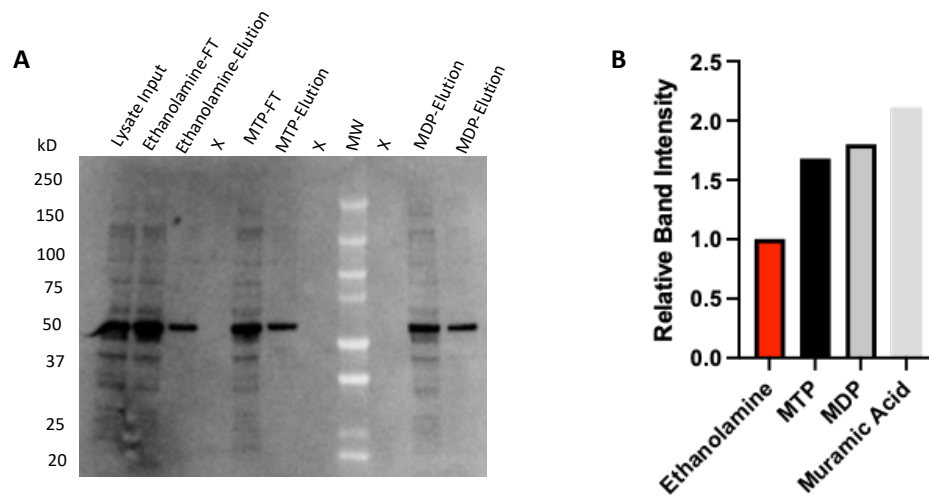


Figure 2.14: Cellular Lysate enrichment biological replicate 1. **A:** Immunoblotting against the C-terminal Spot-Tag. **B:** Densitometric analysis was used to quantify the binding of Cyr1p-LRR and was normalized to ethanolamine. Relative to Ethanolamine, increased binding is observed for PG fragments, MTP, MDP, and MA. X denotes empty lanes

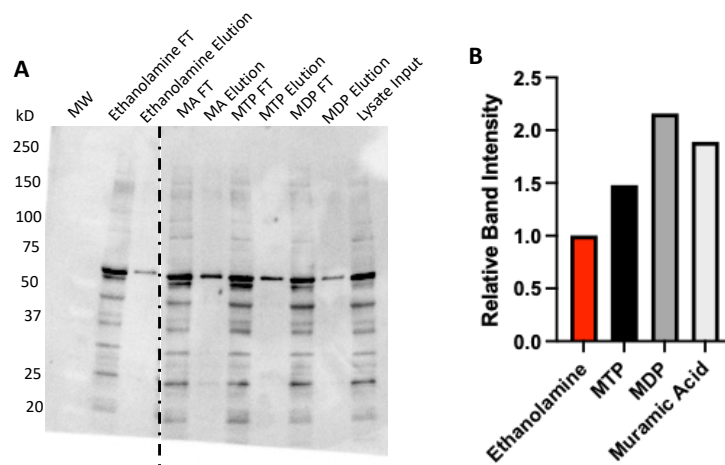


Figure 2.15: Cellular Lysate enrichment biological Replicate 2. A:

Immunoblotting against the C-terminal Spot-Tag. **B:** Densiometric analysis was used to quantify the binding of Cyr1p-LRR and was normalized to ethanolamine. Relative to Ethanolamine, increased binding is observed for PG fragments, MTP, MDP, and MA.

The data demonstrate that the LRR domain can bind bacterial peptidoglycan fragments with greater affinity relative to an ethanolamine control. While not a quantitative assay, this affinity-assay confirms the positive association of the LRR domain with bacterial peptidoglycan fragments, suggesting that the newly expressed LRR domain is functional. This non-quantitative experiment allows for rapid evaluation of the LRR domain with various PG ligands and is amenable to the limitations of working with a membrane protein. It provides an effective middle ground between the biotin-streptavidin pull down assay ¹⁴ and an analytical SPR assay ¹⁶. The former involves complex synthesis to access the bacterial cell wall fragments, while the later requires expensive instrumentation. We envision that this assay could be rapidly expanded with a host of bacterial PG fragments^{36, 34, 37} to quickly assess Cyr1p's binding preferences both from cellular lysates and purified protein.

The Leucine Rich Repeat (LRR) domain of the adenylate cyclase Cyr1p from the human commensal *C. albicans* is a membrane associated protein that can sense and detect bacterial peptidoglycan fragments. We have established a rigorous, reproducible workflow to recombinantly expressed and purified a stable LRR domain from cellular membranes. We have proven the ability of the LRR to interact with bacterial peptidoglycan fragments. This difficult to characterize protein was expressed with an N-terminal His₃ Tag and a small C-terminal Spot-Tag. To the best of our

knowledge, this is the first time this protein has been expressed in a closely related host with such a small affinity tag.

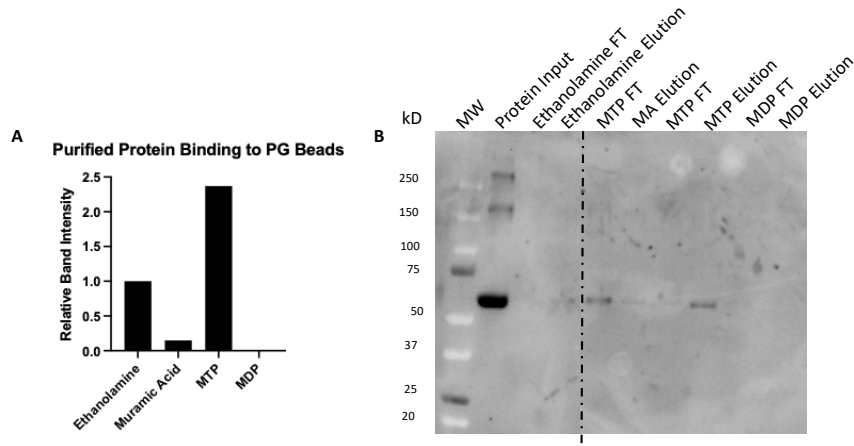


Figure 2.16: Purified protein binding to PG functionalized beads. Background binding to the ethanolamine control is undetectable using purified protein. In addition, purified protein binds MTP with higher affinity relative to ethanolamine control.

Though previously successful in the ability to express and characterize the binding of an LRR construct from Cyr1p to bacterial derived carbohydrates, efforts to further study this construct were limited by the instability of the MBP Tag fusion protein. The inability to obtain purified protein without a denaturing and refolding procedure from inclusion bodies was a limiting factor in the ability to further study the biochemistry of the LRR. Furthermore, the previously reported construct lacked the entire LRR domain, and the necessary N and C terminal caps needed for proper folding, which likely attributed to the instability of the construct.

Here the construct for the Cyr1p's LRR domain was redesigned. AlphaFold2 facilitated a detailed predicted structural analysis, permitting the design of a new construct that spans the majority of the Leucine Rich Repeats in the LRR domain and

most likely encompasses the necessary N and C terminal caps required for proper folding and stability. In addition, the newly designed LRR remains stable after purification and has a small 12 amino acid Spot-Tag that allows for adequate purification and analysis via immunoblotting. This new construct was expressed in a more native host (*S. cerevisiae*). These important changes have allowed for a new LRR construct from Cyr1p that is functional in binding bacterial PG, does not localize to inclusion bodies, and can therefore be purified under native conditions. These findings permit a better understanding of the native properties governing the structure and function of Cyr1p's LRR. It also provides some molecular level insight as to how the LRR can bind bacterial fragments that it is responsive to. We hypothesize that Cyr1p's membrane association are important for protein stability and the ability to properly interact with bacterial PG fragments from its niche via membrane association. In future experiments, this construct will be used to identify accessory proteins and to study the inhibition of bacterial PG binding by small molecules, which will serve as therapeutic leads in the development of new anti-fungals.

REFERENCES

1. Ursell, L. K.; Metcalf, J. L.; Parfrey, L. W.; Knight, R., Defining the human microbiome. *Nutr Rev* **2012**, *70 Suppl 1* (Suppl 1), S38-S44.
2. Mohajeri, M. H.; Brummer, R. J. M.; Rastall, R. A.; Weersma, R. K.; Harmsen, H. J. M.; Faas, M.; Eggersdorfer, M., The role of the microbiome for human health: from basic science to clinical applications. *Eur J Nutr* **2018**, *57* (Suppl 1), 1-14.
3. Crump, G. M.; Zhou, J.; Mashayekh, S.; Grimes, C. L., Revisiting peptidoglycan sensing: interactions with host immunity and beyond. *Chemical Communications* **2020**, *56* (87), 13313-13322.
4. Kobe, B.; Deisenhofer, J., The leucine-rich repeat: a versatile binding motif. *Trends in Biochemical Sciences* **1994**, *19* (10), 415-421.
5. Ng, A.; Xavier, R. J., Leucine-rich repeat (LRR) proteins: integrators of pattern recognition and signaling in immunity. *Autophagy* **2011**, *7* (9), 1082-4.
6. Kobe, B.; Kajava, A. V., The leucine-rich repeat as a protein recognition motif. *Current Opinion in Structural Biology* **2001**, *11* (6), 725-732.
7. Janeway, C. A., Jr., Approaching the asymptote? Evolution and revolution in immunology. *Cold Spring Harb Symp Quant Biol* **1989**, *54 Pt 1*, 1-13.
8. Mayer, F. L.; Wilson, D.; Hube, B., *Candida albicans* pathogenicity mechanisms. *Virulence* **2013**, *4* (2), 119-128.
9. van Tilburg Bernardes, E.; Pettersen, V. K.; Gutierrez, M. W.; Laforest-Lapointe, I.; Jendzjowsky, N. G.; Cavin, J.-B.; Vicentini, F. A.; Keenan, C. M.; Ramay, H. R.; Samara, J.; MacNaughton, W. K.; Wilson, R. J. A.; Kelly, M. M.; McCoy, K. D.; Sharkey, K. A.; Arrieta, M.-C., Intestinal fungi are causally implicated in microbiome assembly and immune development in mice. *Nature Communications* **2020**, *11* (1), 2577.
10. Stop neglecting fungi. *Nature Microbiology* **2017**, *2* (8), 17120.
11. Linder, J. U.; Schultz, J. E., The class III adenylyl cyclases: multi-purpose signalling modules. *Cellular Signalling* **2003**, *15* (12), 1081-1089.
12. Linder, J. U., Class III adenylyl cyclases: molecular mechanisms of catalysis and regulation. *Cellular and Molecular Life Sciences* **2006**, *63* (15), 1736.
13. Klengel, T.; Liang, W.-J.; Chaloupka, J.; Ruoff, C.; Schröppel, K.; Naglik, J. R.; Eckert, S. E.; Mogensen, E. G.; Haynes, K.; Tuite, M. F.; Levin, L. R.; Buck, J.; Mühlischlegel, F. A., Fungal adenylyl cyclase integrates CO₂ sensing with cAMP signaling and virulence. *Curr Biol* **2005**, *15* (22), 2021-2026.

14. Xu, X. L.; Lee, R. T.; Fang, H. M.; Wang, Y. M.; Li, R.; Zou, H.; Zhu, Y.; Wang, Y., Bacterial peptidoglycan triggers *Candida albicans* hyphal growth by directly activating the adenylyl cyclase Cyr1p. *Cell Host Microbe* **2008**, *4* (1), 28-39.
15. Tan, C. T.; Xu, X.; Qiao, Y.; Wang, Y., A peptidoglycan storm caused by β -lactam antibiotic's action on host microbiota drives *Candida albicans* infection. *Nat Commun* **2021**, *12* (1), 2560.
16. Burch, J. M.; Mashayekh, S.; Wykoff, D. D.; Grimes, C. L., Bacterial Derived Carbohydrates Bind Cyr1 and Trigger Hyphal Growth in *Candida albicans*. *ACS Infectious Diseases* **2018**, *4* (1), 53-58.
17. Kyte, J.; Doolittle, R. F., A simple method for displaying the hydropathic character of a protein. *J Mol Biol* **1982**, *157* (1), 105-32.
18. Mitts, M. R.; Grant, D. B.; Heideman, W., Adenylylase in *Saccharomyces cerevisiae* is a peripheral membrane protein. *Mol Cell Biol* **1990**, *10* (8), 3873-83.
19. Altschul, S. F.; Madden, T. L.; Schäffer, A. A.; Zhang, J.; Zhang, Z.; Miller, W.; Lipman, D. J., Gapped BLAST and PSI-BLAST: a new generation of protein database search programs. *Nucleic Acids Res* **1997**, *25* (17), 3389-402.
20. Altschul, S. F.; Wootton, J. C.; Gertz, E. M.; Agarwala, R.; Morgulis, A.; Schäffer, A. A.; Yu, Y. K., Protein database searches using compositionally adjusted substitution matrices. *Febs j* **2005**, *272* (20), 5101-9.
21. Virant, D.; Traenkle, B.; Maier, J.; Kaiser, P. D.; Bodenhöfer, M.; Schmees, C.; Vojnovic, I.; Pisak-Lukáts, B.; Endesfelder, U.; Rothbauer, U., A peptide tag-specific nanobody enables high-quality labeling for dSTORM imaging. *Nature Communications* **2018**, *9* (1), 930.
22. Braun, M. B.; Traenkle, B.; Koch, P. A.; Emele, F.; Weiss, F.; Poetz, O.; Stehle, T.; Rothbauer, U., Peptides in headlock – a novel high-affinity and versatile peptide-binding nanobody for proteomics and microscopy. *Scientific Reports* **2016**, *6* (1), 19211.
23. Daniel Gietz, R.; Woods, R. A., Transformation of yeast by lithium acetate/single-stranded carrier DNA/polyethylene glycol method. In *Methods in Enzymology*, Guthrie, C.; Fink, G. R., Eds. Academic Press: 2002; Vol. 350, pp 87-96.
24. Gietz, R. D.; Schiestl, R. H., High-efficiency yeast transformation using the LiAc/SS carrier DNA/PEG method. *Nature Protocols* **2007**, *2* (1), 31-34.
25. Micsonai, A.; Wien, F.; Bulyáki, É.; Kun, J.; Moussong, É.; Lee, Y. H.; Goto, Y.; Réfrégiers, M.; Kardos, J., BeStSel: a web server for accurate protein secondary structure prediction and fold recognition from the circular dichroism spectra. *Nucleic Acids Res* **2018**, *46* (W1), W315-w322.
26. Micsonai, A.; Wien, F.; Kernya, L.; Lee, Y. H.; Goto, Y.; Réfrégiers, M.; Kardos, J., Accurate secondary structure prediction and fold recognition for circular dichroism spectroscopy. *Proc Natl Acad Sci U S A* **2015**, *112* (24), E3095-103.
27. Skolnick, J.; Gao, M.; Zhou, H.; Singh, S., AlphaFold 2: Why It Works and Its Implications for Understanding the Relationships of Protein Sequence, Structure,

- and Function. *Journal of Chemical Information and Modeling* **2021**, *61* (10), 4827-4831.
28. Jumper, J.; Evans, R.; Pritzel, A.; Green, T.; Figurnov, M.; Ronneberger, O.; Tunyasuvunakool, K.; Bates, R.; Židek, A.; Potapenko, A.; Bridgland, A.; Meyer, C.; Kohl, S. A. A.; Ballard, A. J.; Cowie, A.; Romera-Paredes, B.; Nikolov, S.; Jain, R.; Adler, J.; Back, T.; Petersen, S.; Reiman, D.; Clancy, E.; Zielinski, M.; Steinegger, M.; Pacholska, M.; Berghammer, T.; Bodenstein, S.; Silver, D.; Vinyals, O.; Senior, A. W.; Kavukcuoglu, K.; Kohli, P.; Hassabis, D., Highly accurate protein structure prediction with AlphaFold. *Nature* **2021**, *596* (7873), 583-589.
29. Moringo, N. A.; Bishop, L. D. C.; Shen, H.; Misiura, A.; Carrejo, N. C.; Baiyasi, R.; Wang, W.; Ye, F.; Robinson, J. T.; Landes, C. F., A mechanistic examination of salting out in protein–polymer membrane interactions. *Proceedings of the National Academy of Sciences* **2019**, *116* (46), 22938.
30. Smith, S. M., Strategies for the purification of membrane proteins. *Methods Mol Biol* **2011**, *681*, 485-96.
31. Ahmed, H., *Principles and reactions of protein extraction, purification, and characterization*. CRC press: 2017.
32. le Maire, M.; Champeil, P.; Møller, J. V., Interaction of membrane proteins and lipids with solubilizing detergents. *Biochimica et Biophysica Acta (BBA) - Biomembranes* **2000**, *1508* (1), 86-111.
33. Perez-Iratxeta, C.; Andrade-Navarro, M. A., K2D2: Estimation of protein secondary structure from circular dichroism spectra. *BMC Structural Biology* **2008**, *8* (1), 25.
34. D'Ambrosio, E. A.; Bersch, K. L.; Lauro, M. L.; Grimes, C. L., Differential Peptidoglycan Recognition Assay Using Varied Surface Presentations. *J Am Chem Soc* **2020**, *142* (25), 10926-10930.
35. Hespen, C. W.; Zhao, X.; Hang, H. C., Membrane targeting enhances muramyl dipeptide binding to NOD2 and Arf6–GTPase in mammalian cells. *Chemical Communications* **2022**, 6598-6601.
36. Bersch, K. L.; DeMeester, K. E.; Zagani, R.; Chen, S.; Wodzanowski, K. A.; Liu, S.; Mashayekh, S.; Reinecker, H.-C.; Grimes, C. L., Bacterial Peptidoglycan Fragments Differentially Regulate Innate Immune Signaling. *ACS Central Science* **2021**, *7* (4), 688-696.
37. Lazor, K. M.; Zhou, J.; DeMeester, K. E.; D'Ambrosio, E. A.; Grimes, C. L., Synthesis and Application of Methyl N,O-Hydroxylamine Muramyl Peptides. *Chembiochem* **2019**, *20* (11), 1369-1375.

Chapter 3

PEPTIDOGLYCAN FRAGMENTS DIFFERENTIALLY REGULATE HYPHAL GROWTH IN WILDTYPE CANDIDA ALBICANS

3.1 Introduction

Of the fungal pathogens capable of infecting humans, *Candida albicans* (*C. albicans*) is considered to be the most important, and historically the most successful¹. The success of *C. albicans*'s pathogenicity is directly owned to a morphological transition from budding yeast to pseudohyphae, and true hyphae, as well as the organism's ability to thrive in multiple anatomical sites in the human host by adapting to a variety of micro-ecological environments. Hyphae are an important phase in disease progression, as it can cause tissue damage by invading mucosal epithelial cells and subsequently leading to blood infections². In addition, the transformation of *C. albicans* from yeast to hyphae can help fungi escape phagocytosis of macrophages, resulting in an increased likelihood of invading host tissues thus causing greater damage³.

Yeast cells, the prominent cell morphology under most in vitro conditions, are round and/or oval, have a unicellular morphology, can be involved in biofilm formation, can be toxic or remain symbiotic in blood, and maintain symbiosis in the oral cavity, skin and vagina⁴⁻⁶. Pseudohyphal cells have long elliptic, multicellular forms, which can be induced at pH 6.0, 35°C, on solid limited nitrogen medium, and

via involvement in biofilm formation⁷. Pseudohyphal cells are differentiated from hyphal cells through the presence of constrictions at the neck of the bud and mother cell, with varying width and length⁸. These variations can cause pseudohyphal cells to resemble hyphae at one end, and elongated buds of yeast cells at the other end. Pseudohyphae can therefore be regarded as an intermediate between budding yeast and true hyphae, as true hyphae are distinguished by the absence of constriction in the neck of the mother cell, and parallel sides throughout its length. Furthermore, hyphae and pseudohyphae can be distinguished from one another via mycelium width. The width of hyphal cells has been reported to be approximately 2.0 μm on most media, whereas pseudohyphal cells have a minimum width of 2.8 μm ⁹.

Of particular interest is the formation and maintenance of true hyphae in the presence of coexisting microbial communities. It has been well documented that *C. albicans* infections, which are accompanied with hyphal morphology, are almost always accompanied by bacterial infections¹⁰. Moreover, this is observed not just in disease scenarios, but environmental scenarios in which microorganisms present themselves as biofilm communities that are almost often polymicrobial. This cross-kingdom interaction between *C. albicans* and bacteria parlays microbial advantages such as alterations to host immune responses in the favor of microbial cells, decrease of antimicrobial effectiveness, microbial pathogenesis, and virulence. Microbial advantages garnered through cross-kingdom interactions typically augment the severity of infections and heighten the recalcitrance towards conventional therapies. One of the most prominent examples of this phenomena is the coinfection of *Pseudomonas aeruginosa* and *C. albicans*. This coinfection comprises a canonical

example of clinically relevant fungal-bacterial consortium commonly found in respiratory tract and skin¹¹.

While it is readily documented that *C. albicans* has a particular advantage in its ability to thrive in polymicrobial communities with a heightened degree of pathogenicity, there is little detail about the molecular characteristics that allow for this to ensue. Several stimuli, both external and internal, have been documented to elicit a hyphal response in *C. albicans*. Some of the most potent stimuli of this morphological transition are serum, N-acetyl glucosamine, acidic pH, CO₂, bacterial peptidoglycan fragments, etc.^{9, 12}. In recent years, several studies have shed light on the powerful hyphal stimulating and pathogenic outcomes that bacterial peptidoglycan has on the pathogenicity and virulence of *C. albicans*¹³⁻¹⁶.

This is noteworthy as *C. albicans* infections are almost always isolated with the presence of bacteria, such as *Pseudomonas aeruginosa*¹⁷, and *Staphylococcus aureus*¹⁸. Furthermore, a 2007 review of 141 candidemia patients from 8 Veterans Affairs hospitals and 231 patients from a tertiary care hospital with transplant services demonstrated that 27% of patients presented with polymicrobial blood cultures, 24% had synchronous bacteremia and 3% has more than 1 species of *Candida*¹⁸. In addition, identification of 100 bacteria isolated from patients demonstrated that 69 were Gram (+), and 31 were Gram (-)¹⁸. Despite these findings, mechanisms by which coinfecting bacteria exacerbate *Candida* infections remain elusive at large.

In many aspects, *Candida albicans* can be regarded as a disease of antibiotics¹⁹. Since the late 1940's an association with increased *C. albicans* infections were observed in patients treated with antibiotics²⁰. In fact, the association of increased *C. albicans* infections first became known in the 1950's, to what was largely

referred to as the antibiotics era. In June 1951, the Council on Pharmacy and Chemistry of the American Medical Association (AMA) agreed that a statement should be printed on bottles of the antibiotics aureomycin, chloramphenicol, and terramycin to warn patients receiving these drugs that they may be more susceptible to yeast like organisms²⁰. For quite some time it was thought that the cause of increased incidence of *C. albicans* infections in the presence of antibiotics treatment was due to the loss of competition of neighboring bacterial species. While this holds some precedent, as it has been recently demonstrated that antimicrobial compounds produced by vaginal *Lactobacillus crispatus* are able to strongly inhibit *C. albicans* growth, hyphal formation, as well as the regulation of virulence-related gene expressions²¹, there is still a gap in the persistence of *C. albicans* infections and infection related morphology in the presence of bacterial peptidoglycan fragments alone, without interfering bacterial species, extracellular secretions, etc.

The need to therefore unravel the molecular dynamics of coinfections has become even more urgent. Several studies have sought to unravel this through the ability of the human body to clear *C. albicans* cells such as through activation of invariant natural killer T (iNKT) cells²², or macrophage engulfment²³. Several studies have also scratched the surface denoting the onset and exacerbation of *C. albicans* infections as a direct result of bacterial peptidoglycan fragments in localized environments^{24,25}. This is of extreme significance, as many antibiotics target bacteria through a mechanism that disrupts bacterial cell wall synthesis such as β -lactams and glycopeptide antibiotics, and *C. albicans* infections are known to persist in the presence of antibiotic treatment²⁶. Studies conducted by Manson et al., demonstrated that *C. albicans* colonizes the cecum and stomach in cefoperazone treated mice²⁷.

Cefoperazone is a broad-spectrum antibiotic that has been shown to have a dramatic long-term effect on the indigenous microbiota of mice²⁸. Broad-spectrum antibiotic treatment predisposes mice to *Candida* GI overgrowth and candidiasis and studies have demonstrated that cefoperazone can cause long term alterations of the cecal microbiota²⁹.

The aforementioned studies, though revolutionary, did not specifically analyze individual bacterial peptidoglycan fragments' ability to drive *C. albicans* infections. We aim to unravel communication in coinfection scenarios, through the lens of specific bacterial peptidoglycan fragments such as Muramyl dipeptide (MDP) Muramic acid (MA), and their synthetic derivatives. MDP consists of one carbohydrate and two amino acids, and is found in both Gram (-) and Gram (+) bacteria³⁰. The biologically relevant isomer is MDP-(D). Muramic acid, specifically N-acetyl muramic acid (NAM) is a core structural element found exclusively for bacterial cell wall³¹⁻³³. While bacterial peptidoglycan is dynamic and constantly changing through bacterial growth and division, the NAM building block is a conserved element across all bacterial species^{33, 34}.

Using our repertoire of in house synthesized bacterial peptidoglycan derivatives^{31, 35, 36} we analyzed the ability of these fragments (**Figure 3.1**), to alter the morphology of wildtype *C. albicans* cells, from that of a commensal state (budding) to a pathogenic state (hyphae). Fragments were assessed for their ability to induce and maintain hyphal morphology in wildtype (WT) *C. albicans* through a 22-hour time span. The selected bacterial peptidoglycan fragments are at large, MDP, MA, and glucose derivatives. We aimed to characterize a breadth of MDP ligands that would provide insight into 1) the importance, if any of the orientation of the peptide stem on

the carbohydrate, 2) the impact of functionalization on the 2 carbon in the carbohydrate backbone, and 3) the significance of the peptide stem attached to the carbohydrate moiety. Essentially, we sought to understand the smallest fragment of the bacterial cell wall that *C. albicans* is responsive to by assessing MDP variations and subsequently peeling back the functionalization of the carbohydrate moiety, thereby stripping MDP down to its N-acetyl muramic acid backbone. We were primarily interested in delineating any trends in bacterial cell wall fragments that were potent, mild, or non-inducers of hyphal morphology. *C. albicans* cells have a large degree of morphological plasticity, as they are readily able to interconvert between budding and hyphal growth forms. As such, we sought to understand which bacterial fragments were able to trap cells in the hyphal form, as this is the basis for *C. albicans* infections.

3.2 Materials and Methods

3.2.1 Materials

Candida albicans wildtype cells used in this study were SC5314/ ATCC MYA-2876. Bacterial peptidoglycan fragments MDP- LL ester, 6-amino MMP ester, 6-N-acetyl Muramic acid methyl ester, 2-NH muramic acid, 6-amino MDP-LL-ester, and 6-amino MDP-LL-ester were synthesized in the Grimes Lab by former laboratory member Dr. James Melnyk³⁵. Bacterial peptidoglycan fragments 2-amino- γ amino butyryl MDP and 2-amino β -alanyl MDP were synthesized in the Grimes Lab by former laboratory member Dr. Ashley Brown³⁶. *Candida. albicans* growth curves were conducted on a Molecular Devices SpectraMax i3x plate reader in 96 well plates purchased from Corning Biosciences. All other chemicals, reagents, and consumables were purchased from ThermoFisher or one of their subsidiaries.

3.2.2 Budding *C. albicans* Peptidoglycan Sensitivity

Proliferation of *C. albicans* cells was determined in YPD medium at 30°C overnight. Saturated overnight cultures were diluted to $OD_{600} = 0.1$ into fresh YPD medium. Growth assessment of wildtype *C. albicans* cells in the budding state were conducted at 30°C in the presence of peptidoglycan fragments at 50, 100, and 1000 μM concentrations. Growth curves were conducted in 96 well plates for 24 hours, with absorbance readings at 600 nm every 30 minutes. Plates were agitated for 10 s at medium intensity before each initial reading, and in between readings. Growth analysis were done in triplicates.

3.2.3 Filamentous *C. albicans* Peptidoglycan Sensitivity

Proliferation of *C. albicans* cells was determined in YPD medium at 30°C overnight. Saturated overnight cultures were diluted to $OD_{600} = 0.1$ into fresh YPD medium. Growth assessment of wildtype *C. albicans* cells in the budding state were conducted at 30°C in the presence of peptidoglycan fragments at 50, 100, and 1000 μM concentrations. Growth curves were conducted in 96 well plates for 24 hours, with absorbance readings at 600 nm every 30 minutes. Plates were agitated for 10 s at medium intensity before each initial reading, and in between readings. Growth analyses were conducted in triplicates.

3.2.4 *C. albicans* Wildtype Phenotypic Characterization in the Presence of Bacterial Peptidoglycan Fragments

Proliferation of *C. albicans* cells was determined in YPD medium at 30°C overnight. 1 mL of the saturated overnight cultures was harvested and washed 2x with sterile 1x PBS. Washed cells were resuspended in fresh YPD medium and diluted to $OD_{600} = 0.1$. Cells were incubated with appropriate peptidoglycan fragment at a

concentration of 1 mM in 96 well plate and grown aerobically for 22 hours. 5 μ L of liquid culture was removed at 4, 8, and 22-hour time points. Liquid culture images were captured by differential interference contrast (DIC) microscopy using a Evos M5000 microscope. Images were further processed using the ImageJ software.

3.3 Results and Discussions

3.3.1 Budding *C. albicans* Peptidoglycan Sensitivity

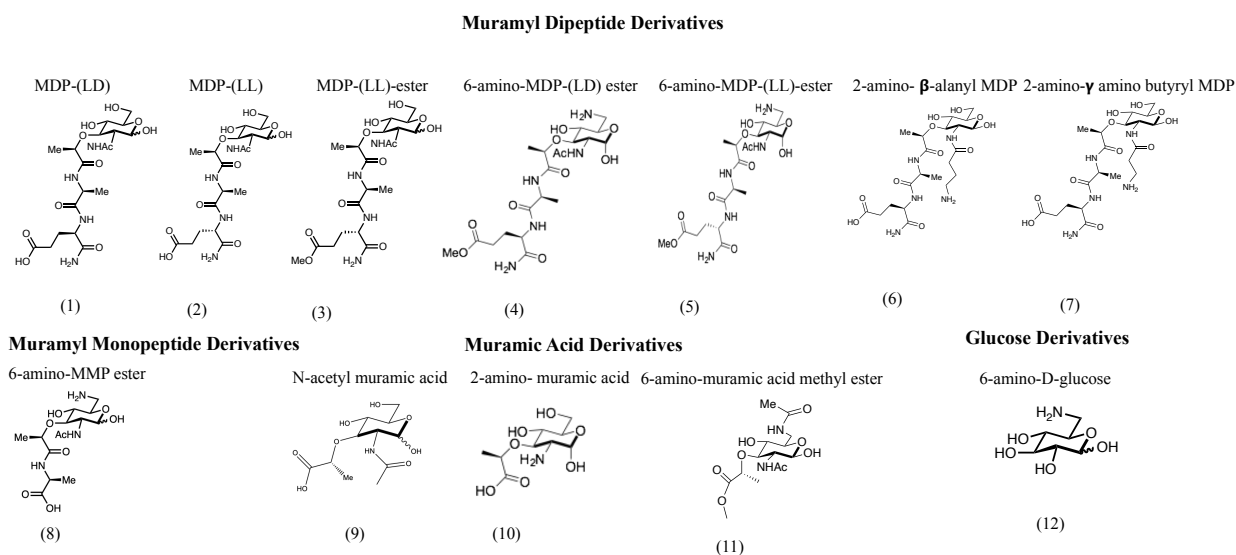


Figure 3.1: Bacterial Peptidoglycan Fragments Synthesized by former members of the Grimes Laboratory. A suite of in house synthesized bacterial peptidoglycan fragments were analyzed for their ability to induce consistent hyphal morphology in wildtype (WT) yeast *C. albicans*. The selected bacterial peptidoglycan fragments are at large, MDP, MA, and glucose derivatives.

Growth assessment in the presence of peptidoglycan fragments in the yeast state (budding, 30°C) showed that none of the fragments tested were lethal to the cells

(**Figure 3.2-3.3**). We therefore continued in our characterization of hyphal morphology at 37°C. Growth curve analysis showed that wildtype cells grew slightly faster in the presence of 1 mM peptidoglycan fragments (12) and (9) (**Figure 3.2**). Since yeast cells are metabolically adapted to survive on a plethora of carbon sources, we moved forward with the possibility that the increased growth observed could be attributed to peptidoglycan fragment consumption as a carbon source for growth.

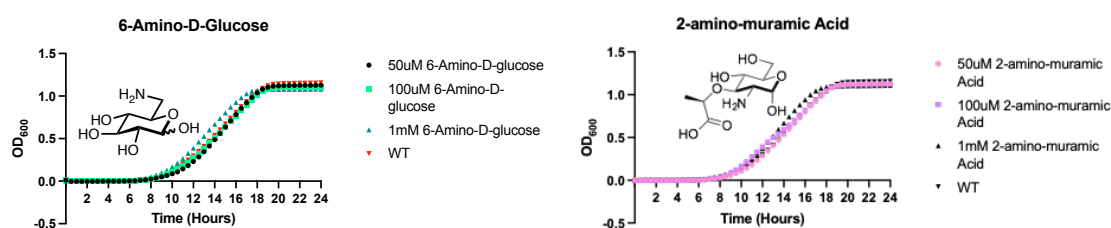


Figure 3.2: Growth of budding yeast characterized in the presence of 6-amino-D - glucose and 2-amino-muramic acid. A slight increase in cellular growth was observed at a concentration of 1mM for both fragments, as evident by a shift in the growth curve to the left.

No observable difference in growth was detected in WT cellular growth in the presence of bacterial peptidoglycan fragments (5), (4), and (8) (**Figure 3.3**). Since cell viability was not a concern with these fragments, we went on to assess their ability to induce hyphal growth in WT cells. Peptidoglycan fragments (1), (6), and (7) were not assayed for their lethality in the budding state. Previous studies have been conducted on MDP and its ability to induce hyphal growth in *C. albicans*, and therefore there was not a concern for lethality to the cells, circumventing the analysis of growth¹³. Additionally, we were limited in our quantity of fragments (6) and (7). As such, we sought best to save the fragments for the analysis of hyphal formation. Growth curves

were also not conducted for fragments (9), (10), and (11) for reasons mentioned above.

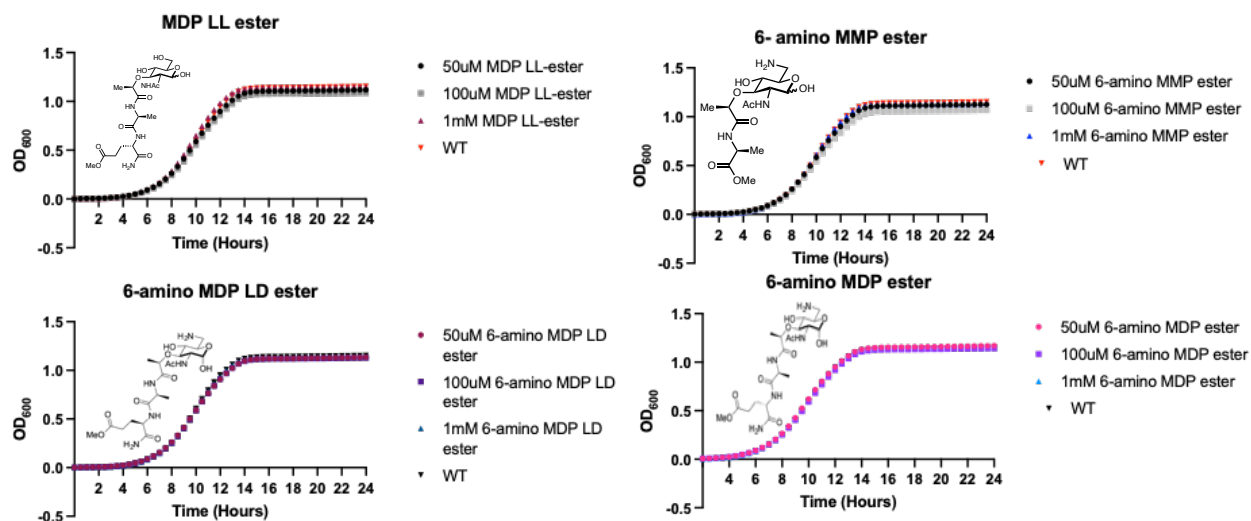


Figure 3.3: Growth of budding yeast in the presence of MDP derivatives. No changes were observed in growth in the presence of these bacterial peptidoglycan fragments at concentrations of 50, 100 and 1000 μM.

3.3.2 Filamentous *C. albicans* Peptidoglycan Sensitivity

Following the growth analysis of budding WT *C. albicans* cells in the presence of varying concentrations of the peptidoglycan fragments, filamentous assays were conducted at 37°C at a concentration of 1 mM. This concentration was selected with confidence, that cellular growth was not inhibited in the budding state. In addition, at 1 mM concentration, a slight alteration in growth was observed for some of the fragments. All fragments tested were compared to WT cellular growth, and cellular growth in the presence of 10% Fetal Bovine Serum (FBS), as this has long been the gold standard for hyphal induction in *C. albicans*^{37,38}. In the presence of

peptidoglycan fragments (12) and (10), cells reached an overall higher OD₆₀₀ in the stationary phase of growth, relative to (1), one of the longest known bacterial peptidoglycan fragments to stimulate hyphal formation, and FBS (**Figure 3.4**).

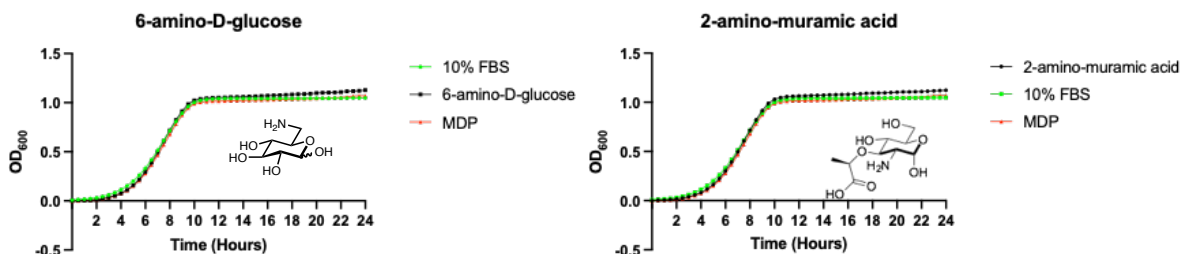


Figure 3.4: Filamentous growth assessment in the presence of 1 mM 6-amino-D-glucose and 2-amino-muramic acid. At 1 mM of each peptidoglycan fragment, a slight increase in filamentous growth is observed, similar to growth as budding yeast.

Relative to filamentous growth in the presence of 1 mM (1), and 10% FBS, *C. albicans* cells reached a slightly lower OD₆₀₀ in the presence of 1 mM (5), (8), and (7) (**Figure 3.5**). Peptidoglycan fragment (4) displayed a unique growth pattern relative to FBS and MDP. During the lag phase of growth, cells treated with 1 mM (4) displayed a slightly slower growth rate, at approximately 6 hours, when cells entered log phase of growth, treated cells grew at a rate similar to FBS and (1) treated cells, and during stationary phase of growth, (4) cells displayed a lower OD₆₀₀ between 9 and 16 hours, after 16 hours, an increase in OD₆₀₀ can be observed, with the treated cells leveling off in stationary phase of growth at a slightly higher OD₆₀₀ compared to (1) and FBS treated cells (**Figure 3.6a**). There was no observable difference between cells treated with (11) relative to cells treated with (1) and FBS (**Figure 3.6b**). Relative to cells grown in 10% FBS and the biologically relevant stereoisomer MDP-

LD) (1), cells achieved an overall lower OD₆₀₀ when treated with the MDP isomer (2) (Figure 3.6c).

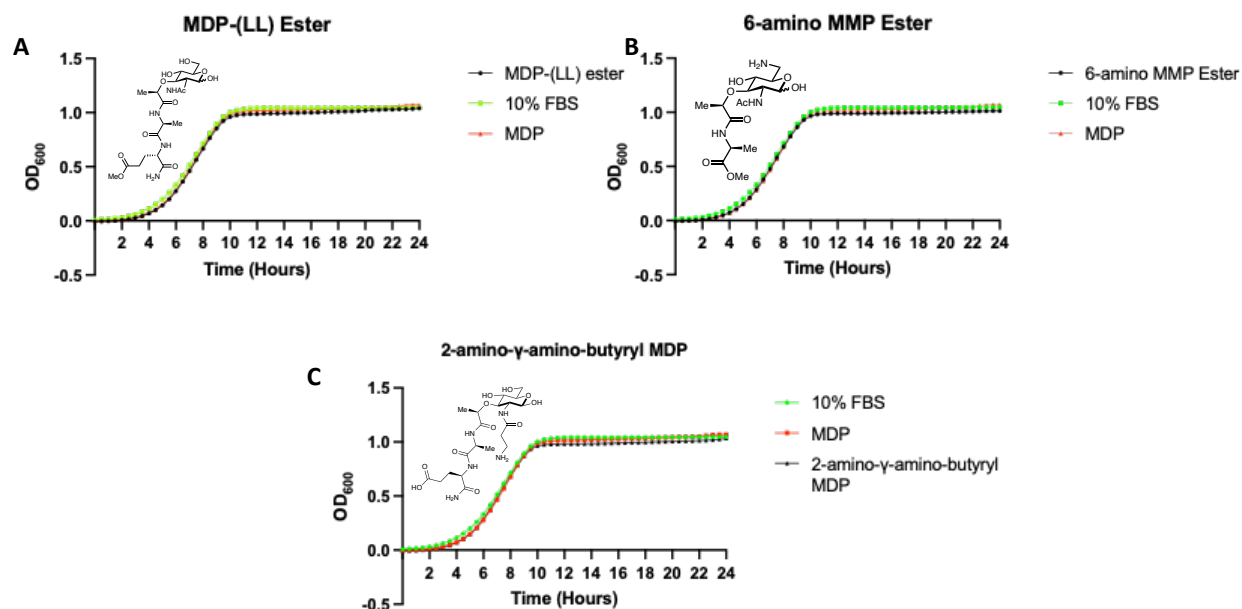


Figure 3.5: Filamentous growth of wildtype cells treated with 1 mM 6-amino MDP-(LL)- ester, 6-amino-MMP ester, and 2-amino-γ-amino-butyryl MDP.

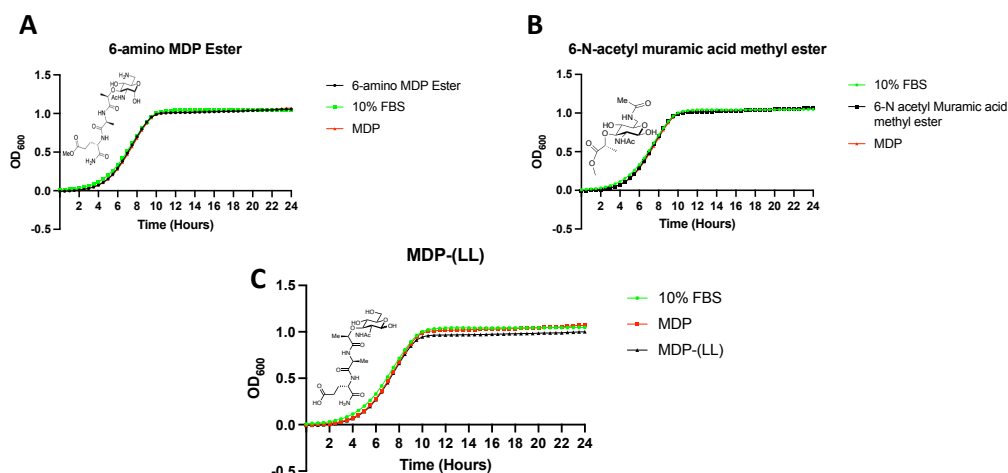


Figure 3.6: Filamentous growth analysis in presence of a: 6-amino MDP ester, b: 6-N-acetyl muramic acid methyl ester, and c: MDP-(LL). Where stereochemistry is not denoted, the biologically active stereoisomer MDP (LL) is implied.

3.3.3 *C. albicans* WT Phenotypic Characterization in the Presence of Bacterial Peptidoglycan Fragments

The above bacterial peptidoglycan fragments were gauged for their ability to 1) induce true hyphae relative to nontreated cells (WT control), 1 mM MDP, 10% FBS, and 2) maintain true hyphae over the course of 22 hours. Cells were treated with 1 mM of each bacterial peptidoglycan fragment and incubated at 37°C in 96 well plates. Cells were analyzed directly from liquid cultures via microscopy. Three different aliquots of cells were analyzed to gather as clear a depiction of each time point.

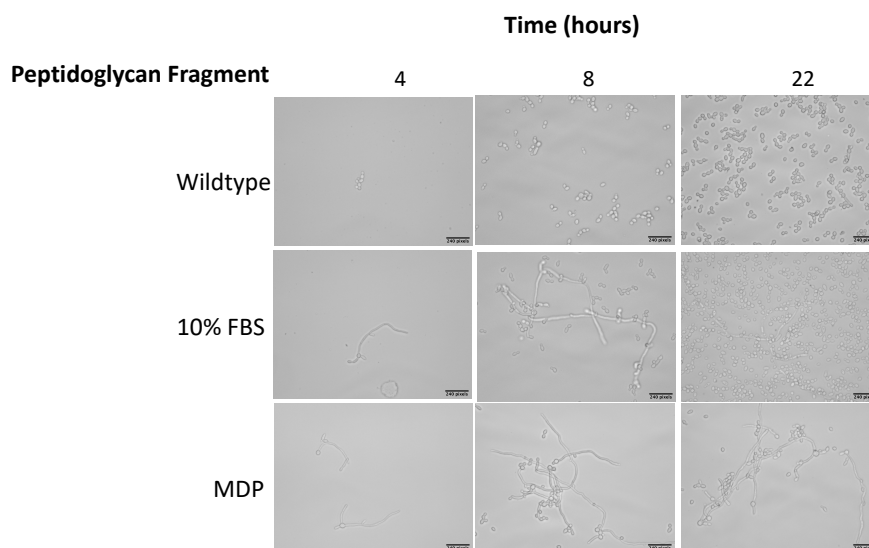


Figure 3.7: Hyphal assessment control used to ensure proper cellular responses. FBS and MDP have been documented hyphal inducers of filamentous growth in *C. albicans*. Where stereochemistry is not denoted, the biologically active stereoisomer MDP-(LD) is implied.

Our hyphal assessment began from a baseline obtained from hyphal induction upon treating WT cells with 10% FBS, and 1 mM fragment (1) (**Figure 3.7**). From there we went on to assess the ability of MDP esters, substituted MDP, muramic acid derivatives, a glucose derivative and an MMP derivative to induce and maintain hyphal growth. MDP esters analyzed were MDP- (LL)-ester (3), 6-amino-MDP-(LL)-ester (5) and 6-amino-MDP-(LD)-ester (4). Of the 3 esters tested, (3) ranked a 5, depicting the ability to induce hyphae and maintain true hyphal growth at 22 hours post treatment (**Figure 3.8**).

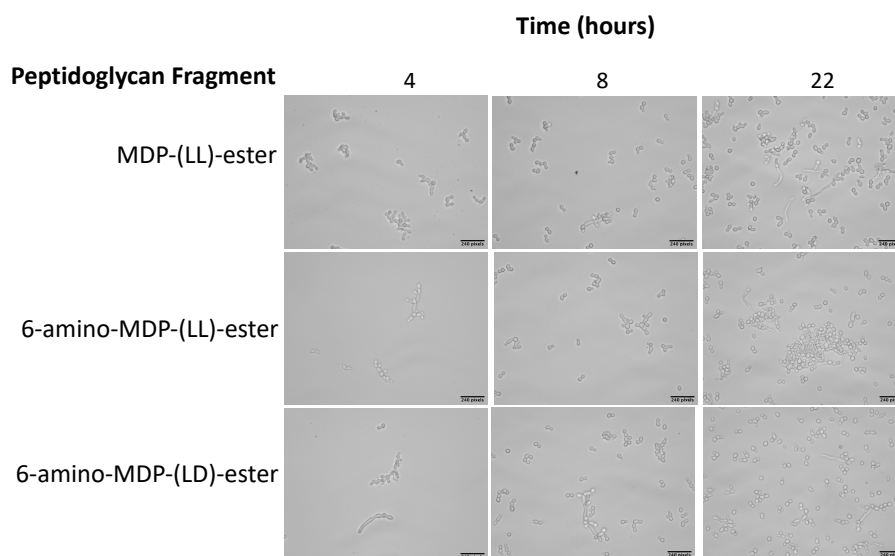


Figure 3.8: Filament assessment in the presence of MDP esters. True hyphae were only observed in the presence of 6-amino MDP ester. MDP ester alone and the 6-amino MDP-(LD)- ester failed to form true hyphae. Where stereochemistry is not denoted, the biologically active stereoisomer MDP-(LL) is implied.

Interestingly, in comparison to (4), fragment (3) was more potent at inducing and maintaining hyphal growth. The ester with the least ability to form and maintain true hyphae was (3), suggesting that not only is the (LL) orientation of the peptide in the ester preferred, but an amine at the 6- position of the muramyl backbone is advantageous in the ability to stimulate true hyphae. Furthermore, analysis of substituted MDP fragments 2-amino- β -alanyl MDP (6), and 2-amino- γ -amino butyryl MDP (7) demonstrated that the former was more potent at not only inducing hyphal growth, but maintaining it at 22 hours, whereas the latter was unable to form true hyphae (Figure 3.9). At 4 hours pseudohyphae was observed in (7) treated cells, but true hyphae were never formed, and at 22 hours cells were observed to occupy only the budding morphology.

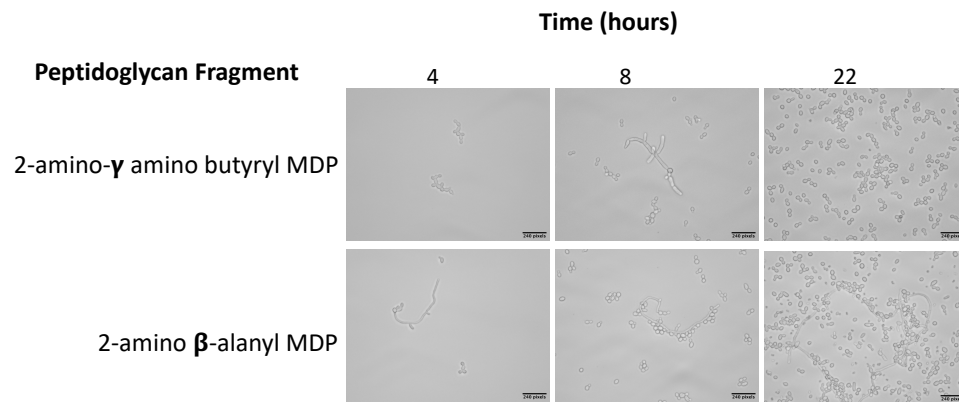


Figure 3.9: Filamentous assessment in the presence of substituted MDP derivatives 2-amino- β -alanyl MDP, and 2-amino- γ -amino butyryl MDP. At 22 hours post induction, 2-amino- β -alanyl MDP maintained hyphae. Comparatively, 2-amino- γ -amino butyryl MDP failed to form true hyphae. At 8 hours, pseudo hyphae can be observed, but cells readily reverted to budding at 22 hours post induction. Where stereochemistry is not denoted, the biologically active stereoisomer MDP- (LL) is implied.

MDP derivative analysis thus far suggest that an amine at the C-6 position on the carbohydrate backbone was advantageous in the ability to form and maintain hyphae in wildtype cells. Though 6-amino-MDP-(LL)-ester was not a more potent hyphal inducer than MDP alone, it was more effective at maintaining true hyphae than 10% FBS. Perhaps 2-amino- β -alanyl MDP may present as a more potent inducer of hyphal induction and maintenance, as it has a bulkier substituent on the 2 position, and may interact tighter with the LRR domain of the adenylate cyclase Cyr1p, as this receptor has been proven to be sensor and signal integrator of bacterial peptidoglycan fragments¹³⁻¹⁵.

We next wanted to strip the MDP fragment down to its carbohydrate backbone to determine the minimum peptidoglycan fragment that can stimulate hyphal growth. As such, we analyzed N-acetyl-muramic acid (NAM) and 2-amino muramic acid for

their ability to induce and maintain hyphal morphology. NAM is a conserved precursor in bacterial cell wall synthesis as well as peptidoglycan turnover, and is therefore biologically relevant as it is found in localized environments upon cleavage by peptidoglycan hydrolases³⁹. At 8 hours post treatment, NAM displayed sparse pseudohyphae, but no true hyphae, whereas at 4 hours 2-amino muramic acid displayed sparse pseudohyphae and was true hyphae at 8 hours. In addition, NAM was unable to maintain pseudohyphae at 22 hours, and almost all cells were observed to have reverted to a budding morphology, whereas 2-amino muramic acid maintained true hyphae at 22 hours post treatment. Furthermore, cells treated with (10) began hyphal induction at 4 hours and maintained true elongated hyphae throughout the 22-hour assessment. In our hands, this was the most potent inducer of hyphal morphology, even more potent than MDP (**Figure 3.10**). Fragment (11) was unable to form true hyphae but did form some pseudohyphae. At 8 hours pseudohyphae was observed, but cells remained budding at large, and by 22 hours, cells were completely reverted to budding (**Figure 3.10**). Analysis of MMP (8) demonstrated that cells though able to form hyphae at 4 and 8 hours, were unable to maintain hyphae at 22 hours (**Figure 3.11**). 6-amino- LD-glucose (12) was able to form hyphae at 4 hours and maintained true hyphae at 22 hours, but the majority of cells remained in a budding state (**Figure 3.11**).

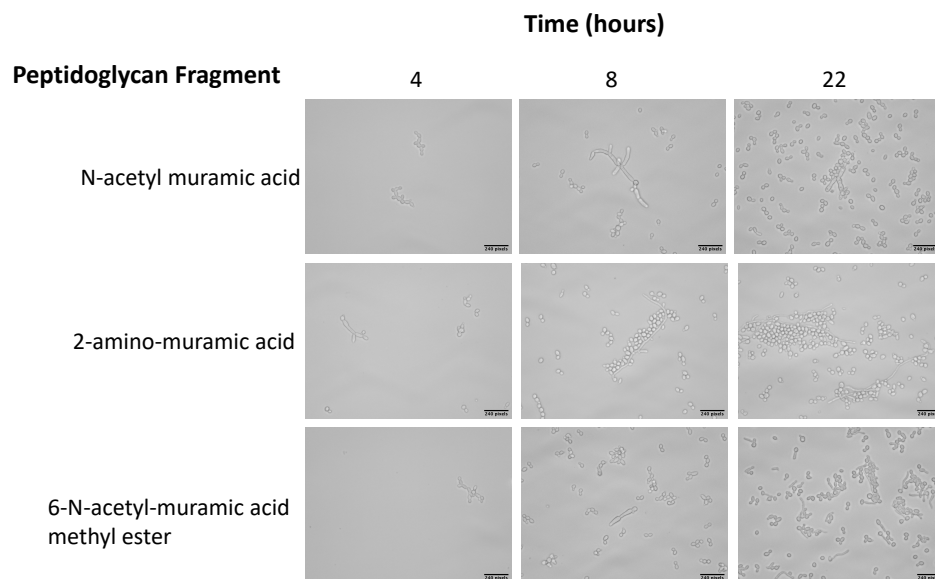


Figure 3.10: Filamentous assessment in the presence of muramic derivatives. 2-amino-muramic acid was the most potent inducer of hyphal morphology comparatively to N-acetyl muramic acid and 6-N-acetyl-muramic acid methyl ester. The former produced hyphae at 8 hours, and maintained this morphology throughout 22 hours, while the latter did not produce true hyphae and displayed pseudohyphae.

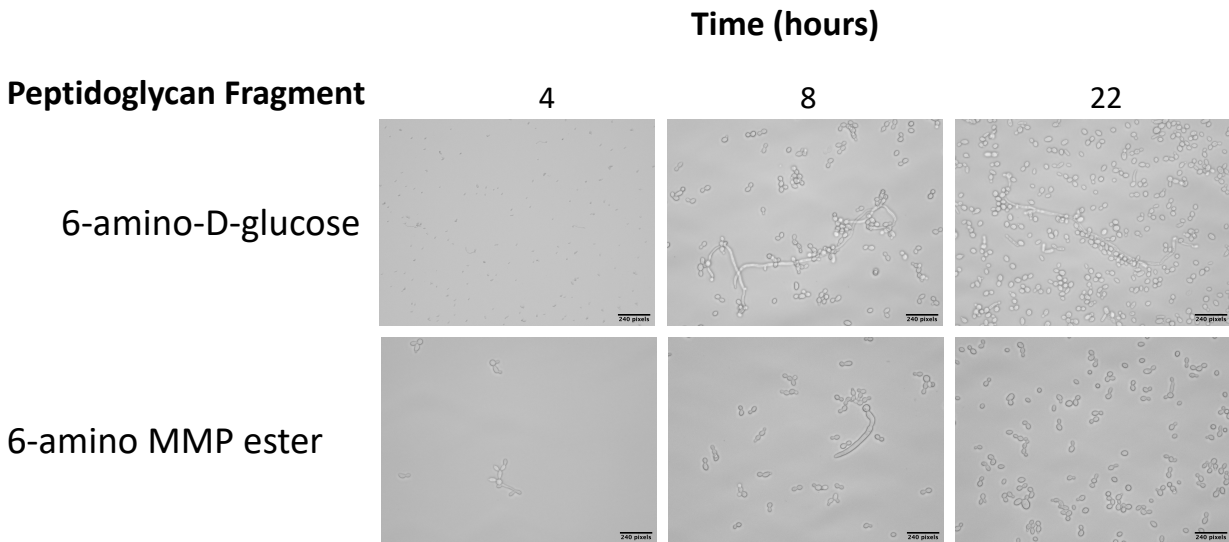


Figure 3.11: Filament assessment is the presence of 6-amino- d-glucose and 6-amino-MMP ester. 6-amino- d-glucose was able to maintain hyphae at 22 hours, but 6-amino MMP ester only induced pseudohyphae at 8 hours, with complete reversion to budding observed at 22 hours.

We probed the ability of wildtype *C. albicans* cells to respond to a plethora of bacterial peptidoglycan fragments by altering its cellular morphology to that of a pathogenic state (filamentous). To do so, we analyzed cells treated with bacterial peptidoglycan fragments via microscopy. Rather than counting cells to determine hyphal percentages, we choose a scale system ranging from 1-5 to arbitrarily identify PG fragments that were true hyphal inducers and maintainers (**Figure 3.12**). Since cells tend to clump together upon hyphal formation we choose not to rely on a counting mechanism for hyphal percentage determination⁴⁰. In our hands, cell counting resulted in a significant amount of variability and loss of data as true hyphal cells are almost always clustered together making it nearly impossible to accurately count all planktonic cells.

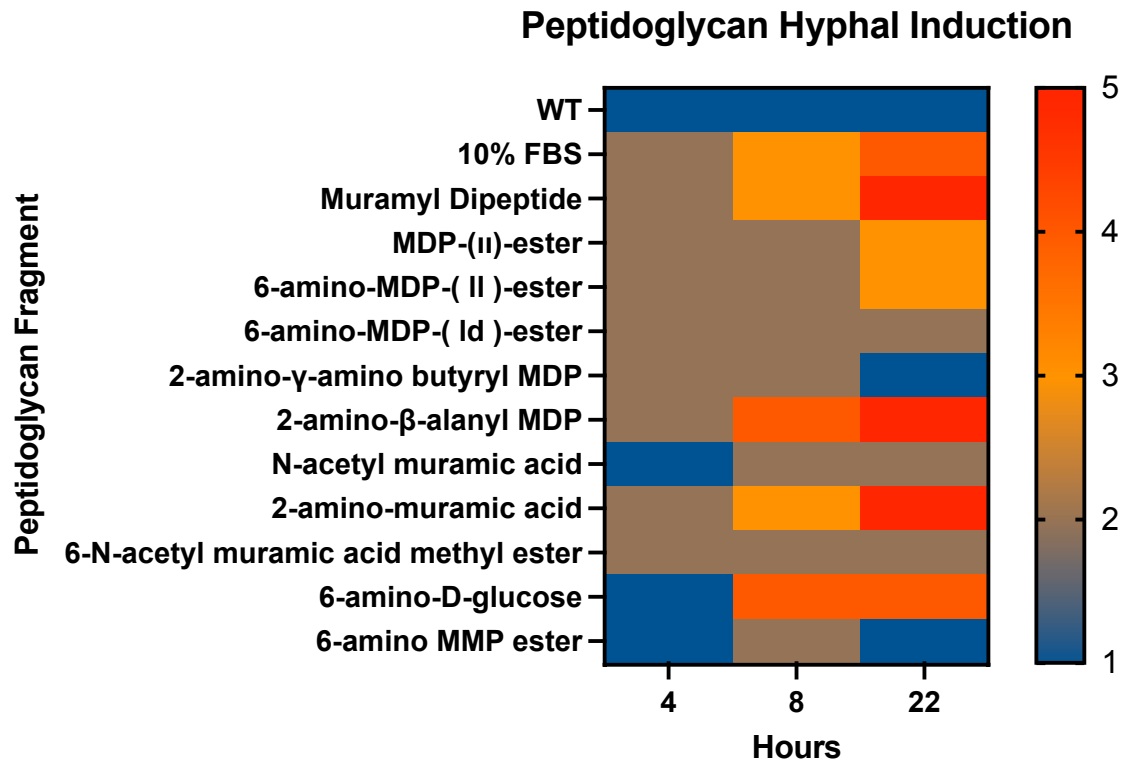


Figure 3.12: Heat map representation of the hyphal inducing ability of peptidoglycan fragments assayed. Fragments that induced and maintained hyphal morphology were MDP, 2-amino-β-alanyl MDP, and 2-amino-muramic acid.

We observed that there are significant differences in the ability of bacterial peptidoglycan fragments to stimulate as well as maintain hyphal formation. In our hands peptidoglycan fragments that were the most potent stimulators of hyphal formation and maintenance relative to Muramyl dipeptide (MDP) and 10% Fetal Bovine Serum (FBS) were 6-amino-MDP-(LL)-ester, 2-amino-β-alanyl MDP, and 2-amino-muramic acid, with the latter being the most potent inducer. Bacterial peptidoglycan fragments MDP-(LL)-ester, 6-amino-MDP-(LD)-ester, and 6-N-acetyl muramic acid methyl ester were able to produce short hyphae that appeared stunted in

their growth. Whereas true hyphae are long filamentous germ tubes that tend to clump together, hyphae formed by these fragments appeared to lack the ability to clump and failed to truly extend. Fragments N-acetyl muramic acid, 6-amino MMP ester, and 2-amino- γ -amino butyryl MDP failed to surpass pseudohyphae and cells were observed to have readily reverted to the budding morphology by 22 hours post treatment.

Collectively, these data suggest that hyphal formation stimulated by bacterial peptidoglycan fragments at large depends on the presence on an amine functional group present on the muramyl moiety either at the 2 or 6 position, rather than the bulkiness of the peptidoglycan fragment. This is supported by lack of hyphal formation in the presence of 6-amino MMP ester, but persistent hyphal formation in the presence of 6-amino-MDP-(LL)-ester. Additionally, previous work done in our lab demonstrated that the LRR domain of Cyr1p is able to bind MTP, which has an additional amino acid in the peptide stem, contains a Lysine as the third peptide in the peptide stem, with (L) stereochemistry¹⁴. Furthermore, we observed a specificity for the stereochemistry of the terminal amino acid in the peptide stem, where 6-amino-MDP-(LL)-ester treated cells presented hyphae 22 hours post induction, whereas 6-amino-MDP-(LD)-ester failed to form true hyphae and remained in a pseudohyphal state.

Noting that 6-amino MMP ester is not sufficient to induce or maintain true hyphae, despite the presence of an amine on the 6-position. We reason that further testing should be conducted with an MMP ester in the absence of a C6 amine, to further analyze the importance of a C6 amine on the carbohydrate backbone and better gauge the importance of the peptide stem. Nonetheless, it appears that in the absence of a peptide stem, a C2 amine off the muramyl moiety is sufficient for hyphal

maintenance at 22 hours. Our analysis also demonstrated that while true hyphae was observed in the presence of 6-amino-D-glucose, cells were still budding at large, suggesting that this compound may be utilized more as a carbon source than hyphal stimulator, as high concentrations of glucose have been implicated in delaying the yeast to hyphae transition, whereas low glucose levels enhance this transition as confirmed by increases in secreted aspartyl proteases (SAP) genes⁴¹. These genes products are considered to be virulent factors of *C. albicans*. In addition, and specifically applicable to this study, as all filamentous assays were conducted in YPD media, studies have demonstrated that high glucose levels appear to delay the hyphae expansion of *C. albicans* even in serum supplemented conditions, whereas low glucose facilitates hyphae development and rapidly enhances SAP5 gene expression during the yeast to hyphae transition⁴¹.

The observation that peptidoglycan fragments differentially regulate hyphal morphology in *C. albicans*, warrants an investigation into transcriptional factors that govern morphology change in this organism. Moreover, the morphological switching from budding to pseudohyphae to budding again in the presence of peptidoglycan fragments such as N-acetyl muramic acid, 6-amino MMP ester, and 2-amino- γ -amino butyryl MDP may be explained by inadequate transcriptional activation of key regulators in the hyphal induction pathway. As such, in chapter 4 we focus on the analysis via RT-PCR of some of the pertinent genes that regulate *C. albicans* morphology.

REFERENCES

1. Silao, F. G. S.; Ljungdahl, P. O., Amino Acid Sensing and Assimilation by the Fungal Pathogen *Candida albicans* in the Human Host. *Pathogens* **2021**, *11* (1).
2. Brown, A.; Haynes, K.; Gow, N. A.; Quinn, J., *Candida* and candidiasis. *Calderone, R., ed* **2002**, 95-106.
3. Uwamahoro, N.; Verma-Gaur, J.; Shen, H.-H.; Qu, Y.; Lewis, R.; Lu, J.; Bambery, K.; Masters, S. L.; Vince, J. E.; Naderer, T., The pathogen *Candida albicans* hijacks pyroptosis for escape from macrophages. *MBio* **2014**, *5* (2), e00003-14.
4. Andes, D. R.; Safdar, N.; Baddley, J. W.; Playford, G.; Reboli, A. C.; Rex, J. H.; Sobel, J. D.; Pappas, P. G.; Kullberg, B. J., Impact of treatment strategy on outcomes in patients with candidemia and other forms of invasive candidiasis: a patient-level quantitative review of randomized trials. *Clinical infectious diseases* **2012**, *54* (8), 1110-1122.
5. Antinori, S.; Milazzo, L.; Sollima, S.; Galli, M.; Corbellino, M., Candidemia and invasive candidiasis in adults: A narrative review. *European journal of internal medicine* **2016**, *34*, 21-28.
6. Samaranayake, L.; MacFarlane, T., The adhesion of the yeast *Candida albicans* to epithelial cells of human origin in vitro. *Archives of oral Biology* **1981**, *26* (10), 815-820.
7. Soll, D. R.; Stasi, M.; Bedell, G., The regulation of nuclear migration and division during pseudo-mycelium outgrowth in the dimorphic yeast *Candida albicans*. *Experimental Cell Research* **1978**, *116* (1), 207-215.
8. Berman, J.; Sudbery, P. E., *Candida albicans*: a molecular revolution built on lessons from budding yeast. *Nature Reviews Genetics* **2002**, *3* (12), 918-931.
9. Chen, H.; Zhou, X.; Ren, B.; Cheng, L., The regulation of hyphae growth in *Candida albicans*. *Virulence* **2020**, *11* (1), 337-348.
10. Shirtliff, M. E.; Peters, B. M.; Jabra-Rizk, M. A., Cross-kingdom interactions: *Candida albicans* and bacteria. *FEMS microbiology letters* **2009**, *299* (1), 1-8.
11. Dižová, S.; Bujdáková, H., Properties and role of the quorum sensing molecule farnesol in relation to the yeast *Candida albicans*. *Die Pharmazie-An International Journal of Pharmaceutical Sciences* **2017**, *72* (6), 307-312.
12. Kornitzer, D., Regulation of *Candida albicans* Hyphal Morphogenesis by Endogenous Signals. *J Fungi (Basel)* **2019**, *5* (1).
13. Xu, X. L.; Lee, R. T.; Fang, H. M.; Wang, Y. M.; Li, R.; Zou, H.; Zhu, Y.; Wang, Y., Bacterial peptidoglycan triggers *Candida albicans* hyphal growth by directly activating the adenylyl cyclase *Cyr1p*. *Cell Host Microbe* **2008**, *4* (1), 28-39.

14. Burch, J. M.; Mashayekh, S.; Wykoff, D. D.; Grimes, C. L., Bacterial Derived Carbohydrates Bind Cyr1 and Trigger Hyphal Growth in *Candida albicans*. *ACS Infectious Diseases* **2018**, *4* (1), 53-58.
15. Crump, G. M.; Rozovsky, S.; Grimes, C. L., Purification and Characterization of a Stable, Membrane-Associated Peptidoglycan Responsive Adenylate Cyclase LRR Domain from Human Commensal *Candida albicans*. *Biochemistry* **2022**.
16. Crump, G. M.; Zhou, J.; Mashayekh, S.; Grimes, C. L., Revisiting peptidoglycan sensing: interactions with host immunity and beyond. *Chemical Communications* **2020**, *56* (87), 13313-13322.
17. Grainha, T.; Jorge, P.; Alves, D.; Lopes, S. P.; Pereira, M. O., Unraveling *Pseudomonas aeruginosa* and *Candida albicans* Communication in Coinfection Scenarios: Insights Through Network Analysis. *Front Cell Infect Microbiol* **2020**, *10*, 550505.
18. Klotz, S. A.; Chasin, B. S.; Powell, B.; Gaur, N. K.; Lipke, P. N., Polymicrobial bloodstream infections involving *Candida* species: analysis of patients and review of the literature. *Diagnostic microbiology and infectious disease* **2007**, *59* (4), 401-406.
19. Huppert, M.; Macpherson, D. A.; Cazin, J., Pathogenesis of *Candida albicans* infection following antibiotic therapy. I. The effect of antibiotics on the growth of *Candida albicans*. *J Bacteriol* **1953**, *65* (2), 171-6.
20. Homei, A.; Worboys, M., Wellcome Trust–Funded Monographs and Book Chapters. In *Fungal Disease in Britain and the United States 1850–2000: Mycoses and Modernity*, Palgrave Macmillan © Aya Homei and Michael Worboys 2013.: Basingstoke (UK), 2013.
21. Wang, S.; Wang, Q.; Yang, E.; Yan, L.; Li, T.; Zhuang, H., Antimicrobial Compounds Produced by Vaginal *Lactobacillus crispatus* Are Able to Strongly Inhibit *Candida albicans* Growth, Hyphal Formation and Regulate Virulence-related Gene Expressions. *Front Microbiol* **2017**, *8*, 564.
22. Tarumoto, N.; Kinjo, Y.; Kitano, N.; Sasai, D.; Ueno, K.; Okawara, A.; Izawa, Y.; Shinozaki, M.; Watarai, H.; Taniguchi, M.; Takeyama, H.; Maesaki, S.; Shibuya, K.; Miyazaki, Y., Exacerbation of Invasive *Candida albicans* Infection by Commensal Bacteria or a Glycolipid Through IFN- γ Produced in Part by iNKT Cells. *The Journal of Infectious Diseases* **2013**, *209* (5), 799-810.
23. Newman, S. L.; Bhugra, B.; Holly, A.; Morris, R. E., Enhanced killing of *Candida albicans* by human macrophages adherent to type 1 collagen matrices via induction of phagolysosomal fusion. *Infect Immun* **2005**, *73* (2), 770-7.
24. Lynch, A. S.; Robertson, G. T., Bacterial and fungal biofilm infections. *Annu Rev Med* **2008**, *59*, 415-28.
25. Tan, C. T.; Xu, X.; Qiao, Y.; Wang, Y., A peptidoglycan storm caused by β -lactam antibiotic's action on host microbiota drives *Candida albicans* infection. *Nat Commun* **2021**, *12* (1), 2560.

26. Sarkar, P.; Yarlagadda, V.; Ghosh, C.; Haldar, J., A review on cell wall synthesis inhibitors with an emphasis on glycopeptide antibiotics. *Medchemcomm* **2017**, *8* (3), 516-533.
27. Mason, K. L.; Erb Downward, J. R.; Mason, K. D.; Falkowski, N. R.; Eaton, K. A.; Kao, J. Y.; Young, V. B.; Huffnagle, G. B., Candida albicans and bacterial microbiota interactions in the cecum during recolonization following broad-spectrum antibiotic therapy. *Infect Immun* **2012**, *80* (10), 3371-80.
28. Theriot, C. M.; Koumpouras, C. C.; Carlson, P. E.; Bergin, II; Aronoff, D. M.; Young, V. B., Cefoperazone-treated mice as an experimental platform to assess differential virulence of Clostridium difficile strains. *Gut Microbes* **2011**, *2* (6), 326-34.
29. Erb Downward, J. R.; Falkowski, N. R.; Mason, K. L.; Muraglia, R.; Huffnagle, G. B., Modulation of Post-Antibiotic Bacterial Community Reassembly and Host Response by Candida albicans. *Scientific Reports* **2013**, *3* (1), 2191.
30. Grimes, C. L.; Ariyananda Lde, Z.; Melnyk, J. E.; O'Shea, E. K., The innate immune protein Nod2 binds directly to MDP, a bacterial cell wall fragment. *J Am Chem Soc* **2012**, *134* (33), 13535-7.
31. DeMeester, K. E.; Liang, H.; Jensen, M. R.; Jones, Z. S.; D'Ambrosio, E. A.; Scinto, S. L.; Zhou, J.; Grimes, C. L., Synthesis of Functionalized N-Acetyl Muramic Acids To Probe Bacterial Cell Wall Recycling and Biosynthesis. *J Am Chem Soc* **2018**, *140* (30), 9458-9465.
32. Park, J. T.; Uehara, T., How bacteria consume their own exoskeletons (turnover and recycling of cell wall peptidoglycan). *Microbiology and Molecular Biology Reviews* **2008**, *72* (2), 211-227.
33. Barnard, M. R.; Holt, S. C., Isolation and characterization of the peptidoglycans from selected gram-positive and gram-negative periodontal pathogens. *Can J Microbiol* **1985**, *31* (2), 154-60.
34. Strominger, J. L.; Park, J. T.; Thompson, R. E., Composition of the cell wall of Staphylococcus aureus: its relation to the mechanism of action of penicillin. *J. biol. Chem* **1959**, *234* (12), 3263-3268.
35. Melnyk, J. E.; Mohanan, V.; Schaefer, A. K.; Hou, C. W.; Grimes, C. L., Peptidoglycan Modifications Tune the Stability and Function of the Innate Immune Receptor Nod2. *J Am Chem Soc* **2015**, *137* (22), 6987-90.
36. Brown, A. R.; Wodzanowski, K. A.; Santiago, C. C.; Hyland, S. N.; Follmar, J. L.; Asare-Okai, P.; Grimes, C. L., Protected N-Acetyl Muramic Acid Probes Improve Bacterial Peptidoglycan Incorporation via Metabolic Labeling. *ACS Chemical Biology* **2021**, *16* (10), 1908-1916.
37. Samaranayake, Y. H.; Cheung, B. P.; Yau, J. Y.; Yeung, S. K.; Samaranayake, L. P., Human serum promotes Candida albicans biofilm growth and virulence gene expression on silicone biomaterial. *PLoS One* **2013**, *8* (5), e62902.
38. Aoki, W.; Ueda, T.; Tatsukami, Y.; Kitahara, N.; Morisaka, H.; Kuroda, K.; Ueda, M., Time-course proteomic profile of Candida albicans during adaptation to a fetal serum. *Pathog Dis* **2013**, *67* (1), 67-75.

39. Irazoki, O.; Hernandez, S. B.; Cava, F., Peptidoglycan muropeptides: release, perception, and functions as signaling molecules. *Frontiers in microbiology* **2019**, *10*, 500.
40. Brand, A.; Gow, N. A., Mechanisms of hypha orientation of fungi. *Curr Opin Microbiol* **2009**, *12* (4), 350-7.
41. Buu, L.-M.; Chen, Y.-C., Impact of glucose levels on expression of hypha-associated secreted aspartyl proteinases in *Candida albicans*. *Journal of Biomedical Science* **2014**, *21* (1), 22.

Chapter 4

ANOMALOUS HYPHAE SPECIFIC GENE EXPRESSION PROFILES IN C.ALBICANS CELLS TREATED WITH BACTERIAL OEOTIDOGLYCAN FRAGMENTS

4.1 Introduction

Candida albicans (*C. albicans*) is the most frequently isolated human fungal pathogen and can cause a variety of infections, especially in an immune compromised population¹. This fungal pathogen can grow in different morphologies: unicellular yeast cells, psuedohyphae, and true hyphae². The morphological plasticity exhibited by this fungal pathogen is a key virulence trait, as formation of hyphae is involved in adhesion to and invasion of host cells and tissues, while yeast cells are required for dissemination into the bloodstream^{3,4}. Each growth form of *C. albicans* is unique in their interactions with host cells. Whereas budding yeast cells are recognized and engulfed by human macrophages, cells that are hyphal in morphology can destroy macrophages by early induction of pyroptosis, toxin production, and host nutrient consumption, among many others⁵⁻⁷.

Several endogenous and environmental stimuli have been proven to affect the morphological transformation of *C. albicans* and subsequent virulence. Common stimuli for to yeast to pseudo/hyphae transition include but are not limited to temperatures of 37°C, serum, neutral pH, and hormones^{1, 8-10}. In addition,

morphological switching is controlled by the protein products of specific *C. albicans* genes, which direct the spore to become a germ tube or mycelium, and subsequently contribute to adhesion. Collectively, the transcription factors that govern this morphological transition are known as hypha specific genes (HSGs) and have been implicated in major signaling pathways (**Figure 4.1**). Signaling pathways identified that respond to filament inducing conditions, including a mitogen-activated protein (MAP) kinase pathway, the cyclic AMP (cAMP)/ protein kinase A (PKA) pathway and a pH response pathway, among others¹¹. Each pathway is associated with specific transcription factors that are either upregulated or downregulated¹²⁻¹⁵. Some of the most studied HSGs include UME6, Hyphal Wall Protein1 (HWP1), Extend of Cell Elongation (ECE1), Agglutin-like Sequence (ALS3), Tup1, and Nrg1 which are all known to regulate major pathways¹⁶.

UME6 is a novel filament-specific regulator of *C. albicans* hyphal extension that encodes an 843 amino-acid protein with a zinc-finger DNA-binding domain¹⁷. Research has demonstrated that UME6 mutant strains of *C. albicans* are completely deficient in hyphal formation under all hyphae stimulating conditions¹⁸. Induction of UME6 occurs via serum and temperatures of 37°C and repression has been associated with the Nrg1-Tup1^{2, 19}. As such, its expression promotes hyphal elongation.

Extent of Cell Elongation 1 (ECE1) is a specific hyphal gene encoding a membrane protein dependent on the cAMP pathway²⁰. The protein is closely related to the extension of hyphae and is hallmarked by an increased expression during mycelial growth but is not absolute for the initial occurrence of morphology. Birse et al., demonstrated that the shape of *C. albicans* does not change in ECE1 deleted cell strains²⁰. Additionally, the ECE1 gene product has been reported to be the transcript

with the highest abundance in *C. albicans* hyphae, independently of the environmental stimuli that triggered filamentation²¹.

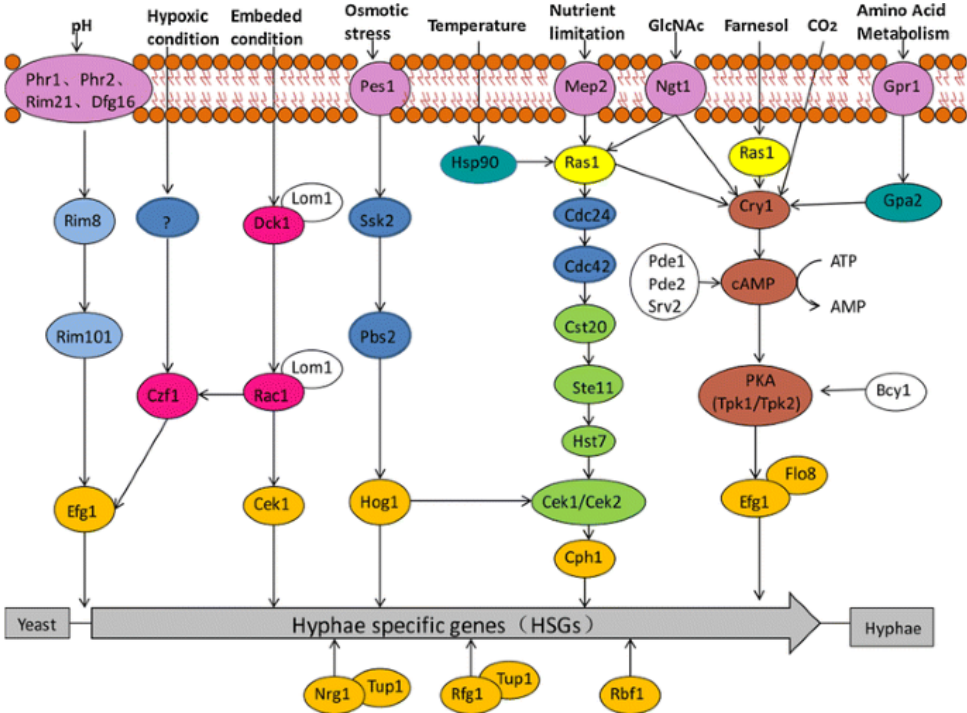


Figure 4.1: Hyphae specific gene regulatory pathways in *C. albicans*. Several major pathways are involved in the regulation of the morphological plasticity of *C. albicans*. Morphological regulation can occur via acidic pH, bacterial peptidoglycan, quorum sensing molecules, etc.

The HWP1 gene is perhaps the most specific gene for hyphal growth, as it encodes a cell wall mannose protein that is essential for normal growth of the mycelium¹⁶. Specifically, it encodes a putative GPI-linked surface protein that has been localized to the cell surface via immunofluorescence labeling studies²². It appears to be a requirement for adhesion, as HWP1-mutated cells demonstrated retained

ability to infect mouse models, though with little virulence²³. Additionally, HWP1 mutant cells infect host in shorter than spans than non HWP1 mutated cells, and is engulfed and cleared by host cells (mouse models) in a relatively short period of time, indicative that HWP1 mutants could not stably adhere to the epithelial mucosal cells²³. Furthermore, deletion analysis of HWP1 demonstrates that the gene is conditionally required for hyphal growth formation. For instance, the ability to form hyphae on solid media was severely reduced in HWP1 heterozygous mutants and eliminated in null mutants²⁴.

The hyphae specific gene ALS3 encodes a multifunctional protein involved in adhesion, invasion, and iron acquisition²⁵⁻²⁷. It is expressed by hyphae and pseudohyphae but not budding cells^{28,29}. The encoded protein is processed intracellularly into eight peptides, of which one is candidalysin³⁰⁻³². Candidalysin is secreted from hyphae into localized environments and mediates host cell cytolysis³³. Promoter analysis reveals that the protein contains two repressor regions, in which hyphae specific repressors Tup1, Nrg1, and Rfg1 downregulate ALS3 transcription by binding to the two repression regions³⁴.

TUP1 was first identified by Braun et al, as a transcriptional repressor of genes whose expression generates filamentation and has also been demonstrated to play key roles of phase switching regulation³⁵. It interacts with other corepressors, whose complexes function with DNA binding proteins to repress gene expression³⁶. Of the DNA binding proteins identified to interact with Tup1 is Nrg1, another hyphal transcriptional repressor. Deletion of TUP1 results in the upregulation of approximately one-third of *C. albicans* genes^{19,37}, and homozygous tup1 mutants are unable to grow as yeast and therefore remain in a constitutive filamentous form

regardless of media³⁸. As such, the activation of Tup1 transcription repressor complexes results in the repression of HSG expression^{19, 35, 37, 39}.

Nrg1 is a DNA-binding protein that represses filamentation growth via the Tup1 pathway and has also been shown to repress UME6 under non-filament conditions⁴⁰. It is also down regulated in response to serum and temperatures as well as neutral pH, thereby suggesting that UME6 and NRG1 may function together in a coordinated manner to control induction of HSGs in response to a plethora of specific inducing conditions and signaling pathways³⁹. Additionally, nrg1 mutants are highly filamentous under non-filamentous conditions similarly to tup1 mutants^{18, 37}.

Several studies have focused on the morphological transitions of *C. albicans* as it pertains to pathogenicity. Many of these studies have included characterization of filament size, filament size differences in biofilm, liquid media, solid support, etc.^{12, 13, 41, 42}. The characterization of transcriptional response to filamentous growth under various stimuli is currently on the cusp of expansion. Of particular interest is the transcriptional response to bacterial peptidoglycan stimuli. To date, not many studies have characterized the transcriptional response to filament inducing stimuli caused bacterial peptidoglycan. Bacterial peptidoglycan is unique to bacterial cells, both Gram (-) and Gram (+) alike. It is a complex polymer consisting of alternating units of N-acetyl muramic acid (NAM), and N-acetyl glucosamine (GlcNac), with a pentapeptide stem branching from the NAM moiety⁴³⁻⁴⁵. The prevalence of *C. albicans* interactions with bacterial cells is heavily documented, as they exist in polymicrobial communities in the human microbiome, and *C. albicans* infections are almost always isolated with bacterial species, both Gram (-) and Gram (+)⁴⁶⁻⁵⁰.

Furthermore, as *C. albicans* infections are exacerbated in the presence of bacteria, and more specifically the presence of bacterial peptidoglycan⁵¹, the underlying mechanism of this relationship remains elusive. Elucidating the transcriptional response garnered by bacterial peptidoglycan, can provide insights into the mechanisms of pathogenicity that ensues when *C. albicans* cells encounter bacterial fragments in the localized environment. We aim to examine the basis for hyphal filament extension caused specifically by bacterial peptidoglycan by focusing on the transcriptional components that are important for controlling induction and maintaining expression of *C. albicans* filamentous growth program.

4.2 Materials and Methods

4.2.1 Materials

Candida albicans wildtype cells used in this study were strain SC5314/ ATCC MYA-2876. Bacterial peptidoglycan fragment 2-amino muramic acid was synthesized in house by our laboratory member Stephen Hyland. N-acetyl muramic acid (NAM) and YPD broth was purchased from Sigma Aldrich and Fetal Bovine Serum (FBS) from R&D Systems Clinical Controls. YeaStar yeast RNA extraction kits were purchased from Zymo Research and the iScript cDNA synthesis kit was purchased from Bio-Rad. 96 well plates were purchased from Corning Biosciences, and all other consumables were purchased from ThermoFisher or their subsidiaries. PCR analysis was conducted on a Bio-Rad CFX96 thermocycler.

4.2.2 Growth of cells for RNA Isolation

C. albicans SC5314 cells were grown overnight to log phase in YPD media. 1 mL of the saturated overnight cells was harvested and washed twice with sterile 1x

Phosphate Buffered Saline (PBS). Washed cells were resuspended into fresh YPD and diluted to OD₆₀₀ 0.5 in replicates of 3. Cells were then treated with 1 mM of either NAM, 10% FBS, water (control) or 2-amino muramic acid. Treated cells were mixed thoroughly and then aliquoted into 96 well plates, with 200 µL per well. The 96 well plates containing cells were then placed into an enclosed plastic container with water at the bottom, (taking care to ensure that the 96 well plate did not come into contact with the water) and incubated at 37°C for 22 hours.

4.2.3 RNA Isolation

RNA isolation was conducted according to the manufacturer's instructions in the YeaStar RNA isolation kit. Briefly, harvested yeast pellets were resuspended in buffer and digested with Zymolyase for 60 minutes at 30°C. Cells were lysed and RNA was extracted from Zymo-Spin column included in the kit. RNA was eluted from the column with 30 µL of nuclease free water under sterile conditions. RNA was quantified using nanodrop and immediately reverse transcribed to cDNA.

4.2.4 cDNA Synthesis

cDNA was synthesized using the Bio-Rad iScript cDNA synthesis kit. 1 µg of RNA was reverse transcribed in replicates of two, according to the manufacturer's instructions. Briefly, 1 µg of RNA template was added to a reaction mix containing 1x iScript Reaction Mix, 1 µL iScript Reverse Transcriptase and nuclease free water to 20 µL total volume. The reaction mix was incubated in a thermal cycler using the following protocol:

Table 4.1: cDNA Synthesis protocol

Priming	5 min at 25°C
Reverse transcription	20 min at 46°C
RT Inactivation	1 min at 95°C
Hold	Hold at 4°C

cDNA concentrations were quantified using a nanodrop. 100 ng working stocks were made from each synthesized sample for qPCR analysis.

4.2.5 RT-qPCR of mRNA levels

PCR reactions were conducted on a 10 μ L scale. The reaction mixture included 1x yellow sample buffer, 10 ng template DNA, 100 nM forward and reverse primers, 1X PowerTrack SYBR Green Master Mix and nuclease free water to 10 μ L final volume. After a 95°C denaturation step for 5 min, the amplification program consisted of 40 cycles of 95°C for 15 s, 60°C for 15 s and 72°C for 30 s. At the end of the program, a melting curve was conducted to verify the specificity of the PCR products. The resulting data were analyzed in Microsoft Excel to determine the relative differences in gene expression, which were normalized to the level of ACT1 mRNA in each sample. The results represent the average of at least two independent preparations of cells (biological replicates). Two sets of assays, each done in triplicate, were carried out on each RNA preparation (technical replicates). Primer sequences used for RT-qPCR analysis are as follows:

Table 4.2: Primers used in this study for RT-qPCR analysis

Gene	Primer Sequence	PCR Product size (bp)	References

ACT1	F-5'-TCCAGAAGCTTTGTTTCAGACCAGC-3' R-5'-TGCATACGTTTCAGCAATACCTGGG-3'	170	52, 53
HWP1	F-5'-GCTCCTGCCACTGAACCTTCCC-3' R-5'-ACTTGAGCCAGCTGGAGCGG-3'	63	52
ECE-1	F-5'-TGGCGTTCCAGATGTTGGCCT-3' R-5'-GCTAAGTGCTACTGAGCCGGCA-3'	227	52
TUP1	CTCTTGGCGACAGGTGCAG GTGGTGACGCCGTCTTCGA	224	54

4.3 Results and Discussions

One of the most important attributes of the human commensal *C. albicans* is the morphological transition from budding growth to a filamentous growth⁵⁵.

Filaments, or germ tubes occur in either pseudohyphal or hyphal form. The hyphal form in particular is associated with virulence characteristics such as tissue invasion, breaching of endothelial cells and lysis of macrophages and neutrophils⁵⁶. Though the importance of hyphal formation has already been established, we aimed to further characterize the formation of hyphae as a direct response to bacterial peptidoglycan fragments. The interactions of *C. albicans* and bacterial peptidoglycan has been well characterized⁵⁷⁻⁶⁰ and is of increasing importance as an exacerbation of *C. albicans* infections is observed in the presence of bacterial peptidoglycan fragments⁵¹.

Despite the documented ability of bacterial peptidoglycan to stimulate the yeast to hyphae transition in *C. albicans*, little is known about the regulatory mechanisms that control this process. In this study, we aimed to correlate the transcriptional regulation of known Hyphae Specific Genes (HSGs) Hyphal Wall Protein 1, Extend of Cellular Elongation 1(ECE1), and Tup1 to hyphal formation in

wildtype *C. albicans* cells stimulated with bacterial peptidoglycan fragments N-acetyl muramic acid (NAM), and 2- amino muramic acid (MA). We compared the transcriptional response from these bacterial peptidoglycan fragments to known hyphal stimulator 10% Fetal Bovine Serum (FBS).

Based on our observations, HWP1 was not consistently upregulated in the presence of hyphal growth. In our FBS positive control samples, HWP1 showed a consistent decrease over the 22-hour time course despite the persistence of hyphal growth upon microscopic analysis of cells (**Figure 4.2**). The least hyphal stimulating bacterial peptidoglycan fragment, based on our phenotypic screening (chapter 3) was NAM. Surprisingly, HWP1 showed increased expression from 4 to 22 hours in NAM treated cells (**Figure 4.3a**). The most potent inducer of hyphal growth based on our phenotypic analysis (refer to chapter 3) was 2-amino muramic acid. Our gene analysis demonstrated downregulation of HWP1 from 4 to 8 hours, with an increase at 22 hours (**Figure 4.3b**). These results are closely related to the HWP1 gene expression profile observed in FBS. For all peptidoglycan treated samples, ECE1 was consistently downregulated across the 22 hours analysis. The HSG repressor TUP1 was downregulated consistently in FBS, and NAM treated samples (**Figures 4.2-4.3**). A similar pattern was observed for the 2-amino muramic acid samples, in which TUP1 expression was increased at the 8-hour time point, but down regulated at 4 and 22 hours (**Figure 4.3b**)

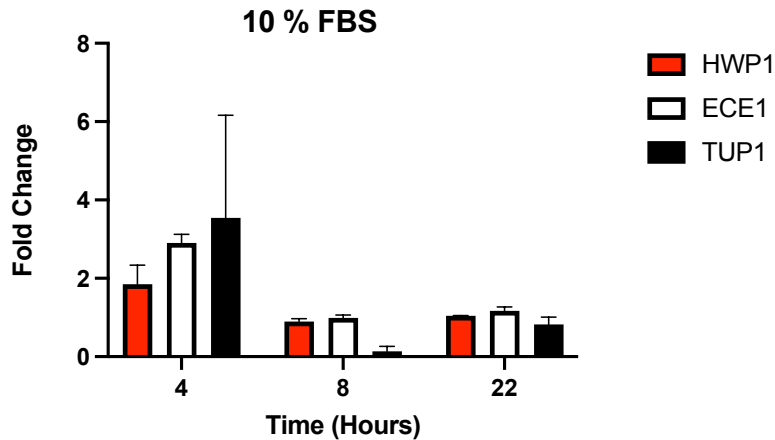


Figure 4.2: Hyphae Specific Gene expression in cells treated with 10% FBS. The HWP1 transcript was not consistently upregulated during the 22-hour time course treatment. TUP1 was downregulated at 8 hours but appeared upregulated at 22 hours relative to the 8-hour time point. ECE1 was downregulated over the treatment course.

Collectively our data failed to demonstrate significant induction of HSGs HWP1 and ECE1. Analysis of filamentous cells formed by treatment with FBS and 2-amino muramic acid indicate that they were indeed true hyphae. These results could suggest that high levels of HSG induction is not required to promote hyphal growth in the presence of bacterial peptidoglycan fragments. In fact, several studies have reported that hyphal morphogenesis and HSG expression can be regulated independently^{21, 52, 61}. While these preliminary data could imply that bacterial peptidoglycan fragments can transduce a signal to induce hyphal morphogenesis that is distinct from transcriptional regulation, additional experimentation must be conducted

with other pertinent HSGs such as UME6, NRG1, and ALS3 to gather a broader transcriptional response.

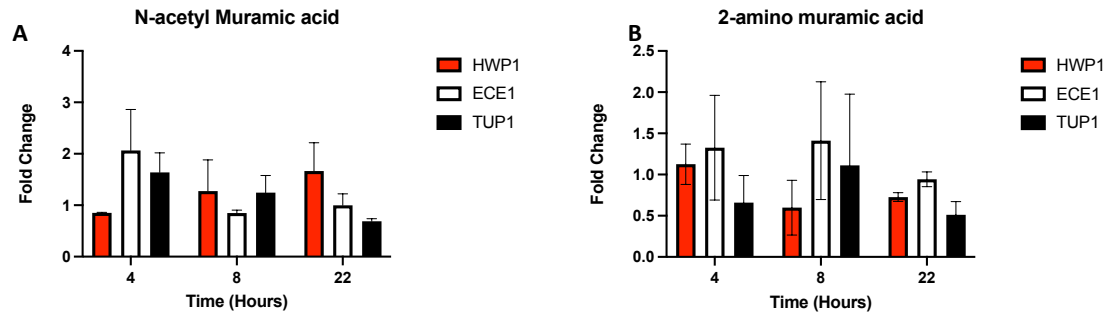


Figure 4.3: Hyphae specific gene expression in cells treated with a) NAM and b) 2-amino muramic acid. NAM treated cells showed a consistent upregulation of HWP1 throughout the 22-hour time course, downregulation of ECE1, and TUP1. MA treated cells displayed no trends in expression patterns of HSGs, as well as HWP1, ECE1, and TUP1 transcripts were neither consistently increased nor decreased throughout the 22-hour analysis window.

The transcriptional regulation of the morphological transition between the budding and pseudohyphal/hyphal form of the human commensal *C. albicans* is a multigene network interwoven with many juxtaposed signaling networks. Of the eight chromosomes that are present in *Candida albicans*, with a total size of 14,324,317bp including 14,283,897 bp in nuclear genome, and 40,420 in the mitochondrial genome, there are 6,419 open reading frames (ORFs) with approximately 20% of ORFs still remaining to be identified⁶². As such, there are many issues surrounding the morphological transitions that require further exploration. Particularly, the presence of other unexplored transcriptional factors, the exact mechanisms of known transcriptional factors, and the details of the signal transduction pathways are yet to be

elucidated. We reason that the anomalies observed in the gene expression profile of HWP1 and ECE1 compared to some literature precedents reflect inadequate knowledge of all known transcriptional regulators of hyphal formation.

These studies, though preliminary, have piqued our interest into the mechanism by which *C. albicans* responds to bacterial peptidoglycan transcriptionally. To further expand our knowledge set, we reason that RNA-sequencing of samples treated with bacterial peptidoglycan fragments will provide a more conclusive picture into the transcriptional program responsible for some of the dynamic bacterial-fungal relationships.

REFERENCES

1. Brown, A.; Haynes, K.; Gow, N. A.; Quinn, J., *Candida and candidiasis*. *Calderone, R., ed* **2002**, 95-106.
2. Ruben, S.; Garbe, E.; Mogavero, S.; Albrecht-Eckardt, D.; Hellwig, D.; Häder, A.; Krüger, T.; Gerth, K.; Jacobsen, I. D.; Elshafee, O.; Brunke, S.; Hünninger, K.; Kniemeyer, O.; Brakhage, A. A.; Morschhäuser, J.; Hube, B.; Vylkova, S.; Kurzai, O.; Martin, R., Ahr1 and Tup1 Contribute to the Transcriptional Control of Virulence-Associated Genes in *Candida albicans*. *mBio* **2020**, *11* (2), e00206-20.
3. Zakikhany, K.; Naglik, J. R.; Schmidt-Westhausen, A.; Holland, G.; Schaller, M.; Hube, B., In vivo transcript profiling of *Candida albicans* identifies a gene essential for interepithelial dissemination. *Cellular microbiology* **2007**, *9* (12), 2938-2954.
4. Mavor, A.; Thewes, S.; Hube, B., Systemic fungal infections caused by *Candida* species: epidemiology, infection process and virulence attributes. *Current drug targets* **2005**, *6* (8), 863-874.
5. Wellington, M.; Koselny, K.; Krysan, D. J., *Candida albicans* morphogenesis is not required for macrophage interleukin 1 β production. *MBio* **2013**, *4* (1), e00433-12.
6. Kasper, L.; König, A.; Koenig, P.-A.; Gresnigt, M. S.; Westman, J.; Drummond, R. A.; Lionakis, M. S.; Groß, O.; Ruland, J.; Naglik, J. R., The fungal peptide toxin Candidalysin activates the NLRP3 inflammasome and causes cytolysis in mononuclear phagocytes. *Nature communications* **2018**, *9* (1), 1-20.
7. Tucey, T. M.; Verma, J.; Harrison, P. F.; Snelgrove, S. L.; Lo, T. L.; Scherer, A. K.; Barugahare, A. A.; Powell, D. R.; Wheeler, R. T.; Hickey, M. J., Glucose homeostasis is important for immune cell viability during *Candida* challenge and host survival of systemic fungal infection. *Cell metabolism* **2018**, *27* (5), 988-1006. e7.
8. Lo, H.-J.; Köhler, J. R.; DiDomenico, B.; Loebenberg, D.; Cacciapuoti, A.; Fink, G. R., Nonfilamentous *C. albicans* mutants are avirulent. *Cell* **1997**, *90* (5), 939-949.
9. Odds, F., *Candida and Candidosis* (Baillière Tindall, London, UK). **1988**.
10. Saville, S. P.; Lazzell, A. L.; Monteagudo, C.; Lopez-Ribot, J. L., Engineered control of cell morphology in vivo reveals distinct roles for yeast and filamentous forms of *Candida albicans* during infection. *Eukaryotic cell* **2003**, *2* (5), 1053-1060.

11. Carlisle, P. L.; Kadosh, D., *Candida albicans* Ume6, a filament-specific transcriptional regulator, directs hyphal growth via a pathway involving Hgc1 cyclin-related protein. *Eukaryot Cell* **2010**, *9* (9), 1320-8.
12. Berman, J.; Sudbery, P. E., *Candida albicans*: a molecular revolution built on lessons from budding yeast. *Nature Reviews Genetics* **2002**, *3* (12), 918-931.
13. Biswas, S.; Van Dijck, P.; Datta, A., Environmental sensing and signal transduction pathways regulating morphopathogenic determinants of *Candida albicans*. *Microbiology and Molecular Biology Reviews* **2007**, *71* (2), 348-376.
14. Ernst, J. F., Transcription factors in *Candida albicans*—environmental control of morphogenesis. *Microbiology* **2000**, *146* (8), 1763-1774.
15. Mitchell, A. P., Dimorphism and virulence in *Candida albicans*. *Current opinion in microbiology* **1998**, *1* (6), 687-692.
16. Fan, Y.; He, H.; Dong, Y.; Pan, H., Hyphae-Specific Genes HGC1, ALS3, HWP1, and ECE1 and Relevant Signaling Pathways in *Candida albicans*. *Mycopathologia* **2013**, *176* (5), 329-335.
17. Kadosh, D.; Johnson, A. D., Induction of the *Candida albicans* filamentous growth program by relief of transcriptional repression: a genome-wide analysis. *Molecular biology of the cell* **2005**, *16* (6), 2903-2912.
18. Zeidler, U.; Lettner, T.; Lassnig, C.; Müller, M.; Lajko, R.; Hintner, H.; Breitenbach, M.; Bito, A., UME6 is a crucial downstream target of other transcriptional regulators of true hyphal development in *Candida albicans*. *FEMS yeast research* **2009**, *9* (1), 126-142.
19. Murad, A.; d'Enfert, C.; Gaillardin, C.; Tourneau, H.; Tekaia, F.; Talibi, D., D. 20 Marechal, V. Marchais, J. Cottin, and AJ Brown. 2001. Transcript profiling in 21 *Candida albicans* reveals new cellular functions for the transcriptional repressors 22 CaTup1, CaMig1 and CaNrg1. *Mol. Microbiol* *42*, 981-93.
20. Birse, C.; Irwin, M.; Fonzi, W.; Sypherd, P., Cloning and characterization of ECE1, a gene expressed in association with cell elongation of the dimorphic pathogen *Candida albicans*. *Infection and immunity* **1993**, *61* (9), 3648-3655.
21. Martin, R.; Albrecht-Eckardt, D.; Brunke, S.; Hube, B.; Hünninger, K.; Kurzai, O., A core filamentation response network in *Candida albicans* is restricted to eight genes. *PloS one* **2013**, *8* (3), e58613.
22. Staab, J. F.; Ferrer, C. A.; Sundstrom, P., Developmental Expression of a Tandemly Repeated, Proline-and Glutamine-rich Amino Acid Motif on Hyphal Surfaces of *Candida albicans* (*). *Journal of Biological Chemistry* **1996**, *271* (11), 6298-6305.
23. Tsuchimori, N.; Sharkey, L. L.; Fonzi, W. A.; French, S. W.; Edwards Jr, J. E.; Filler, S. G., Reduced virulence of HWP1-deficient mutants of *Candida albicans* and their interactions with host cells. *Infection and immunity* **2000**, *68* (4), 1997-2002.
24. Sharkey, L. L.; McNemar, M. D.; Saporito-Irwin, S. M.; Sypherd, P. S.; Fonzi, W. A., *HWP1* Functions in the Morphological Development of *Candida albicans* Downstream of *EFG1*, *TUP1*, and *RBF1*. *Journal of Bacteriology* **1999**, *181* (17), 5273-5279.

25. Almeida, R. S.; Brunke, S.; Albrecht, A.; Thewes, S.; Laue, M.; Edwards Jr, J. E.; Filler, S. G.; Hube, B., The hyphal-associated adhesin and invasin Als3 of *Candida albicans* mediates iron acquisition from host ferritin. *PLoS pathogens* **2008**, *4* (11), e1000217.
26. Phan, Q. T.; Myers, C. L.; Fu, Y.; Sheppard, D. C.; Yeaman, M. R.; Welch, W. H.; Ibrahim, A. S.; Edwards Jr, J. E.; Filler, S. G., Als3 is a *Candida albicans* invasin that binds to cadherins and induces endocytosis by host cells. *PLoS biology* **2007**, *5* (3), e64.
27. Zhao, X.; Oh, S.-H.; Cheng, G.; Green, C. B.; Nuessen, J. A.; Yeater, K.; Leng, R. P.; Brown, A. J.; Hoyer, L. L., ALS3 and ALS8 represent a single locus that encodes a *Candida albicans* adhesin; functional comparisons between Als3p and Als1p. *Microbiology* **2004**, *150* (7), 2415-2428.
28. Argimón, S.; Wishart, J. A.; Leng, R.; Macaskill, S.; Mavor, A.; Alexandris, T.; Nicholls, S.; Knight, A. W.; Enjalbert, B.; Walmsley, R., Developmental regulation of an adhesin gene during cellular morphogenesis in the fungal pathogen *Candida albicans*. *Eukaryotic cell* **2007**, *6* (4), 682-692.
29. Hoyer, L. L.; Payne, T. L.; Bell, M.; Myers, A. M.; Scherer, S., *Candida albicans* ALS3 and insights into the nature of the ALS gene family. *Current genetics* **1998**, *33* (6), 451-459.
30. Moyes, D. L.; Wilson, D.; Richardson, J. P.; Mogavero, S.; Tang, S. X.; Wernecke, J.; Höfs, S.; Gratacap, R. L.; Robbins, J.; Runglall, M., Candidalysin is a fungal peptide toxin critical for mucosal infection. *Nature* **2016**, *532* (7597), 64-68.
31. Bader, O.; Krauke, Y.; Hube, B., Processing of predicted substrates of fungal Kex2 proteinases from *Candida albicans*, *C. glabrata*, *Saccharomyces cerevisiae* and *Pichia pastoris*. *BMC microbiology* **2008**, *8* (1), 1-16.
32. Richardson, J. P.; Mogavero, S.; Moyes, D. L.; Blagojevic, M.; Krüger, T.; Verma, A. H.; Coleman, B. M.; De La Cruz Diaz, J.; Schulz, D.; Ponde, N. O., Processing of *Candida albicans* Ece1p is critical for candidalysin maturation and fungal virulence. *MBio* **2018**, *9* (1), e02178-17.
33. Moyes, D. L.; Naglik, J. R., The mycobiome: influencing IBD severity. *Cell Host Microbe* **2012**, *11* (6), 551-2.
34. Liu, Y.; Filler, S. G., *Candida albicans* Als3, a multifunctional adhesin and invasin. *Eukaryot Cell* **2011**, *10* (2), 168-73.
35. Braun, B. R.; Head, W. S.; Wang, M. X.; Johnson, A. D., Identification and characterization of TUP1-regulated genes in *Candida albicans*. *Genetics* **2000**, *156* (1), 31-44.
36. Kaneko, A.; Umeyama, T.; Utena-Abe, Y.; Yamagoe, S.; Niimi, M.; Uehara, Y., Tcc1p, a novel protein containing the tetratricopeptide repeat motif, interacts with Tup1p to regulate morphological transition and virulence in *Candida albicans*. *Eukaryotic cell* **2006**, *5* (11), 1894-1905.
37. Murad, A. M. A.; Leng, P.; Straffon, M.; Wishart, J.; Macaskill, S.; MacCallum, D.; Schnell, N.; Talibi, D.; Marechal, D.; Tekaia, F., NRG1 represses

- yeast–hypha morphogenesis and hypha-specific gene expression in *Candida albicans*. *The EMBO journal* **2001**, *20* (17), 4742-4752.
38. Braun, B. R.; Johnson, A. D., Control of filament formation in *Candida albicans* by the transcriptional repressor TUP1. *Science* **1997**, *277* (5322), 105-9.
 39. Braun, B. R.; Johnson, A. D., TUP1, CPH1 and EFG1 make independent contributions to filamentation in *Candida albicans*. *Genetics* **2000**, *155* (1), 57-67.
 40. Braun, B. R.; Kadosh, D.; Johnson, A. D., NRG1, a repressor of filamentous growth in *C. albicans*, is down-regulated during filament induction. *Embo j* **2001**, *20* (17), 4753-61.
 41. Brand, A.; Gow, N. A., Mechanisms of hypha orientation of fungi. *Curr Opin Microbiol* **2009**, *12* (4), 350-7.
 42. Soll, D. R.; Stasi, M.; Bedell, G., The regulation of nuclear migration and division during pseudo-mycelium outgrowth in the dimorphic yeast *Candida albicans*. *Experimental Cell Research* **1978**, *116* (1), 207-215.
 43. Irazoki, O.; Hernandez, S. B.; Cava, F., Peptidoglycan muropeptides: release, perception, and functions as signaling molecules. *Frontiers in microbiology* **2019**, *10*, 500.
 44. Park, J. T.; Uehara, T., How bacteria consume their own exoskeletons (turnover and recycling of cell wall peptidoglycan). *Microbiology and Molecular Biology Reviews* **2008**, *72* (2), 211-227.
 45. Barnard, M. R.; Holt, S. C., Isolation and characterization of the peptidoglycans from selected gram-positive and gram-negative periodontal pathogens. *Can J Microbiol* **1985**, *31* (2), 154-60.
 46. Klotz, S. A.; Chasin, B. S.; Powell, B.; Gaur, N. K.; Lipke, P. N., Polymicrobial bloodstream infections involving *Candida* species: analysis of patients and review of the literature. *Diagnostic microbiology and infectious disease* **2007**, *59* (4), 401-406.
 47. Tarumoto, N.; Kinjo, Y.; Kitano, N.; Sasai, D.; Ueno, K.; Okawara, A.; Izawa, Y.; Shinozaki, M.; Watarai, H.; Taniguchi, M.; Takeyama, H.; Maesaki, S.; Shibuya, K.; Miyazaki, Y., Exacerbation of Invasive *Candida albicans* Infection by Commensal Bacteria or a Glycolipid Through IFN- γ Produced in Part by iNKT Cells. *The Journal of Infectious Diseases* **2013**, *209* (5), 799-810.
 48. Mason, K. L.; Erb Downward, J. R.; Mason, K. D.; Falkowski, N. R.; Eaton, K. A.; Kao, J. Y.; Young, V. B.; Huffnagle, G. B., *Candida albicans* and bacterial microbiota interactions in the cecum during recolonization following broad-spectrum antibiotic therapy. *Infect Immun* **2012**, *80* (10), 3371-80.
 49. Wargo, M. J.; Hogan, D. A., Fungal--bacterial interactions: a mixed bag of mingling microbes. *Curr Opin Microbiol* **2006**, *9* (4), 359-64.
 50. Morales, D. K.; Hogan, D. A., *Candida albicans* interactions with bacteria in the context of human health and disease. *PLoS pathogens* **2010**, *6* (4), e1000886.
 51. Tan, C. T.; Xu, X.; Qiao, Y.; Wang, Y., A peptidoglycan storm caused by β -lactam antibiotic's action on host microbiota drives *Candida albicans* infection. *Nat Commun* **2021**, *12* (1), 2560.

52. Naseem, S.; Araya, E.; Konopka, J. B., Hyphal growth in *Candida albicans* does not require induction of hyphal-specific gene expression. *Molecular Biology of the Cell* **2015**, *26* (6), 1174-1187.
53. Shareck, J.; Nantel, A.; Belhumeur, P., Conjugated Linoleic Acid Inhibits Hyphal Growth in *Candida albicans* by Modulating Ras1p Cellular Levels and Downregulating TEC1 Expression. *Eukaryotic Cell* **2011**, *10* (4), 565-577.
54. Toyoda, M.; Cho, T.; Kaminishi, H.; Sudoh, M.; Chibana, H., Transcriptional profiling of the early stages of germination in *Candida albicans* by real-time RT-PCR. *FEMS Yeast Research* **2004**, *5* (3), 287-296.
55. Chen, H.; Zhou, X.; Ren, B.; Cheng, L., The regulation of hyphae growth in *Candida albicans*. *Virulence* **2020**, *11* (1), 337-348.
56. Sudbery, P. E., Growth of *Candida albicans* hyphae. *Nature Reviews Microbiology* **2011**, *9* (10), 737-748.
57. Xu, X. L.; Lee, R. T.; Fang, H. M.; Wang, Y. M.; Li, R.; Zou, H.; Zhu, Y.; Wang, Y., Bacterial peptidoglycan triggers *Candida albicans* hyphal growth by directly activating the adenylyl cyclase Cyr1p. *Cell Host Microbe* **2008**, *4* (1), 28-39.
58. Burch, J. M.; Mashayekh, S.; Wykoff, D. D.; Grimes, C. L., Bacterial Derived Carbohydrates Bind Cyr1 and Trigger Hyphal Growth in *Candida albicans*. *ACS Infectious Diseases* **2018**, *4* (1), 53-58.
59. Crump, G. M.; Zhou, J.; Mashayekh, S.; Grimes, C. L., Revisiting peptidoglycan sensing: interactions with host immunity and beyond. *Chemical Communications* **2020**, *56* (87), 13313-13322.
60. Crump, G. M.; Rozovsky, S.; Grimes, C. L., Purification and Characterization of a Stable, Membrane-Associated Peptidoglycan Responsive Adenylate Cyclase LRR Domain from Human Commensal *Candida albicans*. *Biochemistry* **2022**.
61. Staib, P.; Morschhäuser, J., Chlamydospore formation in *Candida albicans* and *Candida dubliniensis*—an enigmatic developmental programme. *Mycoses* **2007**, *50* (1), 1-12.
62. Odds, F. C.; Brown, A. J.; Gow, N. A., *Candida albicans* genome sequence: a platform for genomics in the absence of genetics. *Genome biology* **2004**, *5* (7), 1-3.

Chapter 5

FUTURE DIRECTIONS

5.1 Characterization of Cyr1p

The biochemical classification of the LRR domain of Cyr1p as a peripheral membrane protein was a major insight into the dynamics of the Cyr1p receptor. Though insightful much work remains to be done to capture the dynamics of the 1690 kDa receptor. In further characterizing this receptor, it necessary to recombinantly express the full-length receptor. Attempts to recombinantly express the full receptor resulted in cell lysis shortly after protein induction. This observation could be due to signaling of the adenylate cyclase in the *S. cerevisiae* expression system. To circumvent this problem, I propose site directed mutagenesis to mutate putative catalytic residues in the binding site of the catalytic domain of the receptor. In doing so, inactive recombinant enzyme can be more amendable to expression and subsequent purification.

5.1.1 Cyr1p-LRR binding pocket elucidation

Previous work in our lab has demonstrated that the LRR domain of the receptor Cyr1p binds the bacterial peptidoglycan Muramyl tripeptide with nM affinity. Photoactivatable crosslinking can be utilized to capture the biding site of MTP via a photoactivatable functionalized MTP ligand. Preliminary work has demonstrated that

this ligand is a suitable candidate for PAL, but optimization on purified protein needs to be conducted (refer to Appendix C).

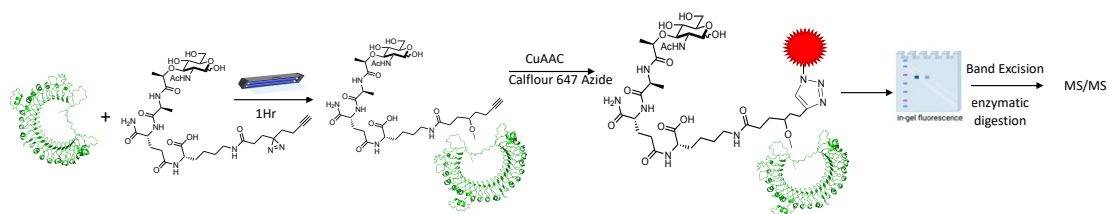


Figure 5.1: Photoactivatable crosslinking of Cyr1p-LRR.

5.2 Peptidoglycan stimulated hyphal growth

To gather a more comprehensive scope of the cellular response to bacterial peptidoglycan fragments, I propose the building up and building down of the bacterial peptidoglycan fragments from MDP to NAM and MDP to MTP respectively. Specifically, I propose to characterize *C. albicans* cellular morphology in the presence of synthetic fragments that are MDP derivatives, carbohydrate backbone derivatives, and MTP derivatives. In chapter 3, a suite of MDP derivatives were analyzed (**Figure 5.2**), but MTP and its derivatives remain to be analyzed (**Figure 5.3**).

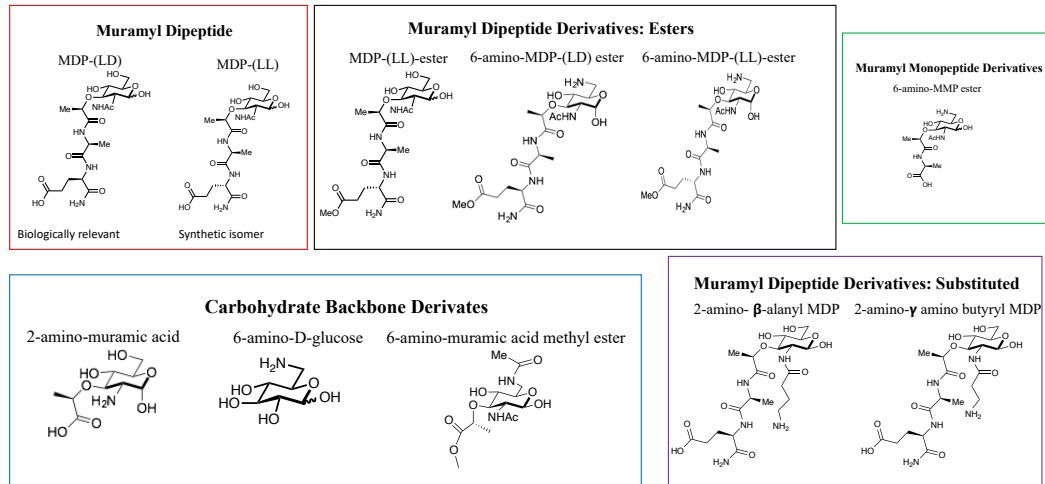


Figure 5.2: Synthetic bacterial peptidoglycan fragments. While some of the fragments were tested for their ability to induce hyphal formation, MDP-(LL) remains to be analyzed.

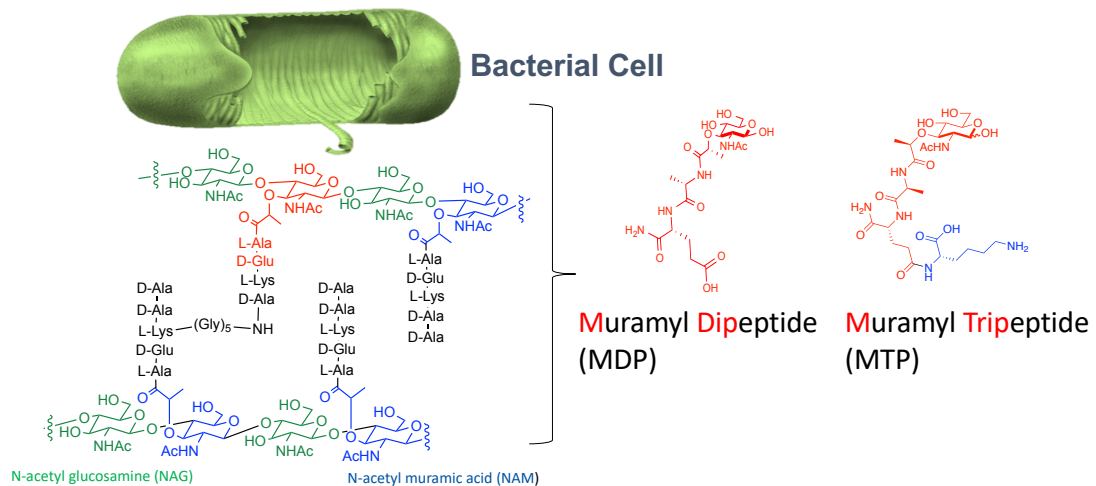


Figure 5.3: Bacterial peptidoglycan fragments. The fragment MTP and its synthetic derivatives remained to be analyzed for their ability to induce hyphae.

5.3 Hyphae transcriptional regulation

Chapter 4 introduced some of the transcriptional components regarding the morphologic regulation of *C. albicans*. My preliminary data suggested that hyphae

specific gene upregulation is not a necessary factor for the phenotypic expression of hyphae. While other studies have confirmed these findings as well, there are still a plethora of genes that can be analyzed to capture a more comprehensive profile of the regulatory pathways involved in bacterial peptidoglycan hyphae stimulation.

Particularly, the gene of *Cyr1p*, *cdc35* needs to be analyzed using the treated samples in chapter 4. Furthermore, the HSPs *ALS3*, *Nrg1* and *UME6* should also be analyzed.

The analysis of these genes can potentially provide insights into the anomalies observed with the genes *HWP1*, *TUP1*, and *ECE1* from chapter 4.

5.4 RNA sequence analysis

The transcriptional discrepancies described in chapter 4 can be fully captured using RNA sequencing analysis. RNA sequence analysis is a useful tool for transcriptome wide analysis of differential gene expression and mRNA splicing. This method can capture the entire transcriptome of *C. albicans* in a bacterial peptidoglycan specific manner, thereby providing major insights into the signaling networks targeted through peptidoglycan sensing and detection.

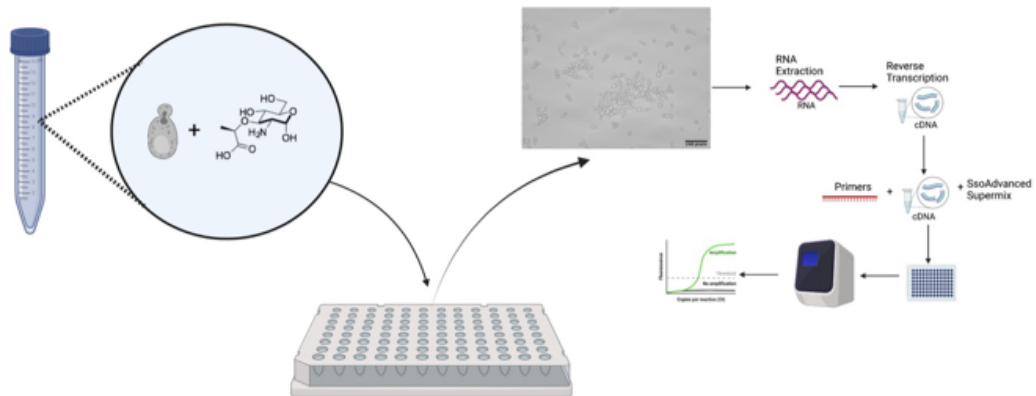


Figure 5.4: Morphological assay to RNA isolation workflow. The morphological assay samples can be further processed to conduct whole RNA sequencing analysis to capture the full range of RNA transcript upregulation and or downregulation.

Appendix A

MOLECULAR CLONING IN *E. COLI*

A.1 Molecular cloning of constructs in *E.coli*

Several constructs with varying purification tags were cloned with the hopes of generating a more stable LRR than the previously expressed *E. coli* construct. The aim was to generate a more stable LRR construct by extending the amino acid composition of the LRR domain to capture the N and C terminal Caps that are pertinent to LRR folding and structure. In addition, we sought to capture the entire span of the LRR domain, which contains 14 repeats. The following table is a compilation of the Cyr1-LRR domain constructs cloned:

Table A.1: Cyr1p-LRR Expression Constructs

Construct No	N-terminal Tag	C-terminal Tag	Expression Host	Amino Acids
1	His ₆ -FH8	His ₆	<i>E.coli</i>	408-915
2	His ₆ -MBP	NA	<i>E.coli</i>	418-1005
3	SpotTag	NA	<i>E.coli</i>	418-1005

A.1.1 Molecular cloning in *E. coli*

Construct 1: PCR was used to extract the LRR domain from residues 408-915 from the CaCYR1 gene that was synthesized by Genscript. Following PCR cleanup and amplicon verification by colony PCR and restriction digest, DNA was inserted

into a modified pET28a vector that contained an N-terminal FH8 tag immediately after a His₆ tag. The modified pET28-FH8 vector was synthesized by Genscript. The Cyl1p-LRR domain was inserted into the modified pET28-FH8 vector utilizing the NotI and XhoI restriction sites and transformed into DH5 α cells. Primers used for amplification were 1) Forward: 5'-TTT TTG CCG CCG CTT CTT GAG ATC ATT GAC ACA TGA TG-3' and 2) Reverse: 5'-TTT TTC TCG AGC AAT TGG TTT GAA GAA ACA TCC AAA-3'.

Construct 2: PCR was used to extract the LRR domain from residues 418-1005 from the CaCYR1 gene that was codon optimized and synthesized by Genscript. Following PCR cleanup and amplicon verification by colony PCR and restriction digest, DNA was inserted into a pMal-c6X vector. The LRR domain was inserted into the pMAL-c6x vector utilizing the NotI and EcoRI restriction sites and transformed into DH5 α cells. Primers used for amplification were 1) Forward: 5'- TTTTT gcggccgc TCAAGAACTACGTTGATGT-3' and 2) reverse: 5'- TTTTT gaattc CAGAATTTGATAACTTCGGTT-3'.

Construct 3: PCR was used to extract the LRR domain from residues 418-1005 from the CaCYR1 gene that was codon optimized and synthesized by Genscript. Following PCR cleanup and amplicon verification by colony PCR and restriction digest, DNA was inserted into a pSPOT1 vector. The LRR domain was inserted into the pSPOT1 vector utilizing EcoRI and XhoI restriction sites and transformed into DH5 α cells. Primers used for amplification were 1) Forward: 5'- TTTTT gaattcATG TCAAGAACTACGTTGATGT-3' and 2) Reverse: 5'- TTTTT ctcgag CAGAATTTGATAACTTCGGTT-3'.

After transformation into DH5 α cells, selected colonies were grown to a dense culture on a 10mL scale, and plasmids were isolated using a Qiagen plasmid purification kit the following day. Purified plasmids were verified by next generation sequencing through the University of Delaware Biotechnology Institute. Plasmids were then transformed into BL21 RIPL-codon optimized cells for expression analysis.

A.2 Expression of Cyr1-LRR domain constructs in *E. coli*

The fusion proteins were expressed in 1 L cultures of LB media containing the appropriate antibiotics: Kanomycin (50 $\mu\text{g}/\text{mL}$) for constructs 1 and 3, and carbenicillin (100 $\mu\text{g}/\text{mL}$) for construct 2 at 30°C until an optical density of 0.6-0.8 was reached at 600nm. Protein expression was induced by the addition of IPTG to a final concentration of 1.0 mM overnight at 15°C. *E. coli* cells were pelleted by centrifugation at 5000 g for 20 minutes and the supernatant was discarded. Pellets were stored at -80°C until use.

Appendix B

MOLECULAR CLONING OF GFP TAGGED LRR IN SACCHAROMYCES CEREVISIAE

B.1 Molecular Cloning of GFP tagged Cyr1-LRR in *S. cerevisiae*

PCR was used to extract the LRR domain from residues 418-1005 from the CaCYR1 gene that was codon optimized and synthesized by Genscript. The codon optimized CaCYR1 gene was cloned into a pESC-URA expression vector with an N-terminal His₆ tag and a C-terminal yeGFP tag utilizing the restriction sites BamH1 and SmaI at the N and C termini respectively. Following PCR cleanup and amplicon verification by colony PCR and restriction digest, DNA was ligated into a yeGFP plasmid utilizing BamH1 and SmaI restriction sites at the N and C termini respectively. Primers used for amplification were 1) Forward: 5'-TTTTTGGATCCGCCACCATGTCAGGTTCAAG-3' and 2) Reverse: 5'-AGGCTCGAGAAAGTTATCAAATTCCCGGGAAAAA-3'.

B.2 Molecular cloning of Full-length Cyr1 in *S. cerevisiae*

Full-length, codon optimized Cyr1 (1690 amino acids), was synthesized by Genscript and cloned into a pESC-URA expression vector with an N-terminal StrepII tag and a C-terminal Spot-Tag utilizing the restriction sites EcoRI and NotI at the N and C termini respectively. The pESC-URA plasmid containing the full-length Cyr1 was transformed into *S. cerevisiae* cells EY1202 (refer to chapter 2) via the lithium acetate method.

Appendix C

PHOTOAFFINITY LABELING ANALYSIS OF CYR1-LRR

C.1 Introduction

With initial data showing a nM binding event between the MBP-tagged LRR domain and the synthetic bacterial peptidoglycan fragment, muramyl tripeptide (MTP)¹, we sought to elucidate the binding site of MTP within the LRR domain using photoaffinity labeling (PAL). PAL is a powerful technique employed in chemical proteomics, to study protein-protein interactions, and protein-ligand interactions among others². Since its development in 1962, a multitude of photocrosslinkers have emerged³. Though photocrosslinkers can be largely divided into three photoreactive groups, Benzophenones, aryl azides, and diazirines, the mechanism of action of all groups, rely on photoirradiation to generate reactive intermediates to establish a covalent modification with the protein of interest. Labeled protein of interest can be visualized utilizing fluorophores, immunoprecipitation, and mass spectrometry.

A former laboratory member Dr. Siavash Mashayekh developed a multifunctional crosslinker to study the potential binding site of the Cyr1-LRR domain. The photoactivatable crosslinker probe consists of MTP as the ligand for the Cyr1-LRR domain, an alkyne diazirine photoactivatable crosslinker group, and a biorthogonal alkyne handle for use in copper-catalyzed azide-alkyne click chemistry (CuAAC) (Figure 1).

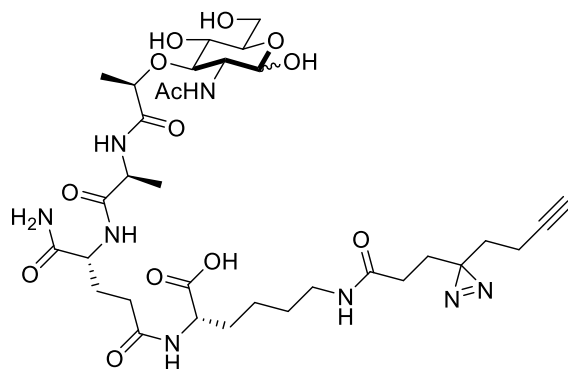


Figure C.1: MTP photoactivatable probe. MTP was functionalized with a diazirine moiety and a bioorthogonal alkyne handle for use in copper-catalyzed azide-alkyne click chemistry.

Cells were lysed in lysis buffer (50 mM HEPES, 0.1 mM MgCl₂, 0.1 mM EGTA, 150 mM NaCl, 10% glycerol, 1 mM PMSF, pH 7.4, and protease inhibitor cocktail). Lysate was centrifuged at 60K RPM for 2hrs at 4°C. Membrane fractions were resuspended in lysis buffer with the addition of 1% Fos-choline-12 (refer to chapter 2). Protein solubilization was conducted at 4°C overnight. Solubilized protein was clarified by centrifugation at 60K RPM for 2hrs at 4°C. Solubilized protein was dialyzed into fresh lysis buffer overnight. Solubilized protein was incubated at 4°C overnight with and without MTP-diazirine probe. Samples were aliquoted into 21 well plates and either irradiated with UV light for 1hr or kept on ice protected from light (-UV control). Following irradiation, CalFluor 647 Azide was attached to the probe using CuAAC chemistry (refer to Table 1).

Table C.1: Components of the PAL experiment.

Component	Amount (μL)
20% SDS	1.25
10mM calflour 647 Azide	0.5
50mM TCEP	0.5
1.7mM TBTA	1.5
50mM CuSO ₄	0.5
DMSO	0.5
100mM Aminoguanidine	1.25

6 μ L of the above reaction mixture was added to 19 μ L of lysate-probe complexes, or appropriate negative controls. For the CuAAC negative control, water was added in place of 50 mM CuSO₄. Click reaction ensued for 1 hr at room temperature, after which 5 μ L of 6X loading dye was added to the reaction mixture to prepare for SDS-PAGE analysis. SDS-PAGE gels were imaged using a GE Typhoon scanning imager.

C.2 Results and Discussions

The synthesized crosslinker probe was used in a photoaffinity labeling experiment with cellular lysate from Spot-tagged Cyr1-LRR expressed in *S. cerevisiae* (refer to chapter 2). Cells were lysed as described in chapter 2, and membranes fractionized. Cyr1-LRR was solubilized from fractionized membranes and solubilized proteins were dialyzed into lysis buffer overnight into lysis buffer. Lysate was incubated with the MTP probe, and the sample was irradiated under 365nm UV light to generate the necessary reactive carbene intermediate to covalently anchor the probe to the LRR. The terminal alkyne was then utilized as the handle in a CuAAC to install a CalFlour 647 azide fluorophore (Table 1). Protein-probe-fluorophore complexes were separated via SDS-PAGE and analyzed via in-gel fluorescence using a GE Typhoon gel imaging scanner. In-gel fluorescence demonstrated a higher fluorescent

intensity in UV-irradiated samples incubated with probe, relative to negative control samples that were not incubated with the probe or was not subjected to UV irradiation. These preliminary results indicate that the MTP crosslinker can bind to the Cyr1-LRR domain and with further optimization, can aid in the elucidation of the MTP binding site within the LRR (Figure 1).

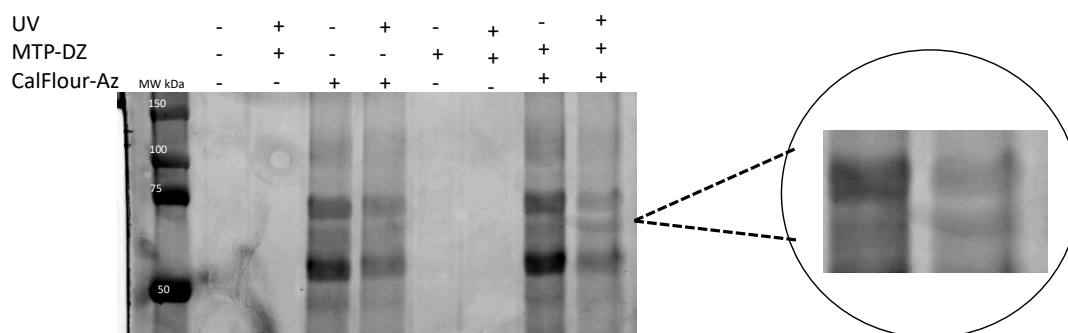


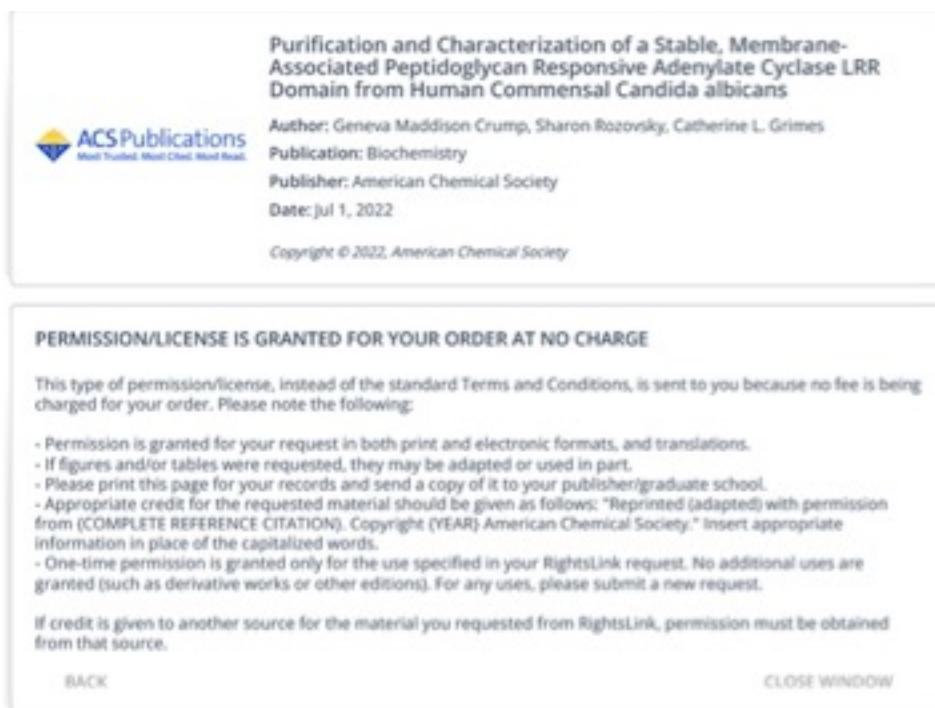
Figure C.2: Preliminary photoactivatable crosslinking of Cyr1p-LRR. In gel fluorescence demonstrates increased fluorescent intensity in the presence of UV light in Cyr1p-LRR and probe complexes.

C.3 REFERENCES

1. Burch, J. M.; Mashayekh, S.; Wykoff, D. D.; Grimes, C. L., Bacterial Derived Carbohydrates Bind Cyr1 and Trigger Hyphal Growth in *Candida albicans*. *ACS Infectious Diseases* **2018**, *4* (1), 53-58.
2. Murale, D. P.; Hong, S. C.; Haque, M. M.; Lee, J.-S., Photo-affinity labeling (PAL) in chemical proteomics: a handy tool to investigate protein-protein interactions (PPIs). *Proteome Science* **2017**, *15* (1), 14.
3. Singh, A.; Thornton, E. R.; Westheimer, F. H., The photolysis of diazoacetylchymotrypsin. *J Biol Chem* **1962**, *237*, 3006-8.

Appendix D

PUBLICATION PERMISSIONS



Purification and Characterization of a Stable, Membrane-Associated Peptidoglycan Responsive Adenylate Cyclase LRR Domain from Human Commensal *Candida albicans*

ACS Publications
Most Trusted. Most Cited. Most Read.

Author: Geneva Maddison Crump, Sharon Rozovsky, Catherine L. Grimes
Publication: Biochemistry
Publisher: American Chemical Society
Date: Jul 1, 2022

Copyright © 2022, American Chemical Society

PERMISSION/LICENSE IS GRANTED FOR YOUR ORDER AT NO CHARGE

This type of permission/license, instead of the standard Terms and Conditions, is sent to you because no fee is being charged for your order. Please note the following:

- Permission is granted for your request in both print and electronic formats, and translations.
- If figures and/or tables were requested, they may be adapted or used in part.
- Please print this page for your records and send a copy of it to your publisher/graduate school.
- Appropriate credit for the requested material should be given as follows: "Reprinted (adapted) with permission from (COMPLETE REFERENCE CITATION). Copyright (YEAR) American Chemical Society." Insert appropriate information in place of the capitalized words.
- One-time permission is granted only for the use specified in your RightsLink request. No additional uses are granted (such as derivative works or other editions). For any uses, please submit a new request.

If credit is given to another source for the material you requested from RightsLink, permission must be obtained from that source.

BACK CLOSE WINDOW

Figure Appendix D.1: Permission for use of material from the publication: Purification and Characterization of a Stable, Membrane-Associated Peptidoglycan Responsive Adenylate Cyclase LRR Domain from Human Commensal *Candida albicans*.



Sales Operations
 Thomas Graham House
 Science Park, Milton Road
 Cambridge CB4 0WF, UK

Tel +44 (0) 1223 420066

Email contracts-copyright@rsc.org

www.rsc.org

Permission Request Form for RSC Material

To request permission to use material from material published by The Royal Society of Chemistry (RSC), please complete and return this form.

From: Name: Geneva Maddison Crum E-mail: crumpg@udel.edu
 Address: 19 Purchase St
Easton, MA 02375

I am preparing the following work for publication:

Article/Chapter Title _____
 Journal/Book Title _____
 Editor/Author(s) Geneva Maddison Crump, Junhui Zhou, Siavash Mashayekl
 Publisher _____

I would very much appreciate your permission to use the following material:

Journal/Book Title Chemical Communications
 Article/Chapter Title Revisiting Peptidoglycan Sensing: interactions with host imm
 Editor/Author(s) Geneva Maddison Crump, Junhui Zhou, Siavash Mashayekl
 DOI 10.1039/D0CC02605K
 Year of Publication 2020
 Description of Material Feature Article
 Page(s) All pages

I will acknowledge the original source as specified at the <https://rsc.li/permissions>.

Signed: Geneva Maddison Crump Date: 09/13/2022

The Royal Society of Chemistry hereby grants permission for the use of the material specified above in the work described and in all subsequent editions of the work for distribution throughout the world, in all media including electronic and microfilm. You may use the material in conjunction with computer-based electronic and information retrieval systems, grant permissions for photocopying, reproductions and reprints, translate the material and to publish the translation, and authorise document delivery and abstracting and indexing services. Please note that if the material specified above or any part of it appears with credit or acknowledgement to a third party then you must also secure permission from that third party before reproducing that material. The Royal Society of Chemistry is a signatory to the STM Guidelines on Permissions (available on request).

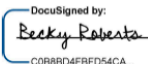
Signed:  _____ Date: 14/9/2022 | 9:31 AM BST
C088BD4FBFD54CA...

Figure D.2: Permission for use of the following publication: *Revisiting peptidoglycans sensing: interactions with host immunity and beyond.*

SPRINGER NATURE LICENSE
TERMS AND CONDITIONS

Oct 14, 2022

This Agreement between Ms. Geneva Crump ("You") and Springer Nature ("Springer Nature") consists of your license details and the terms and conditions provided by Springer Nature and Copyright Clearance Center.

License Number 5407750857803

License date Oct 14, 2022

Licensed Content
Publisher Springer Nature

Figure D.3: Permission for the use of Figure 4.1 from the following publication:
Hyphae-Specific Genes HGC1, ALS3, HWP1, and ECE1, and Relevant
Signaling Pathways in *Candida albicans*.